Functional Analysis of Plant Glutamate Receptors

Michelle Beth Price

Dissertation submitted to the faculty of the
Virginia Polytechnic Institute and State University
in partial fulfillment of the requirements for the degree of

Doctor of Philosophy
In
Plant Pathology, Physiology, and Weed Science

Sakiko Okumoto, Chair
Eva Collakova
Glenda E. Gillaspy
Guillaume Pilot
Boris A. Vinatzer

September 10th, 2013
Blacksburg, Virginia

Keywords: glutamate receptors, amino acids, sensing, plants, calcium channels

Functional Analysis of Plant Glutamate Receptors

Michelle Beth Price

Abstract

The plant glutamate receptors (GLRs) are homologs of mammalian ionotropic glutamate receptors (iGluRs) and are hypothesized to be potential amino acid sensors in plants. Since their first discovery in 1998, the members of plant GLRs have been implicated in diverse processes such as C/N ratio sensing, root formation, pollen germination and plant-pathogen interaction. However, the exact properties of these channels, such as the spectrum of ligands, ion specificities, and subunit compositions are still not well understood.

It is well established that animal iGluRs form homo- or hetero-tetramers in order to form ligand-gated cation channels. The first aspect of this research was to determine if plant GLRs likewise require different subunits to form functional channels. A modified yeast-2-hybrid system approach was initially taken and applied to 14 of the 20 *At*GLRs to identify a number of candidate interactors in yeast. Förster resonance energy transfer (FRET), which measures the transfer of energy between interacting molecules, was performed in mammalian cells to confirm interaction between a few of those candidates. Interestingly, despite an abundance of overlapping co-localization between heteromeric combinations, only homomeric interactions were identified between GLRs 1.1 and 3.4 in HEK293 cells.

Further, amino acids have been implicated in signaling between plants and microbes, but the mechanisms for amino acid perception in defense responses are far from being understood. Recently it was demonstrated that calcium responses initiated by

bacterial and fungal microbe-associated molecular patterns (MAMPs) were diminished in seedlings treated with known agonists and antagonists of mammalian iGluRs, suggesting potential roles of GLRs in pathogen responses. Analysis of publicly available microarray data shows altered gene expression of a sub-fraction of GLRs in response to pathogen infection and bacterial elicitors. Thus, the second goal of my PhD research was aimed at determining whether GLRs are involved in the interaction between plants and pathogens. Gene expression changes of a number of candidate GLRs as well as pathogen growth was examined in response to the plant pathogen *Pseudomonas syringae* pv. tomato DC3000. Interestingly, single gene and multi-gene deficient plants responded differently with regards to pathogen susceptibility, likely as a result of functional compensation between GLRs.

Acknowledgements

I am grateful for the love and support of my family, friends, and colleagues while at Virginia Tech. I would like to thank Sakiko Okumoto for accepting me into her lab and guiding and encouraging me in conducting research. I am especially thankful to the Molecular Plant Sciences program and community, without whom I would not have found the passion to persevere in obtaining my doctorate degree. The members, and previous members, of my committee, Eva Collakova, Glenda Gillaspy, John Jelesko, Guillaume Pilot, and Boris Vinatzer have been very supportive in helping me to develop a diversity of techniques and apply them to my research. In addition, they have been very helpful in guiding me towards obtaining an ideal research position in biotech industry. I am very thankful to the Latham Hall community for their friendship, riveting conversations (both scientific and otherwise), and overall helpfulness. Further, all of this could not have been achieved without the loving support of my husband T.J. and daughter Rachel, my mom and step-dad Patricia and Timothy Basham, and my wonderful in-laws Heather, Kim, Audrey and Sam. I love you all!

Attributions

Several colleagues have contributed to research conducted in this dissertation.

Sakiko Okumoto, Ph.D. is professor in the Department of Plant Pathology, Physiology, and Weed Sciences at Virginia Tech as well as the advisor for this research. She assisted in many late nights of data collection, project guidance, and revision of this dissertation.

Chapter 2: Evolutionary Origins of Plant Glutamate Receptors

John Jelesko is professor in the Department of Plant Pathology, Physiology, and Weed Sciences at Virginia Tech as well as former advisor to this research. He conducted phylogenetic analysis of plant glutamate receptors.

Chapter 3: Identification of Subunits Necessary for GLR Channel Functionality

Carmine Graniello is a research technician in the Okumoto Lab and assisted with attempts to perform co-immunoprecipitation of GLR proteins *in planta*. **Guillaume Pilot** is a professor in PPWS as well as committee member**, Rejane Pratelli** is a postdoc of the Pilot Lab, and **Shi Yu** is a graduate student of the Pilot Lab who all provided technical support for protein extraction and co-immunoprecipitation of proteins. In addition, Guillaume Pilot provided control constructs and guidance for the mating-based split ubiquitin assays.

Chapter 4: Examination of Subcellular Localization and Inter-subunit Interaction in Plants

Altaf Ahmad was a former postdoc in the Okumoto Lab who developed genomic DNA-fluorescent protein fusions of GLR3.3 and 3.4.

Chapter 5: Determination of the role of plant glutamate receptors in response to pathogen infection

Jocelyn Funes was an undergraduate assistant in the Okumoto Lab, and **Carmine Graniello** is a research technician in the Okumoto Lab. Both were very instrumental in assisting with and conducting pathogen growth studies in GLR mutant plants. **Christopher Clarke** is a postdoc in the Vinatzer Lab who assisted with protocol development for pathogen growth assays as well as provided pathogen strains.

Chapter 6: Characterization of a novel mutant phenotype

Gunjune Kim is a graduate student in the Westwood Lab and **Zachary Adelman** is a faculty member in the Department of Entomology at Virginia Tech. They conducted assemblies and guided interpretation of Next Generation Sequencing data. **Kathy Lowe** is a research technician at the Veterinary School of Virginia Tech who assisted with protocol development and SEM imaging of tissue. **Eva Collakova** is a professor in PPWS who provided guidance in metabolite profiling of mutant plants. **Takeshi Fujino** is a former postdoc in the Brunner Lab who provided guidance in tissue fixation and microtome sectioning of plant tissue.

Table of Contents

Summary of Figures

CHAPTER 5

CHAPTER 6

Summary of Tables

CHAPTER 1:LITERATURE REVIEW OF AMINO ACID SENSING MECHANISMS IN PLANTS

AMINO ACIDS AS SIGNALING MOLECULES

Background

As sessile organisms, plants need to sense the availability of minerals to modulate developmental programs and maximize fitness. Nitrogen (N) is quantitatively the most important mineral nutrient, and often the limiting factor for plant growth in the field. The availability of N has a profound short- and long-term effect on plant physiology, which involves developmental reprogramming to maximize N use efficiency (Marschner 1997). While the details of such regulation are starting to be unveiled through systems approaches, the very first step – the sensing of N – is largely unknown in plants.

The assimilation of inorganic nitrogen molecules, namely nitrate and ammonia, into amino acids through glutamine synthetase/glutamine oxoglutarate aminotransferase (GS-GOGAT) is a critical biochemical process in plant growth and development (Taiz L 2006).

Genome-wide studies of plant responses to amino acids have revealed that a large number of genes (approximately 81% of genes regulated by external N) are regulated by organic N levels, particularly those of glutamine and/or glutamate (Gutierrez, Stokes et al. 2008). Because of their essential role in the regulation of nitrogen assimilation, it is plausible that amino acids serve as a potential mechanism for N signaling in plants (Lam, Chiao et al. 2006, Miller, Fan et al. 2008, Vidal and Gutierrez 2008).

Amino acids and the regulation of nitrogen metabolism

Amino acids, formed as the result of the assimilation of inorganic N, serve as N signaling molecules in other organisms, and are considered the prime candidate for organic N signals in plants. Ample evidence demonstrates that amino acid levels affect the activities of key enzymes and transporters in the nitrogen assimilation pathway through transcriptional and post-transcriptional processes. For example, the initial amino acids formed during nitrogen assimilation, glutamine and glutamate, regulate nitrogen assimilation through a feed-back inhibition mechanism (Oliveira, Brenner et al. 2001). In addition, gene expression of cytosolic and plastidic glutamine synthetases, GLN1 and GLN2 respectively, which convert ammonium and 2-oxoglutarate to glutamine, are regulated by the levels of amino acids, particularly glutamine, glutamate, aspartate, and asparagine in *Arabidopsis* and tobacco (Vincentz, Moureaux et al. 1993, Oliveira, Brenner et al. 2001, Fritz, Mueller et al. 2006, Sulieman, Fischinger et al. 2010). The non-protein amino acid GABA (γ-amino-butyric acid), when supplied to plant growth medium, is capable of modulating not only the activity of key enzymes in nitrogen assimilation, but also the uptake of nitrate itself (Barbosa, Singh et al. 2010). Further, amino acids are capable

of modulating uptake of inorganic and organic nitrogen (Rawat, Silim et al. 1999, Nazoa, Vidmar et al. 2003, Hirner, Ladwig et al. 2006).

In addition to gene regulation at the transcriptional level, amino acids have been shown to trigger rapid responses when supplied externally to plant cells. For example, exogenous application of amino acids to plants causes a transient cytosolic calcium increase and membrane depolarization (Dennison and Spalding 2000, Dubos, Huggins et al. 2003, Demidchik, Essah et al. 2004, Qi, Stephens et al. 2006, Stephens, Qi et al. 2008). Further, GABA and D-Ser, have been shown to trigger Ca^{2+} transients in pollen grains (Yu, Liang et al. 2006, Michard, Lima et al. 2011). These studies suggest that plants have endogenous mechanisms of monitoring the concentration of amino acid levels, enabling modulation of nitrogen metabolism.

POTENTIAL MECHANISMS OF AMINO ACID SENSING IN PLANTS

Introduction

Due to the importance of nitrogen in fundamental biological processes common to all kingdoms of life such as protein and nucleic acid synthesis, it is reasonable to speculate that some mechanisms recognizing the levels of nitrogen would be conserved between organisms. Sequencing of the model plant *Arabidopsis* and other plant genomes allowed for identification of proteins that are homologous to the ones involved in amino acid sensing in other organisms. In this section, proteins that function as amino acid sensors in other organisms are summarized. Notably, homologs of all these proteins have been discovered in plants, suggesting some conservation in amino acid sensing mechanisms in a wide range of organisms.

PII Proteins

PII proteins are highly conserved among eukaryotes and prokaryotes, and may play a role in signal transduction in plants In bacteria and cyanobacteria, PII proteins regulate the uptake of ammonium and nitrate/nitrite, modulate the activity of key enzymes in nitrogen assimilation such as glutamine synthetase, and interact with transcriptional regulators of nitrogen metabolism (Arcondeguy, Jack et al. 2001, Coutts, Thomas et al. 2002, Forchhammer 2004, Osanai and Tanaka 2007). The conformation and modification status of PII is determined by the levels of 2-oxoglutarate and glutamine, which in turn triggers interactions with a number of target proteins (Leigh and Dodsworth 2007). For example, in *Escherichia coli*, when 2-oxoglutarate accumulates, GlnK is uridylated and is then able to bind to a trans-membrane ammonia channel, AmtB (Leigh and Dodsworth 2007). Once ammonia is assimilated into glutamine, glutamine then binds to uridyl-transferase to decrease uridylation of GlnK (Leigh and Dodsworth 2007). Additional targets of bacterial PII proteins include the NtrB/NtrC signal transduction system, in which the membrane associated kinase NtrB phosphorylates activates the transcription factor NtrC under nitrogen limiting conditions; N-acetyl glutamate kinase (NAGK) in cyanobacteria, which regulates arginine biosynthesis; and the transcriptional activator of nitrogen fixation NifA under extreme nitrogen depletion in γ-proteobacteria (Leigh and Dodsworth 2007). Bacterial PII proteins are thus considered "master regulators" capable of sensing the nitrogen state of the cell, transmitting the nitrogen signal through direct interaction with enzymes, transporters and regulatory proteins, and regulating processes such as transport, gene expression, enzyme activity, and protein modification resulting in regulation of nitrogen metabolism (Leigh and Dodsworth 2007).

In *Arabidopsis*, a PII homolog (Glb1) sharing 50% identity to *Escherichia coli* PII has been identified, with no other homologs in the *Arabidopsis* genome. Glb1 is a nuclear-encoded,

chloroplast-localized protein (Feria Bourrellier, Valot et al. 2010), and is negatively regulated at the transcriptional level by the concentrations of the amino acids asparagine, glutamine, and glutamate (Hsieh, Lam et al. 1998). Crystal structure of Glb1showed that, like its bacterial counterparts, Glb1 contains a B-loop signature motif which may be important for interactions with small molecule effectors like 2-oxoglutarate and ATP, suggesting that this protein may represent a potential mechanism of metabolite sensing conserved in both bacteria and plants (Oliveira, Brenner et al. 2001, Mizuno, Moorhead et al. 2007). So far, two chloroplastic enzymes, acetyl CoA-carboxylase (ACCase) and N-acetyl glutamate kinase (NAGK), have been identified as direct targets of the plant PII protein Glb1 (Feria Bourrellier, Valot et al. 2010), which are also known targets of cyanobacterial PII proteins (Maheswaran, Urbanke et al. 2004). ACCase and NAGK are key enzymes initiating the synthesis of fatty acids in plastids and arginine biosynthesis, respectively (Ferrario-Mery, Besin et al. 2006, Feria Bourrellier, Valot et al. 2010).

Recently, the transcription factor *WRINKLED1*, which controls the expression levels of multiple genes involved in fatty acid accumulation and seed maturation, was demonstrated to directly control AtGlb1 expression (Baud, Feria Bourrellier et al. 2010). Knockout of Glb1 did not exhibit a developmental or altered growth response under nitrogen sufficient conditions, but did exhibit a weak phenotype showing increased levels of starch and glucose only under nitrogen-limiting growth conditions (Ferrario-Mery, Besin et al. 2006, Feria Bourrellier, Valot et al. 2010). Interestingly, however, these mutants do contain decreased amounts of long chain desaturated fatty acids in seeds (Baud, Feria Bourrellier et al. 2010). These data suggest that unlike their microbial counterparts, plant PII proteins are probably not “master regulators” of nitrogen. Rather, the role of Glb1 appears to be centered on fine-tuning the allocation of carbon

to fatty acid biosynthesis (Baud, Feria Bourrellier et al. 2010), and its role in maintenance of carbon/nitrogen might be limited to nitrogen limiting conditions (Feria Bourrellier, Valot et al. 2010).

Mammalian Target of Rapamycin (mTOR)

In yeast and mammals, target of rapamycin (TOR) is a serine/threonine kinase that regulates cell growth through sensing of nutrient status and modulating cellular catabolism accordingly (Jewell, Russell et al. 2013). The mammalian TOR (mTOR) complex (mTORC1) is composed of mTOR, RAPTOR which aids in substrate recognition and regulates mTOR, mammalian lethal with SEC13 protein 8 (MLST8), PRAS40, and DEPTOR (DEP-domain containing mTOR-interacting protein) (Kim, Sarbassov et al. 2002, Kim, Sarbassov et al. 2003, Wullschleger, Loewith et al. 2006, Jewell, Russell et al. 2013). This complex is a master regulator of nutrient, energy, and redox status as well as protein synthesis and is controlled by insulin, growth factors, oxidative stress, and amino acids (Kim, Sarbassov et al. 2002, Hay and Sonenberg 2004, Jewell, Russell et al. 2013).

Interestingly, growth factors alone are not sufficient to activate mTORC1, with the level of amino acids (namely leucine, glutamine, and arginine) and energy availability being critical to ensure resources are available for modulating developmental and metabolic processes (Hara, Yonezawa et al. 1998, Nicklin, Bergman et al. 2009, Bauchart-Thevret, Cui et al. 2010, Jewell, Russell et al. 2013). Direct sensing of leucine by LeuRS (leucy-transfer RNA synthetase) activates mTORC1 (Avruch, Long et al. 2009, Efeyan, Zoncu et al. 2013, Jewell, Russell et al. 2013), which is then recruited to the surface of endosomes and lysosomes to Rheb-GTP through interaction with Rag-GTPases and RAPTOR (Duran and Hall 2012, Efeyan, Zoncu et al. 2012,

Efeyan, Zoncu et al. 2013, Jewell, Russell et al. 2013). The signals which influence mTORC1 activity do so through modulation of phosphorylation of TSC1/TSC2 complex, where TSC2 is a GTPase-activating protein (GAP) that interacts with the Rheb G protein to hydrolyze GTP to GDP in the cell, thus providing energy necessary for activation (Beauchamp and Platanias 2012, Duran and Hall 2012, Jewell, Russell et al. 2013).

In plants, all necessary components of mTORC1 are conserved (Robaglia, Thomas et al. 2012), and homozygous *tor* mutants are lethal following in the cell growth component of cell division during the globular stage of embryogenesis (Menand, Desnos et al. 2002). While the TOR pathway in plants has not been fully investigated, evidence is emerging for a role similar to that of its yeast and mammalian counterparts as a "master regulator" of nutrient status, where components of nitrogen assimilation and recycling (glutamine synthetase, glutamate dehydrogenase, PP2A, and nitrite reductase) are targeted (MacKintosh 1992, Deprost, Yao et al. 2007, Ahn, Han et al. 2011, Robaglia, Thomas et al. 2012).

Amino Acid Transporters/Sensors (Transceptors)

Some identified transporters are known to have dual functions as both transporters and sensors, many of which are found in yeast and mammals (Didion, Regenberg et al. 1998, Franchi-Gazzola, Dall'Asta et al. 2006, Hundal and Taylor 2009). Recently, a nitrate transporter CHL1 (NRT1.1) from *Arabidopsis* was identified as the first transporter/sensor in plants responsible for the primary nitrate response (Ho, Lin et al. 2009). Such transceptors for amino acids are best understood in yeast and all transceptors for amino acids transporter/sensor identified to date belong to the amino acid/polyamine/organocation (APC) superfamily of amino acid transporters (Wipf, Ludewig et al. 2002). The amino acid permeases Ssy1 and Gap1 are

branched-chain and general amino acid transporters, respectively, localized in the plasma membrane and are known to be involved in sensing the amino acid leucine (Didion, Regenberg et al. 1998, Wipf, Ludewig et al. 2002, Hundal and Taylor 2009). In mammals, sodium-dependent neutral amino acid transporter 2 (SNAT2) is a neutral amino acid transporter that senses extracellular availability of amino acids such as glutamine, glycine, alanine, and proline and modulates the free intracellular amino acid pool accordingly (Franchi-Gazzola, Dall'Asta et al. 2006, Gaccioli, Huang et al. 2006). Perception of extracellular amino acids through membrane transport by these sensors initiates multiple signaling cascades in which the target of rapamycin (TOR) pathway plays a central role (Zuo, De Jager et al. 1997, Jacinto and Hall 2003, Kang, Kim et al. 2006). Plants have more than 90 potential amino acid transporters, including 14 members of the APC superfamily, thus, there is a possibility that some of them may work as sensors of amino acids, but so far none have been identified (Wipf, Ludewig et al. 2002, Rentsch, Schmidt et al. 2007).

Glutamate Receptors (GluRs)

In mammals, sensing of amino acids such as glutamate, glycine, and γ-aminobutyric acid (GABA) in regulation of gated ion channels is well-established. Glutamate is involved in exciting ionotropic receptors and modulating signaling at metabotropic receptors (receptors which indirectly activate ion channels through secondary messengers upon ligand binding), while glycine and GABA are major inhibitory neurotransmitters in the central nervous system (Schwartz 2000). These amino acids play key roles in mediating cell-to-cell signaling in the mammalian nervous system by behaving as ligands for gated ion channels, where an influx of cations through the channel depolarizes synaptic membranes triggering a signaling cascade. The

abundance, localization and subunit compositions of mammalian GluRs play an essential role in neuronal plasticity (Chiu, DeSalle et al. 1999, Dingledine, Borges et al. 1999, Schwartz 2000). Curiously, earlier studies demonstrated that glutamate and glycine, which function as neurotransmittors, are capable of triggering membrane depolarization in plants, and suggests that an amino-acid gated channel might also exist in plants (Dennison and Spalding 2000, Dubos, Huggins et al. 2003, Meyerhoff, Muller et al. 2005).

PLANT GLUTAMATE-LIKE RECEPTORS (GLRs)

Introduction

Genome-wide searches for putative nitrogen sensors based on amino acid and protein homology to animal glutamate receptors resulted in the identification of gene homologs in flowering plants (Lam, Chiu et al. 1998, Chiu, DeSalle et al. 1999, Chiu, Brenner et al. 2002, Davenport 2002), as well as Bryophytes and Lycophytes (see Chapter 2). Many studies have been published since the identification of plant GLRs, indicating the function of glutamate receptors in a wide variety of processes. Our current knowledge of the structure, channel compositions and physiological functions of plant GLRs are summarized here.

Secondary and Tertiary Structures

Mammalian ionotropic GluRs are classified into 4 classes based on their pharmacological response to agonists and antagonists: AMPA (α-amino-3-hydroxy-5-methyl-4-isoxazole propionate), KA (kainate), and NMDA (N-methyl-D-aspartate) and δ (no known ligands)(Connaughton 1995, Mayer 2011). These classifications are not rigid however, as a

result of sequence similarity and cross-reactivity between classes, often resulting in functional grouping of AMPA, δ and KA together as the non-NMDA receptors (Connaughton 1995, Kandel, Schwartz et al. 2000). Homologs of glutamate receptors can be found in bacteria, metazoans and plants. They share the basic structure of domains that make up the ligand-binding site and transmembrane domains, but there is a significant difference in the structures that may have implications in the function of these channels.

The minimal structure of an ionotropic glutamate receptor consists of a ligand binding domain (LBD) and a channel forming domain (Figure 1-1). A LBD consists of two subdomains, GlnH1/S1 and GlnH2/S2, which are considered to have evolved from periplasmic binding proteins of bacteria because of significant homology in primary sequence (Nakanishi, Shneider et al. 1990). Indeed, crystal structures of ligand binding domains of all glutamate receptors analyzed so far has revealed striking structural similarities between the ligand binding domains and bacterial glutamine binding protein (Armstrong, Sun et al. 1998, Armstrong and Gouaux 2000, Naur, Vestergaard et al. 2005). The channel forming domain consists of two or three complete trans-membrane domains (M1 and M3 in prokaryotic channels; M1, M3, and M4 in eukaryotic channels) and one partial trans-membrane domain (M2) that forms a pore-loop (P-loop) structure (Kandel, Schwartz et al. 2000). The structure formed by M1, M3 and P-loop resembles the structure of tetrameric potassium channels such as KcsA, with inverted topology (MacKinnon 2003).

While bacterial ionotropic glutamate receptors consist only of the ligand binding domain and the channel forming domain (Chen, Cui et al. 1999), eukaryotic glutamate receptors possess an additional amino terminal domain (ATD). Similar to LBD, ATD shares sequence and structural similarity with bacterial periplasmic binding proteins (Figure 1-2). The ATDs are

responsible for the interaction between the subunits, which in turn contributes to determining the subunit composition of the channel (Jin, Singh et al. 2009). Further, the ATD of NMDA receptors can bind a wide range of molecules and ions that work as modulators of the channel activities (Lipton, Kim et al. 1997). Plant glutamate receptors share the signature "three plus one" trans-membrane domains M1 to M4 as well as the putative ligand binding domains GlnH1 and GlnH2, which show high amino acid sequence identity (63%-16%), particularly with the M3 domain (63%), with animal NMDA-receptor iGluRs (Lam, Chiu et al. 1998, Chiu, DeSalle et al. 1999). In addition, the predicted membrane topology and orientation of the protein, with the ligand-binding domains exposed to the external side of the membrane, are considered to be conserved (Lam, Chiu et al. 1998, Dubos, Huggins et al. 2003, Dubos, Willment et al. 2005, Furukawa, Singh et al. 2005).

Structure and Subunit Composition

In mammals, functional, ligand-gated channels can be formed from either homo- or hetero- multimers of four subunits within the same agonist class (Rosenmund, Stern-Bach et al. 1998). NMDA receptors form obligatory hetero-tetramers consisting of two glycine-binding subunits and glutamate-binding subunits (Monyer, Sprengel et al. 1992), whereas some AMPA and kainate receptors can form functional homo-tetramers (Mano and Teichberg 1998). The subunit composition dictates the functional properties of the channel, resulting in a large number of receptor types which function differently *in vivo* (Mayer 2005). In addition, alternative splicing and RNA editing of glutamate receptors further increases the diversity of the receptor complexes (Egebjerg and Heinemann 1993, Gereau and Swanson 2008).

In 2009, the crystal structure of the homo-tetrameric rat AMPA receptor GluA2 was resolved, shedding light onto the assembly of the entire channel (Sobolevsky, Rosconi et al. 2009). The resolved crystal structure has a "Y"-shape, where the ATD and LBD spread outward from the more compact channel-forming domains (Figure 1-2). The tetramer is formed as "dimer of dimers", and the ATD and LBD exhibits approximate overall 2-fold molecular symmetry to the axis perpendicular to the membrane. The trans-membrane domain, on the other hand, assumes a 4-fold rotational symmetry that is remarkably similar to the bacterial potassium channel KcsA (Doyle, Morais Cabral et al. 1998).

The structure revealed extensive inter-subunit interaction through ATDs (interface ~330 $Å^2$), which was essentially identical to what was observed in the crystal structures of isolated ATDs (Sobolevsky, Rosconi et al. 2009, Mayer 2011). On the other hand, the inter-subunit interaction in LBDs is much smaller (interface ~224 $Å^2$), hence the role of LBD in the subunit assembly is considered to be minimal. This result corroborates the previous studies using isolated ATD domains: ATDs of two interacting subunits exhibit very high affinity (e.g. 11nM for GluR6 and KA2 heterodimer, 0.7μM for NR1 and NR2 heterodimer) to each other compared to the affinity for itself (Karakas, Simorowski et al. 2011, Kumar, Schuck et al. 2011). Therefore, while ATD might not be the only domain that dictates the interaction partners (Pasternack, Coleman et al. 2002), it is considered to play an important role in the correct assembly of subunits.

The subunit compositions of plant glutamate receptors are largely unknown. Examination of calcium conductance and mutant analyses in response to amino acids (specifically Met, Phe, Leu, Tyr, Asn, and Thr) revealed *At*GLR1.4 forms an ion-channel gated by multiple hydrophobic amino acids (Tapken, Anschutz et al. 2013). Also, *At*GLR3.4 can form a homo-meric channel

when expressed in HEK293 cells (Vincill, Bieck et al. 2012). On the other hand, co-expression analysis using single-cell sampling revealed that, at least in Arabidopsis leaf epidermal and mesophyll cells, there are five to six GLRs co-expressed on average, therefore hetero-tetramer formation is quite likely (Roy, Gilliham et al. 2008). In studies using T-DNA insertion mutants of *At*GLR3.3 and 3.4, it was shown that the response to all six amino acids that can induce membrane depolarization (Ala, Cys, Asn, Glu, Ser, and Gly) were affected in *glr3.3* mutants, while in *glr3.4* mutants responses were affected in only a subset of amino acids (Stephens, Qi et al. 2008). These results support a model where GLR3.3 is included in all receptor complexes in the cell type tested (hypocotyl) whereas a sub-fraction of complexes include at least GLR3.3 and 3.4. A recent study demonstrated that GLRs 3.2 and 3.4 are capable of physically interacting with one another in phloem and T-DNA insertion mutants of both *glr3.2* and *glr3.4* display an increase in aberrant lateral root primordia in Arabidopsis seedlings (Vincill, Clarin et al. 2013). Interestingly, however, no physical interaction was detected between GLRs 3.2 or 3.4 and GLR3.3, counter to the model based on previous genetic evidence (Stephens, Qi et al. 2008, Vincill, Clarin et al. 2013). The discrepancy between these experiments can be attributed to the current limitations in detecting physical protein-protein interaction as a result of incompatible protein conformation (where proximity and orientation are non-ideal) and lack of understanding of conditions and constituents necessary for channel subunit dynamics. Further investigations are necessary to understand the subunit compositions of GLRs *in vivo*.

Pharmacological Studies

NMDA-receptor iGluRs bind glutamate to mediate synaptic depolarization in the postsynaptic membranes. As discussed in the next section, the ligand-binding domain of plant

GLRs shares homology at the amino acid level with mammalian NMDA-receptors. Thus, several groups have investigated whether plant GLRs are influenced similarly to their mammalian counterparts in response to agonists and antagonists (Lam, Chiu et al. 1998, Brenner, Martinez-Barboza et al. 2000). The possible *in vivo* function of plant GLRs was examined by investigating whether plant glutamate receptors respond analogously to mammalian glutamate receptors to the known competitive antagonist 6,7-dinitroquinoxaline-2,3-(1*H*,4*H*)-dione (DNQX)(Lam, Chiu et al. 1998). When *Arabidopsis* seedlings were treated with DNQX, plants grown in light exhibited a dose- and light-dependent increase in hypocotyl elongation and reduced light-induced chlorophyll synthesis (Lam, Chiu et al. 1998). Likewise, when light-grown *Arabidopsis* seedlings were treated with *S*(+)-β-methyl-α,β-diaminopropionic acid (BMAA), an agonist of AMPA-kainate glutamate receptors and a glutamate analog, hypocotyl elongation was increased while cotyledon opening was impaired (Brenner, Martinez-Barboza et al. 2000). BMAA-induced hypocotyls responses are alleviated when exogenous glutamate is applied, suggesting that there may be a conserved mechanism for ligand-binding between mammalian and plant glutamate receptors (Brenner, Martinez-Barboza et al. 2000).

The fact that two different compounds capable of interacting with mammalian iGluRs, DNQX and BMAA, each induce hypocotyl elongation in light grown seedlings suggests a role for AtGLRs in photomorphogenic development (Brenner, Martinez-Barboza et al. 2000). However, this evidence is circumstantial due to lack of experimental evidence demonstrating direct binding of ligands to plant GLRs and also lack of heterologous expression data demonstrating altered function of these channels in the presence or absence of potential antagonists and agonists.

Electrophysiological Analyses

Channel selectivity of plant GLRs are not completely understood at this point. Early studies indicated that plant GLRs function as non-selective cation channels (NSCCs). Plants over-expressing the *Arabidopsis* GLR3.1 gene exhibited a phenotype consistent with Ca^{2+} deficiency that was reversed when supplemented with exogenous Ca^{2+}. These plants also exhibited an increased sensitivity to K^+, Na^+, and Mg^{2+}cations, consistent with their putative roles as NSCCs (Kim, Kwak et al. 2001). Expression of *At*GLR3.7 in *Xenopus* oocytes enhanced plasma membrane conductance of $Ba^{2+,}$ Ca^{2+}, and Na^+ ions, providing further evidence that plant GLRs function as NSCCs (Roy, Gilliham et al. 2008). Grafting experiments in which the pore region of GLR1.1 and 1.4 were transplanted into rat AMPA and kainite receptors indicated that the pore regions of these receptors are capable of conducting K^+, Na^+, and Ca^{2+} (Tapken and Hollmann 2008). On the other hand, recently, it has been demonstrated that both *At*GLRs 1.4, and 3.4, when expressed heterologously in *Xenopus* oocytes and HEK293 cells respectively, are capable of acting as calcium-permeable non-selective cation channels (Tapken and Hollmann 2008, Vincill, Bieck et al. 2012, Tapken, Anschutz et al. 2013). Interestingly, though, the ligand specificity is very different between the two channels, where *At*GLR1.4 is most responsive to Met, Trp, Phe, Leu, Tyr, Asn, and Thr (Tapken, Anschutz et al. 2013), or more hydrophobic amino acids, while *At*GLR3.4 is most responsive to Asn, Ser, and Gly (Vincill, Bieck et al. 2012). Also, the two channels vary in their specificity for cation conductance, where *At*GLR1.4 is a non-selective cation conductor and *At*GLR3.4 conducts calcium specifically, at least in their respective heterologous expression system (Vincill, Bieck et al. 2012, Tapken, Anschutz et al. 2013). This suggests that the plant GLRs might have different agonist profiles, possibly

depending on 1) whether and which GLRs comprise the channel, and 2) the location and function of the GLR channel in the plant.

Physiological functions of GLRs

In the 15 years following the first documentation of plant GLRs, a large number of studies aimed to understand their physiological functions. In particular, genetics tools available in the model plant *Arabidopsis* have largely contributed to our current understanding of plant GLRs' functions. As of the time of this dissertation, plant GLRs are suggested to play a role in a remarkably wide variety of physiological processes.

Role of GLRs in Carbon-Nitrogen Balance

Antisense *At*GLR1.1 plants have been examined for phenotypes under various treatments such as, agonist and antagonist treatments, various cations, as well as sucrose, mannitol, glucose, and sorbitol to attempt to elucidate a function for this gene (Kang and Turano 2003). Decreased accumulation of GLR1.1 transcript, as a result of expression of antisense *At*GLR1.1, corresponded to a decrease in protein and transcript abundance in carbon and nitrogen metabolic enzymes such as cytosolic glutamine synthase (GS1), cytosolic aspartate aminotransferase (AAT2), nitrate reductase (NR1), nitrite reductase (NiR), nitrate transporter (CHL1), and hexokinase (HXK1), and an increase in abscisic acid (ABA) biosynthesis gene (ABA1). In addition, the levels of ABA are higher in antisense plants compared with wild-type (Kang and Turano 2003). These results suggest a role for GLR1.1 in regulation of carbon and nitrogen metabolism and ABA biosynthesis and signaling (Kang and Turano 2003, Kang, Mehta et al. 2004).

Membrane Depolarization Induced by Amino Acids

Mutants in two *Arabidopsis* GLR genes, GLR3.3 and GLR3.4, exhibit impaired membrane depolarization and cytosolic Ca^{2+} responses to extracellular glutamate and other amino acids compared to wild-type, suggesting that these genes are directly or indirectly involved in the perception of extracellular amino acids (Qi, Stephens et al. 2006, Stephens, Qi et al. 2008). Recently, it has been demonstrated that mammalian human embryonic kidney (HEK293) cells over-expressing *At*GLR3.4 are capable of conducting calcium inwardly with respect to the membrane in response to the amino acids glycine and asparagine (Vincill, Bieck et al. 2012). Interestingly, plants deficient in *At*GLR3.3 expression exhibited abolished cytosolic calcium response known to be initiated upon treatment with glutathione tripeptide (GSH, γ-Glu-Cys-Gly), indicating that calcium responses induced by GSH are at least partly acting through *At*GLR3.3 channels (Li, Wang et al. 2013). In addition, deficiency of *At*GLR1.4 expression in seedlings results in a significant decrease in methionine-induced membrane depolarization, consistent with the increased cation conductance seen in oocytes over-expressing GLR1.4, a response which was not seen with the non-agonist glutamate (Tapken, Anschutz et al. 2013).

Lateral Root Formation

Examination of promoter activities and mRNA abundance shows that the majority of Clade 3 genes are expressed more highly in the root than shoot (Chiu, Brenner et al. 2002, Roy, Gilliham et al. 2008). Mining of the microarray data of specific root cell types revealed that *At*GLRs3.2 and 3.4 were expressed predominately in the phloem (Moreno-Risueno, Van Norman et al. 2010), and the co-expression of these two genes was confirmed by localization of native

promoter-gene-fluorescent protein fusions, both of which localized to the sieve plates in the phloem (Vincill, Clarin et al. 2013). Interestingly, both single and double gene knock-outs of *At*GLR3.2 and 3.4 show an increase in the number of lateral root primordia, but not emerged lateral roots, compared to wild-type, suggesting their roles in lateral root formation (Vincill, Clarin et al. 2013). As of yet, it is unclear whether the function of these GLRs in lateral root primordia initiation is dependent on their role as amino acid-gated cation channels, and what the exact mechanism is through which GLRs modulated the lateral root formation.

Pollen Tube Elongation

It is well-established that changes in apical cytosolic calcium concentration are a central regulator of pollen tube growth, though the mechanism through which the calcium gradient is established is unclear (Swarbreck, Colaco et al. 2013). A compelling, though indirect, role of GLRs in pollen tube growth has been observed through application of the known mammalian ionotropic glutamate receptors (iGluRs) pharmacological antagonists CNQX, DNQX, and AP-5 (Michard, Lima et al. 2011). Application of these antagonists resulted in significant inhibition of pollen tube growth and calcium oscillations (Michard, Lima et al. 2011). Interestingly, application of D-serine and glycine, but not the well-established iGluR agonist L-glutamate, significantly promoted pollen tube growth and prompted an influx of calcium as observed through patch-clamp analysis (Michard, Lima et al. 2011). Further, *glr1.2* mutants display deformed pollen tips and tubes, which phenocopies that seen in the wild-type pollens treated with CNQX, and the mutant plants show decreased male fertility. Importantly, the cytosolic calcium oscillation amplitude, in *glr1.2* mutants are decreased, strongly suggesting a role for GLR1.2 in modulating pollen tube growth (Michard, Lima et al. 2011).

Response to Plant Pathogens

Amino acids have been implicated in signaling between plant and infectious pathogens. In response to *Agrobacterium tumefaciens* infection, plants activate synthesis of the amino acid γ-aminobutyric acid (GABA)(Chevrot, Rosen et al. 2006, Haudecoeur, Planamente et al. 2009). GABA is known to promote the degradation of the quorum sensing signal OC8HSL (N-(3-oxooctanoyl) homoserine lactone), which controls conjugation and amplification of the Ti (Tumor-inducing) plasmid as well as severity of tumoral symptoms during infection (Chevrot, Rosen et al. 2006, Haudecoeur, Planamente et al. 2009). The branched chain amino acid (Bra) transporter system is responsible for the transport of GABA through the bacterial membrane (Hosie, Allaway et al. 2002, Chevrot, Rosen et al. 2006). The presence of GABA activates the lactonase AttM, leading to the degradation of the quorum sensing signal by an unknown mechanism, suggesting that GABA may be used by the plant as a way to control bacterial growth (Chevrot, Rosen et al. 2006). Interestingly, the amino acid proline antagonizes GABA-induced degradation of OC8HSL, thus demonstrating a system in which amino acids serve as signaling molecules during plant-pathogen interactions (Haudecoeur, Planamente et al. 2009). During infection with the fungal pathogen *Cladosporium fulvum*, the concentrations of most amino acids and total nitrogen content increase (Solomon and Oliver 2001). Despite this, the mechanisms for amino acid perception in defense responses are far from being understood.

Analysis of publicly available microarray data shows increased expression of a sub-fraction of GLRs in response to pathogen infection, as well as by mutations in the negative regulators of signal transduction caused by bacterial pathogens (Zimmermann, Hirsch-Hoffmann et al. 2004, Thilmony, Underwood et al. 2006, Cheung, Zeng et al. 2007). Bacterial challenge

with *Pseudomonas syringae* pv. tomato DC3000 (Pto DC3000), a pathogen capable of causing bacterial speck on *Arabidopsis*, results in differential expression of a subset of GLRs, particularly those in subfamily 1 (Zimmermann, Hirsch-Hoffmann et al. 2004). Interestingly, *P. syringae* pv. tomato DC3000 carrying avrRpm1, an avirulence gene recognized by RPM1 in *Arabidopsis* (Ritter and Dangl 1995), or pathovars of which *Arabidopsis* is not a host, such as *P. syringae pv. phaseolicola* (Mishina and Zeier 2007), tend to increase expression of GLR subfamily 1 genes compared to the compatible pathogen, DC3000 (Zimmermann, Hirsch-Hoffmann et al. 2004).

Recently, it was demonstrated that calcium responses initiated by bacterial and fungal microbe-associated molecular patterns (MAMPs) were diminished in seedlings treated with known agonists and antagonists of mammalian iGluRs (Kwaaitaal, Huisman et al. 2011). In addition, potential GLR agonists aspartate and glutamate appear to desensitize the calcium response to bacterial MAMPs flg22 and elf18 (Kwaaitaal, Huisman et al. 2011). Since glutamate receptors are likely to act as non-selective cation channels and expression is induced in response to incompatible pathogens (non-host or gene-for-gene resistance), they might play a role in signal transduction during pathogen challenge that leads to the initiation of plant defense responses.

New evidence implicates that GLR3.3 mediates GSH-mediated immunity in Arabidopsis. Glutathione, (GSH or γ-Glu-Cys-Gly) is a major antioxidant tripeptide capable of acting as a neurotransmitter and modulating iGluRs in the central nervous system of animals (Levy, Sucher et al. 1991, Juurlink 1999, Dringen 2000, Oja, Janaky et al. 2000, Aoyama, Watabe et al. 2008). In plants, GSH plays an important role in ROS (reactive oxygen species) scavenging and signaling during oxidative stress responses, where plants with reduced GSH biosynthesis exhibit

enhanced disease susceptibility to virulent strains of *Pseudomonas syringae* and *Phytophthora brassicae* plant pathogens (Parisy, Poinssot et al. 2007, Dubreuil-Maurizi and Poinssot 2012). Microarray analysis of defense and signaling-related genes in WT and *glr3.3* mutants in response to GSH were examined, revealing that GLR3.3 plays a role in mediating early transcriptional responses to GSH in Arabidopsis leaf tissue (Li, Wang et al. 2013). Further, deficiency in GLR3.3 expression resulted in an increased susceptibility to *P. syringae* pathogen infection as monitored by bacterial growth curve analysis (Li, Wang et al. 2013). Interestingly, the amino acid cysteine, along with the peptide GSH, was capable of suppressing pathogen growth in WT compared to *glr3.3* mutants, indicating a "priming" of defense response through an AtGLR3.3-dependent pathway (Li, Wang et al. 2013).

FIGURES

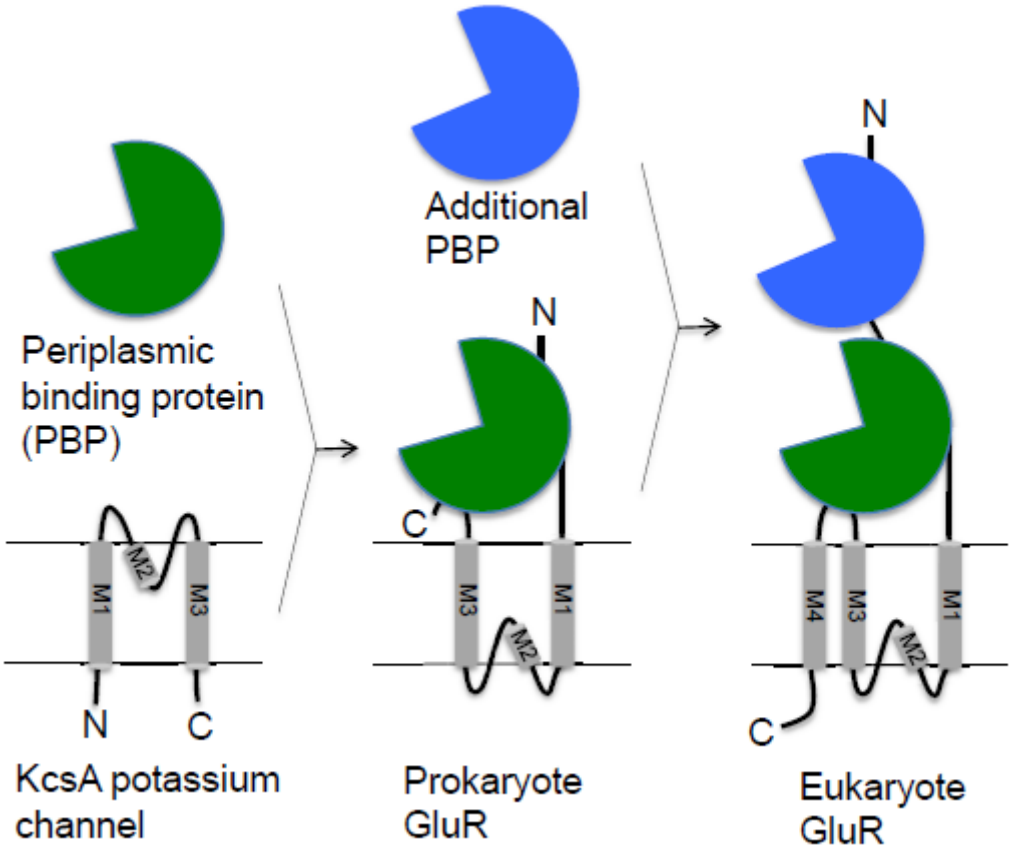

Figure 1-1. Schematic representations of prokaryotic and eukaryotic glutamate receptors. The proposed origins of ligand binding domain (LBD, green) and amino terminal domain (ATD, blue), and the channel domain. Bacterial periplasmic binding protein and potassium channel are shown for comparison. Proposed gene fusion events that gave rise to the eukaryotic glutamate receptors are represented by arrows. Figure as originally published in Price, M.B., J. Jelesko, and S. Okumoto (2012) Glutamate receptor homologs in plants: functions and evolutionary origins, Front Plant Sci 3:235. doi: 10.3389/fpls.2012.00235. Figure used with permission from *Frontiers in Plant Science*.

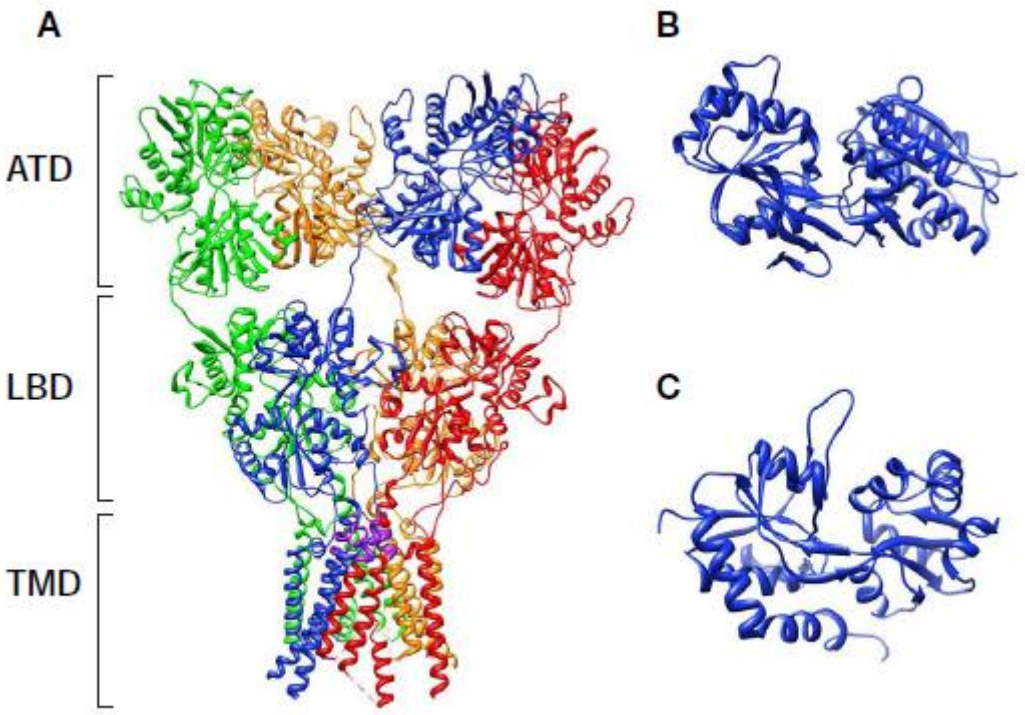

Figure 1-2. The crystal structure of the rat glutamate receptor GluA2.

(A) Structure of the intact channel (3KG2; (Sobolevsky, Rosconi et al. 2009)). Four subunits are shown in different colors. The "SYTANLAA" motif, which consists of the narrowest part of the channel in each subunit, is marked in purple. (B, C) The structures of isolated ATD (3H5V; (Jin, Singh et al. 2009)) and LBD (2UXA; (Greger, Akamine et al. 2006)), respectively. Note the "venus-flytrap" like structure in both domains. Figure as originally published in Price, M.B., J. Jelesko, and S. Okumoto (2012) Glutamate receptor homologs in plants: functions and evolutionary origins, Front Plant Sci 3:235. doi: 10.3389/fpls.2012.00235.

LITERATURE CITED

Ahn, C. S., J. A. Han, H. S. Lee, S. Lee and H. S. Pai (2011). "The PP2A regulatory subunit Tap46, a component of the TOR signaling pathway, modulates growth and metabolism in plants." Plant Cell **23**(1): 185-209.

Aoyama, K., M. Watabe and T. Nakaki (2008). "Regulation of neuronal glutathione synthesis." J Pharmacol Sci **108**(3): 227-238.

Arcondeguy, T., R. Jack and M. Merrick (2001). "P(II) signal transduction proteins, pivotal players in microbial nitrogen control." Microbiol Mol Biol Rev **65**(1): 80-105.

Armstrong, N. and E. Gouaux (2000). "Mechanisms for activation and antagonism of an AMPA-sensitive glutamate receptor: crystal structures of the GluR2 ligand binding core." Neuron **28**(1): 165-181.

Armstrong, N., Y. Sun, G. Q. Chen and E. Gouaux (1998). "Structure of a glutamate-receptor ligand-binding core in complex with kainate." Nature **395**(6705): 913-917.

Avruch, J., X. Long, S. Ortiz-Vega, J. Rapley, A. Papageorgiou and N. Dai (2009). "Amino acid regulation of TOR complex 1." Am J Physiol Endocrinol Metab **296**(4): E592-602.

Barbosa, J. M., N. K. Singh, J. H. Cherry and R. D. Locy (2010). "Nitrate uptake and utilization is modulated by exogenous gamma-aminobutyric acid in Arabidopsis thaliana seedlings." Plant Physiol Biochem **48**(6): 443-450.

Bauchart-Thevret, C., L. Cui, G. Wu and D. G. Burrin (2010). "Arginine-induced stimulation of protein synthesis and survival in IPEC-J2 cells is mediated by mTOR but not nitric oxide." Am J Physiol Endocrinol Metab **299**(6): E899-909.

Baud, S., A. B. Feria Bourrellier, M. Azzopardi, A. Berger, J. Dechorgnat, F. Daniel-Vedele, L. Lepiniec, M. Miquel, C. Rochat, M. Hodges and S. Ferrario-Mery (2010). "PII is induced by WRINKLED1 and fine-tunes fatty acid composition in seeds of Arabidopsis thaliana." Plant J **64**(2): 291-303.

Beauchamp, E. M. and L. C. Platanias (2012). "The evolution of the TOR pathway and its role in cancer." Oncogene.

Brenner, E. D., N. Martinez-Barboza, A. P. Clark, Q. S. Liang, D. W. Stevenson and G. M. Coruzzi (2000). "Arabidopsis mutants resistant to S(+)-beta-methyl-alpha, beta-diaminopropionic acid, a cycad-derived glutamate receptor agonist." Plant Physiol **124**(4): 1615-1624.

Chen, G. Q., C. Cui, M. L. Mayer and E. Gouaux (1999). "Functional characterization of a potassium-selective prokaryotic glutamate receptor." Nature **402**(6763): 817-821.

Cheung, M. Y., N. Y. Zeng, S. W. Tong, F. W. Li, K. J. Zhao, Q. Zhang, S. S. Sun and H. M. Lam (2007). "Expression of a RING-HC protein from rice improves resistance to Pseudomonas syringae pv. tomato DC3000 in transgenic Arabidopsis thaliana." J Exp Bot **58**(15-16): 4147-4159.

Chevrot, R., R. Rosen, E. Haudecoeur, A. Cirou, B. J. Shelp, E. Ron and D. Faure (2006). "GABA controls the level of quorum-sensing signal in Agrobacterium tumefaciens." Proc Natl Acad Sci U S A **103**(19): 7460-7464.

Chiu, J., R. DeSalle, H. M. Lam, L. Meisel and G. Coruzzi (1999). "Molecular evolution of glutamate receptors: a primitive signaling mechanism that existed before plants and animals diverged." Mol Biol Evol **16**(6): 826-838.

Chiu, J. C., E. D. Brenner, R. DeSalle, M. N. Nitabach, T. C. Holmes and G. M. Coruzzi (2002). "Phylogenetic and expression analysis of the glutamate-receptor-like gene family in Arabidopsis thaliana." Mol Biol Evol **19**(7): 1066-1082.

Connaughton, V. (1995). Glutamate and Glutamate Receptors in the Vertebrate Retina. Webvision: The Organization of the Retina and Visual System. H. Kolb, E. Fernandez and R. Nelson. Salt Lake City (UT).

Coutts, G., G. Thomas, D. Blakey and M. Merrick (2002). "Membrane sequestration of the signal transduction protein GlnK by the ammonium transporter AmtB." EMBO J **21**(4): 536-545.

Davenport, R. (2002). "Glutamate receptors in plants." Ann Bot **90**(5): 549-557.

Demidchik, V., P. A. Essah and M. Tester (2004). "Glutamate activates cation currents in the plasma membrane of Arabidopsis root cells." Planta **219**(1): 167-175.

Dennison, K. L. and E. P. Spalding (2000). "Glutamate-gated calcium fluxes in Arabidopsis." Plant Physiol **124**(4): 1511-1514.

Deprost, D., L. Yao, R. Sormani, M. Moreau, G. Leterreux, M. Nicolai, M. Bedu, C. Robaglia and C. Meyer (2007). "The Arabidopsis TOR kinase links plant growth, yield, stress resistance and mRNA translation." EMBO Rep **8**(9): 864-870.

Didion, T., B. Regenberg, M. U. Jorgensen, M. C. Kielland-Brandt and H. A. Andersen (1998). "The permease homologue Ssy1p controls the expression of amino acid and peptide transporter genes in Saccharomyces cerevisiae." Mol Microbiol **27**(3): 643-650.

Dingledine, R., K. Borges, D. Bowie and S. F. Traynelis (1999). "The glutamate receptor ion channels." Pharmacol Rev **51**(1): 7-61.

Doyle, D. A., J. Morais Cabral, R. A. Pfuetzner, A. Kuo, J. M. Gulbis, S. L. Cohen, B. T. Chait and R. MacKinnon (1998). "The structure of the potassium channel: molecular basis of K+ conduction and selectivity." Science **280**(5360): 69-77.

Dringen, R. (2000). "Metabolism and functions of glutathione in brain." Prog Neurobiol **62**(6): 649-671.

Dubos, C., D. Huggins, G. H. Grant, M. R. Knight and M. M. Campbell (2003). "A role for glycine in the gating of plant NMDA-like receptors." Plant J **35**(6): 800-810.

Dubos, C., J. Willment, D. Huggins, G. H. Grant and M. M. Campbell (2005). "Kanamycin reveals the role played by glutamate receptors in shaping plant resource allocation." Plant J **43**(3): 348-355.

Dubreuil-Maurizi, C. and B. Poinssot (2012). "Role of glutathione in plant signaling under biotic stress." Plant Signal Behav **7**(2): 210-212.

Duran, R. V. and M. N. Hall (2012). "Regulation of TOR by small GTPases." EMBO Rep **13**(2): 121-128.

Efeyan, A., R. Zoncu, S. Chang, I. Gumper, H. Snitkin, R. L. Wolfson, O. Kirak, D. D. Sabatini and D. M. Sabatini (2013). "Regulation of mTORC1 by the Rag GTPases is necessary for neonatal autophagy and survival." Nature **493**(7434): 679-683.

Efeyan, A., R. Zoncu and D. M. Sabatini (2012). "Amino acids and mTORC1: from lysosomes to disease." Trends Mol Med **18**(9): 524-533.

Egebjerg, J. and S. F. Heinemann (1993). "Ca2+ permeability of unedited and edited versions of the kainate selective glutamate receptor GluR6." Proc Natl Acad Sci U S A **90**(2): 755-759.

Feria Bourrellier, A. B., B. Valot, A. Guillot, F. Ambard-Bretteville, J. Vidal and M. Hodges (2010). "Chloroplast acetyl-CoA carboxylase activity is 2-oxoglutarate-regulated by interaction of PII with the biotin carboxyl carrier subunit." Proc Natl Acad Sci U S A **107**(1): 502-507.

Ferrario-Mery, S., E. Besin, O. Pichon, C. Meyer and M. Hodges (2006). "The regulatory PII protein controls arginine biosynthesis in Arabidopsis." FEBS Lett **580**(8): 2015-2020.

Forchhammer, K. (2004). "Global carbon/nitrogen control by PII signal transduction in cyanobacteria: from signals to targets." FEMS Microbiol Rev **28**(3): 319-333.

Franchi-Gazzola, R., V. Dall'Asta, R. Sala, R. Visigalli, E. Bevilacqua, F. Gaccioli, G. C. Gazzola and O. Bussolati (2006). "The role of the neutral amino acid transporter SNAT2 in cell volume regulation." Acta Physiol (Oxf) **187**(1-2): 273-283.

Fritz, C., C. Mueller, P. Matt, R. Feil and M. Stitt (2006). "Impact of the C-N status on the amino acid profile in tobacco source leaves." Plant Cell Environ **29**(11): 2055-2076.

Furukawa, H., S. K. Singh, R. Mancusso and E. Gouaux (2005). "Subunit arrangement and function in NMDA receptors." Nature **438**(7065): 185-192.

Gaccioli, F., C. C. Huang, C. Wang, E. Bevilacqua, R. Franchi-Gazzola, G. C. Gazzola, O. Bussolati, M. D. Snider and M. Hatzoglou (2006). "Amino acid starvation induces the SNAT2

neutral amino acid transporter by a mechanism that involves eukaryotic initiation factor 2alpha phosphorylation and cap-independent translation." J Biol Chem **281**(26): 17929-17940.

Gereau, R. W. and G. Swanson (2008). The Glutamate Receptors. New York, Humana Press.

Greger, I. H., P. Akamine, L. Khatri and E. B. Ziff (2006). "Developmentally regulated, combinatorial RNA processing modulates AMPA receptor biogenesis." Neuron **51**(1): 85-97.

Gutierrez, R. A., T. L. Stokes, K. Thum, X. Xu, M. Obertello, M. S. Katari, M. Tanurdzic, A. Dean, D. C. Nero, C. R. McClung and G. M. Coruzzi (2008). "Systems approach identifies an organic nitrogen-responsive gene network that is regulated by the master clock control gene CCA1." Proc Natl Acad Sci U S A **105**(12): 4939-4944.

Hara, K., K. Yonezawa, Q. P. Weng, M. T. Kozlowski, C. Belham and J. Avruch (1998). "Amino acid sufficiency and mTOR regulate p70 S6 kinase and eIF-4E BP1 through a common effector mechanism." J Biol Chem **273**(23): 14484-14494.

Haudecoeur, E., S. Planamente, A. Cirou, M. Tannieres, B. J. Shelp, S. Morera and D. Faure (2009). "Proline antagonizes GABA-induced quenching of quorum-sensing in Agrobacterium tumefaciens." Proc Natl Acad Sci U S A **106**(34): 14587-14592.

Hay, N. and N. Sonenberg (2004). "Upstream and downstream of mTOR." Genes Dev **18**(16): 1926-1945.

Hirner, A., F. Ladwig, H. Stransky, S. Okumoto, M. Keinath, A. Harms, W. B. Frommer and W. Koch (2006). "Arabidopsis LHT1 is a high-affinity transporter for cellular amino acid uptake in both root epidermis and leaf mesophyll." Plant Cell **18**(8): 1931-1946.

Ho, C. H., S. H. Lin, H. C. Hu and Y. F. Tsay (2009). "CHL1 functions as a nitrate sensor in plants." Cell **138**(6): 1184-1194.

Hosie, A. H., D. Allaway, C. S. Galloway, H. A. Dunsby and P. S. Poole (2002). "Rhizobium leguminosarum has a second general amino acid permease with unusually broad substrate specificity and high similarity to branched-chain amino acid transporters (Bra/LIV) of the ABC family." J Bacteriol **184**(15): 4071-4080.

Hsieh, M. H., H. M. Lam, F. J. van de Loo and G. Coruzzi (1998). "A PII-like protein in Arabidopsis: putative role in nitrogen sensing." Proc Natl Acad Sci U S A **95**(23): 13965-13970.

Hundal, H. S. and P. M. Taylor (2009). "Amino acid transceptors: gate keepers of nutrient exchange and regulators of nutrient signaling." Am J Physiol Endocrinol Metab **296**(4): E603-613.

Jacinto, E. and M. N. Hall (2003). "Tor signalling in bugs, brain and brawn." Nat Rev Mol Cell Biol **4**(2): 117-126.

Jewell, J. L., R. C. Russell and K. L. Guan (2013). "Amino acid signalling upstream of mTOR." Nat Rev Mol Cell Biol **14**(3): 133-139.

Jin, R., S. K. Singh, S. Gu, H. Furukawa, A. I. Sobolevsky, J. Zhou, Y. Jin and E. Gouaux (2009). "Crystal structure and association behaviour of the GluR2 amino-terminal domain." EMBO J **28**(12): 1812-1823.

Juurlink, B. H. (1999). "Management of oxidative stress in the CNS: the many roles of glutathione." Neurotox Res **1**(2): 119-140.

Kandel, E. R., J. H. Schwartz and T. M. Jessell (2000). Principles of Neural Science. New York, McGraw-Hill.

Kang, J., S. Mehta and F. J. Turano (2004). "The putative glutamate receptor 1.1 (AtGLR1.1) in Arabidopsis thaliana regulates abscisic acid biosynthesis and signaling to control development and water loss." Plant Cell Physiol **45**(10): 1380-1389.

Kang, J. and F. J. Turano (2003). "The putative glutamate receptor 1.1 (AtGLR1.1) functions as a regulator of carbon and nitrogen metabolism in Arabidopsis thaliana." Proc Natl Acad Sci U S A **100**(11): 6872-6877.

Kang, S., H. B. Kim, H. Lee, J. Y. Choi, S. Heu, C. J. Oh, S. I. Kwon and C. S. An (2006). "Overexpression in Arabidopsis of a plasma membrane-targeting glutamate receptor from small radish increases glutamate-mediated Ca2+ influx and delays fungal infection." Mol Cells **21**(3): 418-427.

Karakas, E., N. Simorowski and H. Furukawa (2011). "Subunit arrangement and phenylethanolamine binding in GluN1/GluN2B NMDA receptors." Nature **475**(7355): 249-253.

Kim, D. H., D. D. Sarbassov, S. M. Ali, J. E. King, R. R. Latek, H. Erdjument-Bromage, P. Tempst and D. M. Sabatini (2002). "mTOR interacts with raptor to form a nutrient-sensitive complex that signals to the cell growth machinery." Cell **110**(2): 163-175.

Kim, D. H., D. D. Sarbassov, S. M. Ali, R. R. Latek, K. V. Guntur, H. Erdjument-Bromage, P. Tempst and D. M. Sabatini (2003). "GbetaL, a positive regulator of the rapamycin-sensitive pathway required for the nutrient-sensitive interaction between raptor and mTOR." Mol Cell **11**(4): 895-904.

Kim, S. A., J. M. Kwak, S. K. Jae, M. H. Wang and H. G. Nam (2001). "Overexpression of the AtGluR2 gene encoding an Arabidopsis homolog of mammalian glutamate receptors impairs calcium utilization and sensitivity to ionic stress in transgenic plants." Plant Cell Physiol **42**(1): 74-84.

Kumar, J., P. Schuck and M. L. Mayer (2011). "Structure and assembly mechanism for heteromeric kainate receptors." Neuron **71**(2): 319-331.

Kwaaitaal, M., R. Huisman, J. Maintz, A. Reinstadler and R. Panstruga (2011). "Ionotropic glutamate receptor (iGluR)-like channels mediate MAMP-induced calcium influx in Arabidopsis thaliana." Biochem J **440**(3): 355-365.

Lam, H. M., Y. A. Chiao, M. W. Li, Y. K. Yung and S. Ji (2006). "Putative nitrogen sensing systems in higher plants." Journal of Integrative Plant Biology **48**(8): 873-888.

Lam, H. M., J. Chiu, M. H. Hsieh, L. Meisel, I. C. Oliveira, M. Shin and G. Coruzzi (1998). "Glutamate-receptor genes in plants." Nature **396**(6707): 125-126.

Leigh, J. A. and J. A. Dodsworth (2007). "Nitrogen regulation in bacteria and archaea." Annu Rev Microbiol **61**: 349-377.

Levy, D. I., N. J. Sucher and S. A. Lipton (1991). "Glutathione prevents N-methyl-D-aspartate receptor-mediated neurotoxicity." Neuroreport **2**(6): 345-347.

Li, F., J. Wang, C. Ma, Y. Zhao, Y. Wang, A. Hasi and Z. Qi (2013). "Glutamate Receptor Like Channel 3.3 is involved in mediating glutathione-triggered cytosolic Ca2+ transients, transcriptional changes and innate immunity responses in Arabidopsis." Plant Physiol.

Lipton, S. A., W. K. Kim, Y. B. Choi, S. Kumar, D. M. D'Emilia, P. V. Rayudu, D. R. Arnelle and J. S. Stamler (1997). "Neurotoxicity associated with dual actions of homocysteine at the N-methyl-D-aspartate receptor." Proc Natl Acad Sci U S A **94**(11): 5923-5928.

MacKinnon, R. (2003). "Potassium channels." FEBS Lett **555**(1): 62-65.

MacKintosh, C. (1992). "Regulation of spinach-leaf nitrate reductase by reversible phosphorylation." Biochim Biophys Acta **1137**(1): 121-126.

Maheswaran, M., C. Urbanke and K. Forchhammer (2004). "Complex formation and catalytic activation by the PII signaling protein of N-acetyl-L-glutamate kinase from Synechococcus elongatus strain PCC 7942." J Biol Chem **279**(53): 55202-55210.

Mano, I. and V. I. Teichberg (1998). "A tetrameric subunit stoichiometry for a glutamate receptor-channel complex." Neuroreport **9**(2): 327-331.

Marschner, H. (1997). Functions of Mineral Nutrients: Macronutrients Mineral Nutrition of Higher Plants. San Diego, CA, Academic Press Inc**:** 231-254.

Mayer, M. L. (2005). "Glutamate receptor ion channels." Curr Opin Neurobiol **15**(3): 282-288.

Mayer, M. L. (2011). "Emerging models of glutamate receptor ion channel structure and function." Structure **19**(10): 1370-1380.

Menand, B., T. Desnos, L. Nussaume, F. Berger, D. Bouchez, C. Meyer and C. Robaglia (2002). "Expression and disruption of the Arabidopsis TOR (target of rapamycin) gene." Proc Natl Acad Sci U S A **99**(9): 6422-6427.

Meyerhoff, O., K. Muller, M. R. Roelfsema, A. Latz, B. Lacombe, R. Hedrich, P. Dietrich and D. Becker (2005). "AtGLR3.4, a glutamate receptor channel-like gene is sensitive to touch and cold." Planta **222**(3): 418-427.

Michard, E., P. T. Lima, F. Borges, A. C. Silva, M. T. Portes, J. E. Carvalho, M. Gilliham, L. H. Liu, G. Obermeyer and J. A. Feijo (2011). "Glutamate receptor-like genes form Ca2+ channels in pollen tubes and are regulated by pistil D-serine." Science **332**(6028): 434-437.

Miller, A. J., X. Fan, Q. Shen and S. J. Smith (2008). "Amino acids and nitrate as signals for the regulation of nitrogen acquisition." Journal of Experimental Botany **59**(1): 111-119.

Mishina, T. E. and J. Zeier (2007). "Bacterial non-host resistance: interactions of Arabidopsis with non-adapted Pseudomonas syringae strains." Physiol Plant **131**(3): 448-461.

Mizuno, Y., G. B. Moorhead and K. K. Ng (2007). "Structural basis for the regulation of N-acetylglutamate kinase by PII in Arabidopsis thaliana." J Biol Chem **282**(49): 35733-35740.

Monyer, H., R. Sprengel, R. Schoepfer, A. Herb, M. Higuchi, H. Lomeli, N. Burnashev, B. Sakmann and P. H. Seeburg (1992). "Heteromeric NMDA receptors: molecular and functional distinction of subtypes." Science **256**(5060): 1217-1221.

Moreno-Risueno, M. A., J. M. Van Norman, A. Moreno, J. Zhang, S. E. Ahnert and P. N. Benfey (2010). "Oscillating gene expression determines competence for periodic Arabidopsis root branching." Science **329**(5997): 1306-1311.

Nakanishi, N., N. A. Shneider and R. Axel (1990). "A family of glutamate receptor genes: evidence for the formation of heteromultimeric receptors with distinct channel properties." Neuron **5**(5): 569-581.

Naur, P., B. Vestergaard, L. K. Skov, J. Egebjerg, M. Gajhede and J. S. Kastrup (2005). "Crystal structure of the kainate receptor GluR5 ligand-binding core in complex with (S)-glutamate." FEBS Lett **579**(5): 1154-1160.

Nazoa, P., J. J. Vidmar, T. J. Tranbarger, K. Mouline, I. Damiani, P. Tillard, D. Zhuo, A. D. Glass and B. Touraine (2003). "Regulation of the nitrate transporter gene AtNRT2.1 in Arabidopsis thaliana: responses to nitrate, amino acids and developmental stage." Plant Mol Biol **52**(3): 689-703.

Nicklin, P., P. Bergman, B. Zhang, E. Triantafellow, H. Wang, B. Nyfeler, H. Yang, M. Hild, C. Kung, C. Wilson, V. E. Myer, J. P. MacKeigan, J. A. Porter, Y. K. Wang, L. C. Cantley, P. M. Finan and L. O. Murphy (2009). "Bidirectional transport of amino acids regulates mTOR and autophagy." Cell **136**(3): 521-534.

Oja, S. S., R. Janaky, V. Varga and P. Saransaari (2000). "Modulation of glutamate receptor functions by glutathione." Neurochem Int **37**(2-3): 299-306.

Oliveira, I. C., E. Brenner, J. Chiu, M. H. Hsieh, A. Kouranov, H. M. Lam, M. J. Shin and G. Coruzzi (2001). "Metabolite and light regulation of metabolism in plants: lessons from the study of a single biochemical pathway." Braz J Med Biol Res **34**(5): 567-575.

Osanai, T. and K. Tanaka (2007). "Keeping in touch with PII: PII-interacting proteins in unicellular cyanobacteria." Plant Cell Physiol **48**(7): 908-914.

Parisy, V., B. Poinssot, L. Owsianowski, A. Buchala, J. Glazebrook and F. Mauch (2007). "Identification of PAD2 as a gamma-glutamylcysteine synthetase highlights the importance of glutathione in disease resistance of Arabidopsis." Plant J **49**(1): 159-172.

Pasternack, A., S. K. Coleman, A. Jouppila, D. G. Mottershead, M. Lindfors, M. Pasternack and K. Keinanen (2002). "Alpha-amino-3-hydroxy-5-methyl-4-isoxazolepropionic acid (AMPA) receptor channels lacking the N-terminal domain." J Biol Chem **277**(51): 49662-49667.

Qi, Z., N. R. Stephens and E. P. Spalding (2006). "Calcium entry mediated by GLR3.3, an Arabidopsis glutamate receptor with a broad agonist profile." Plant Physiol **142**(3): 963-971.

Rawat, S. R., S. N. Silim, H. J. Kronzucker, M. Y. Siddiqi and A. D. Glass (1999). "AtAMT1 gene expression and NH4+ uptake in roots of Arabidopsis thaliana: evidence for regulation by root glutamine levels." Plant J **19**(2): 143-152.

Rentsch, D., S. Schmidt and M. Tegeder (2007). "Transporters for uptake and allocation of organic nitrogen compounds in plants." FEBS Lett **581**(12): 2281-2289.

Ritter, C. and J. L. Dangl (1995). "The avrRpm1 gene of Pseudomonas syringae pv. maculicola is required for virulence on Arabidopsis." Mol Plant Microbe Interact **8**(3): 444-453.

Robaglia, C., M. Thomas and C. Meyer (2012). "Sensing nutrient and energy status by SnRK1 and TOR kinases." Curr Opin Plant Biol **15**(3): 301-307.

Rosenmund, C., Y. Stern-Bach and C. F. Stevens (1998). "The tetrameric structure of a glutamate receptor channel." Science **280**(5369): 1596-1599.

Roy, S. J., M. Gilliham, B. Berger, P. A. Essah, C. Cheffings, A. J. Miller, R. J. Davenport, L. H. Liu, M. J. Skynner, J. M. Davies, P. Richardson, R. A. Leigh and M. Tester (2008). "Investigating glutamate receptor-like gene co-expression in Arabidopsis thaliana." Plant Cell Environ **31**(6): 861-871.

Schwartz, J. H. (2000). Many Neuroactive Peptides Serve as Neuotransmitters. Principles of Neural Science. E. R. Kandel, J. H. Schwartz and T. M. Jessell. New York, McGraw-Hill**:** 280-296.

Schwartz, J. H. (2000). Many Neuroactive Peptides Serve as Transmitters. Principles of Neural Science. E. R. Kandel, Schwartz, J. H., Jessell, T.M. New York, McGraw-Hill**:** 280-296.

Sobolevsky, A. I., M. P. Rosconi and E. Gouaux (2009). "X-ray structure, symmetry and mechanism of an AMPA-subtype glutamate receptor." Nature **462**(7274): 745-756.

Solomon, P. S. and R. P. Oliver (2001). "The nitrogen content of the tomato leaf apoplast increases during infection by Cladosporium fulvum." Planta **213**(2): 241-249.

Stephens, N. R., Z. Qi and E. P. Spalding (2008). "Glutamate receptor subtypes evidenced by differences in desensitization and dependence on the GLR3.3 and GLR3.4 genes." Plant Physiol **146**(2): 529-538.

Sulieman, S., S. A. Fischinger, P. M. Gresshoff and J. Schulze (2010). "Asparagine as a major factor in the N-feedback regulation of N2 fixation in Medicago truncatula." Physiol Plant **140**(1): 21-31.

Swarbreck, S., R. Colaco and J. Davies (2013). "Plant calcium-permeable channels." Plant Physiol.

Taiz L, Z. E. (2006). Plant Physiology. Sunderland, Massachusetts, Sinauer Associates.

Tapken, D., U. Anschutz, L. H. Liu, T. Huelsken, G. Seebohm, D. Becker and M. Hollmann (2013). "A plant homolog of animal glutamate receptors is an ion channel gated by multiple hydrophobic amino acids." Sci Signal **6**(279): ra47.

Tapken, D. and M. Hollmann (2008). "Arabidopsis thaliana glutamate receptor ion channel function demonstrated by ion pore transplantation." J Mol Biol **383**(1): 36-48.

Thilmony, R., W. Underwood and S. Y. He (2006). "Genome-wide transcriptional analysis of the Arabidopsis thaliana interaction with the plant pathogen Pseudomonas syringae pv. tomato DC3000 and the human pathogen Escherichia coli O157:H7." Plant J **46**(1): 34-53.

Vidal, E. A. and R. A. Gutierrez (2008). "A systems view of nitrogen nutrient and metabolite responses in Arabidopsis." Current Opinion in Plant Biology **11**(5): 521-529.

Vincentz, M., T. Moureaux, M. T. Leydecker, H. Vaucheret and M. Caboche (1993). "Regulation of Nitrate and Nitrite Reductase Expression in Nicotiana-Plumbaginifolia Leaves by Nitrogen and Carbon Metabolites." Plant Journal **3**(2): 315-324.

Vincill, E. D., A. M. Bieck and E. P. Spalding (2012). "Ca(2+) conduction by an amino acid-gated ion channel related to glutamate receptors." Plant Physiol **159**(1): 40-46.

Vincill, E. D., A. E. Clarin, J. N. Molenda and E. P. Spalding (2013). "Interacting Glutamate Receptor-Like Proteins in Phloem Regulate Lateral Root Initiation in Arabidopsis." Plant Cell.

Wipf, D., U. Ludewig, M. Tegeder, D. Rentsch, W. Koch and W. B. Frommer (2002). "Conservation of amino acid transporters in fungi, plants and animals." Trends in Biochemical Sciences **27**(3): 139-147.

Wullschleger, S., R. Loewith and M. N. Hall (2006). "TOR signaling in growth and metabolism." Cell **124**(3): 471-484.

Yu, G., J. Liang, Z. He and M. Sun (2006). "Quantum dot-mediated detection of gamma-aminobutyric acid binding sites on the surface of living pollen protoplasts in tobacco." Chem Biol **13**(7): 723-731.

Zimmermann, P., M. Hirsch-Hoffmann, L. Hennig and W. Gruissem (2004). "GENEVESTIGATOR. Arabidopsis microarray database and analysis toolbox." Plant Physiol **136**(1): 2621-2632.

Zuo, J., P. L. De Jager, K. A. Takahashi, W. Jiang, D. J. Linden and N. Heintz (1997). "Neurodegeneration in Lurcher mice caused by mutation in delta2 glutamate receptor gene." Nature **388**(6644): 769-773.

CHAPTER 2:EVOLUTIONARY ORIGIN OF PLANT GLUTAMATE RECEPTORS

Some of the content of this chapter was published in *Frontiers in Plant Science* and is made available as an electronic reprint with the permission of the journal. The paper can be found at the following URL on the Frontiers website:
http://www.frontiersin.org/Journal/Abstract.aspx?ART_DOI=10.3389/fpls.2012.00235&name=plant_traffic_and_transport

INTRODUCTION

In this short chapter, the evolutionary origin of plant GLRs is examined using deep-phylogeny analysis. As mentioned in Chapter 1, main structural components (amino-terminal domain, ligand-binding domain, and three and half transmembrane domains) are conserved between plant and animal glutamate receptors. In addition, at least two GLRs from plants were confirmed to be amino acid gated channels (Vincill, Bieck et al. 2012, Tapken, Anschutz et al. 2013). Therefore, it is likely that some of the sensory mechanisms, through which GLRs bind to amino acid and conduct cations, are conserved between plants and animals.

Prior phylogenetic analysis using both parsimony and neighbor joining suggests that plant and animal glutamate receptors diverged from a common ancestor as opposed to convergent evolution of genes with similar structure and function (Chiu, DeSalle et al. 1999). Examination of amino acid sequence similarity between plant GLRs and various kinds of ion channels such as animal ionotropic glutamate receptors (iGluRs), potassium channels, acetylcholine receptors, and $GABA_A$ receptors suggested that the plant GLRs are most closely

related to animal iGluRs (Chiu, DeSalle et al. 1999, Chiu, Brenner et al. 2002), although their N-terminus might share common ancestor with $GABA_B$ receptors as well (Turano, Panta et al. 2001). Meanwhile, GLR-like proteins which lack the amino-terminal domain are also found in bacteria, including cyanobacteria (Mayer, Olson et al. 2001, Price, Jelesko et al. 2012). Phylogenetic relationships between glutamate receptor homologs in all three kingdoms have not been examined thus far in literature. Tremendous advance in massively parallel sequencing made far greater number of genome sequences available compared to the time the above studies were published, making deeper and more precise phylogenetic analyses possible.

Therefore, we performed a comprehensive analysis using the full genomic sequences of plant GLRs in order to achieve better phylogenetic placement. In particular, phylogenetic distance between plant and cyanobacterial GLRs were compared to examine whether the plant GLRs could have derived from cyanobacterial ancestor of chloroplasts.

RESULTS AND DISCUSSION

The deep phylogenetic relationships between plants, metazoans, and bacteria GLRs were investigated using statistically-oriented phylogenetic methods that are amenable to formal hypothesis testing of alternative molecular evolution models. GLR homologs were identified using the AtGLR1.1 and the human NMDA receptor NR1-3 sequences as queries using a sensitive similarity search algorithm (SSEARCH) enforcing a criteria for establishing homology(i.e. common ancestry) that combined both a maximum expectation value of e^{-4} and mutual hits by both query sequences. A bootstrap Maximum Likelihood (ML) phylogenetic analysis indicated a tripartite basal split between bacterial, plant, and other eukaryotic GLR homologs (Figure 2-1)(Price, Jelesko et al. 2012). This topology had good bootstrap support and

was generally consistent with the separation of bacteria from eukaryotes in the tree of life (ToL), in agreement with previously published results (Janovjak, Sandoz et al. 2011). Cyanobacterial glutamate receptors clustered tightly with other bacterial homologs, suggesting against the possibility that the plant glutamate receptors have a cyanobacterial origin. The hypothesis of a cyanobacterial origin of plant GLRs was also statistically rejected by likelihood ratio testing of phylogenetic analyses using alternatively constrained topologies (Table 2-1)(Price, Jelesko et al. 2012).

The basal positioning of the plant GLR homologs relative to other eukaryotic GLR homologs was also consistent with a very ancient separation of plant GLRs from other eukaryotic GLRs. Indeed, likelihood ratio testing indicated that a model of monophyletic plant-eukaryotic association was not a statistically significant better fit to the data than either monophyletic plant-bacteria association or monophyletic eukaryotic-bacteria association models (Table 2-1)(Price, Jelesko et al. 2012). Thus, plant GLRs were no more closely related to eukaryotic GluR homologs than either the plant or mammalian GluRs were to the bacterial GluRs. These results indicate a very ancient separation of plant, eukaryotic, and bacterial GLRs that dates back to perhaps as far as the separation of the last universal common ancestor (LUCA) in the ToL, or to the very early evolution of the Eukaryotic domain. The GLR molecular evolutionary model is consistent with the current placement of the Plantae (Archeaplastids) as one of the five super-groups of eukaryote taxonomy (Simpson and Roger 2002, Adl, Simpson et al. 2005, Keeling, Burger et al. 2005). Thus, the plant GLR homologs should be considered as phylogenetically distinct from metazoan GLRs as they are from the bacterial GLRs.

Among plant GLRs, that Clade 1 from plant GLRs only included genes from *Arabidopsis thaliana* and its close relative, *Arabidopsis lyrata*. In order to investigate whether the Clade 1

genes are indeed specific to close relatives of Arabidopsis, an additional phylogenetic analysis was performed. Additional homologs of *At*GLR1.1 were searched in Plant Genome Database (http://www.plantgdb.org/), which includes predicted protein annotations from whole genome shotgun sequences (WGS) that are not included in RefSeq protein database. Predicted protein sequences from the genomes of *Brachypodium distachyon, Brassica rapa, Celtis bungeana, Gossypium hirsutum, Glycine max, Hordeum vulgare, Lotus Japonicas, Oriza sativa, Poplus trichocarpa, Sorghum bicolor, Setaria italica, Triticum aestivum, Solanum lycopersicum,* and *Zea mays* were queried with *At*GLR1.1 protein sequence using SSEARCH with the same parameters (maximum expectation value of e^{-4}). All sequences that had maximum expectation value higher than AtGLR2.5, which is distinctly placed in Clade 2, were included in the phylogenetic analysis. Figure 2.2 shows the result of expanded phylogenetic analysis (Price, Jelesko et al. 2012). Interestingly, the result shows that GLR1 is part of a very derived and well-supported clade comprised of paralogs that are found only in the Brassicas. Whether Clade 1 GLRs have evolved distinct roles in this order of plants remains to be investigated.

MATERIALS AND METHODS

Homologous GLR-like sequences were identified using methods that emphasize mutual protein sequences identified in SSEARCHs using well accepted related GLR query sequences (Jelesko 2012). Specifically, the *At*GLR1.1 protein sequences (Genbank NM_111282) and the human glutamate receptor variant NR1-3 (Genbank NM_007327) were used to query a local Genbank RefSeq protein database (April 6, 2012) using SSEARCH (Pearson 1996). Protein sequences with expectation values of e^{-4} and smaller were initially selected, and 1,277 sequences were present in both SSEARCHs, thereby defining the initial "GLR-like" sequences. In order to

reduce the computational complexity of the phylogenetic analysis, but not bias the overall sampling of GLR-like phylogenetic diversity, every fourth initial GLR-like sequence was selected. Apparent fast evolving GLR sequences were deleted to avoid long branch attraction artifacts (Felsenstein 1978, Bergsten 2005). This resulted in a final dataset of 321 sequences with GenBank accessions listed in Table 2-2, which were aligned using MAFFT (Katoh, Kuma et al. 2005). ProtTest v 3.0 (Darriba, Taboada et al. 2011) identified the optimal evolutionary model as WAG+I+G+F. One hundred unconstrained Maximum Likelihood (ML) phylogenetic analyses were performed using GARLI v. 2.0 (Zwickl 2006). The imposed phylogenetic constraints were as follows: plant with bacteria, eukaryotes with bacteria, plants with eukaryotes, and plants with cyanobacteria. One hundred ML analyses were performed for each constraint and the best Ln Likelihood (LnL) value from each constraint were compared using the Likelihood Ratio Test fitted to a Chi-squared distribution to assign P-values to the alternative pair-wise phylogenetic hypotheses.

FIGURES

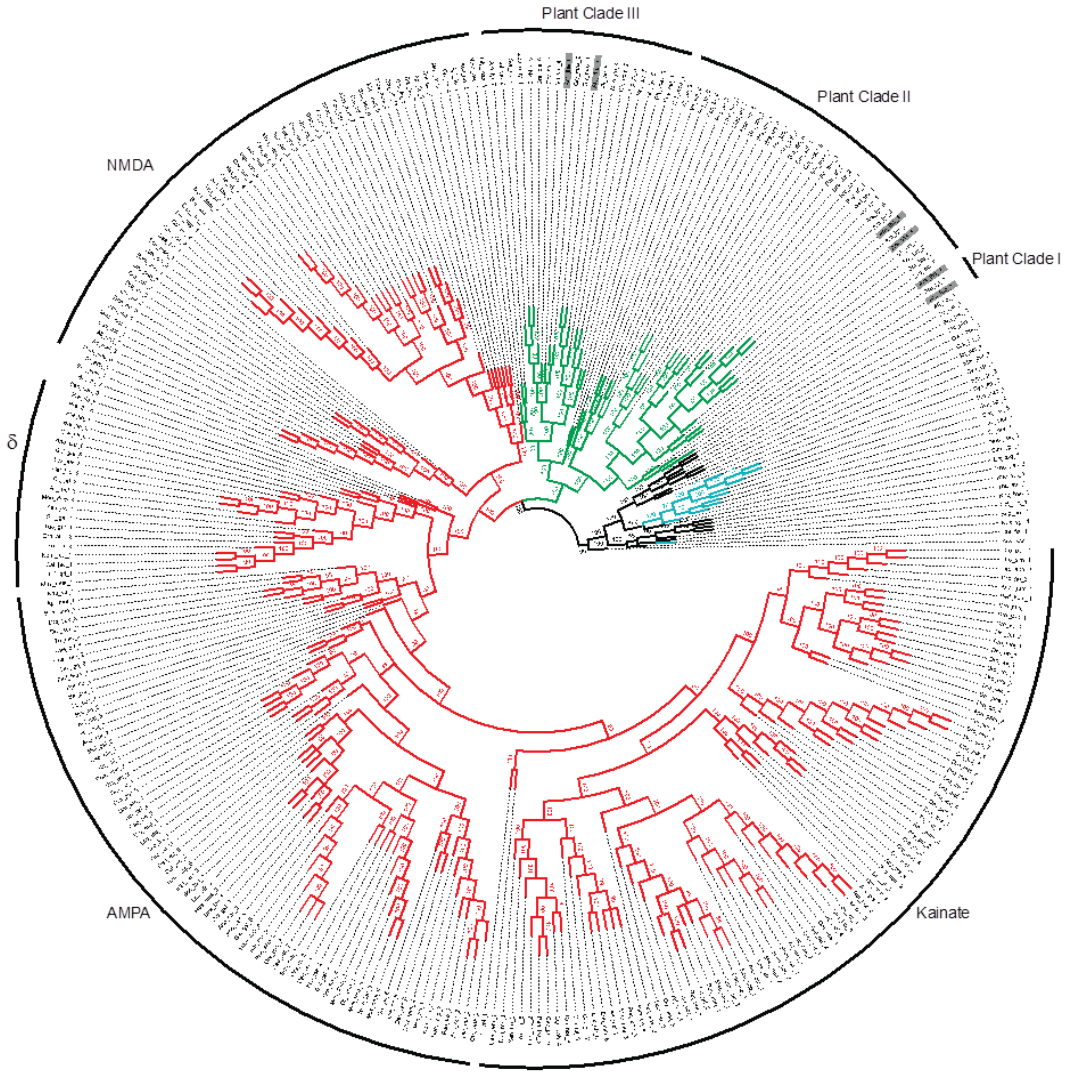

Figure 2-1. Phylogenetic tree of plant, animal, and bacterial glutamate receptors. Metazoan, bacteria, cyanobacteria, plant proteins are marked in red, black, cyan, and green, respectively. NMDA, AMPA, and Kainate subfamilies of mammalian receptors are also indicated. Figure as originally published in Price, M.B., J. Jelesko, and S. Okumoto (2012) Glutamate receptor homologs in plants: functions and evolutionary origins, Front Plant Sci

3:235. doi: 10.3389/fpls.2012.00235. Figure used with permission from *Frontiers in Plant Science*.

Figure 2-2. Extended phylogenetic tree including additional plant GLRs.

GLR1 paralogs that are found only in the Brassicas. Color coding of organisms are the same as that in Figure 2.1.

TABLES

Table 2-1. Likelihood Ratio Testing of Alternative Phylogenetic Models.

Alternative constrained phylogenetic models	2*ΔLnL	P-value
Monophyletic Plants with Eukaryotes vs. Unconstrained	0.00233	0.9617
Monophyletic Plants with Eukaryotes vs. Monophyletic Eukaryotes with Bacteria	0.00000	1.0000
Monophyletic Plants with Eukaryotes vs. Monophyletic Plants with Bacteria	0.00000	1.0000
Monophyletic Plants with Eukaryotes vs. Monophyletic Plants with Cyanobacteria	348.0987	<0.0001

The optimal LnL score from 100 replicate ML phylogenetic analyses enforcing a particular monophyletic constraint was compared to that enforcing a different phylogenetic constraint using the Ln Likelihood Ratio Test, fit to a Chi-squared distribution with one degree of freedom. Monophyletic plants with eukaryotes constituted the null hypothesis. Table as originally published in Price, M.B., J. Jelesko, and S. Okumoto (2012) Glutamate receptor homologs in plants: functions and evolutionary origins, Front Plant Sci 3:235. doi: 10.3389/fpls.2012.

Table 2-2. Genbank Accessions and published protein names for GLR-Like sequences used in Figure 2-1.

GLR-like code:	Published protein names:	Genbank ID:	Species:
Ara_tha_1	GLR1.1	NP_187061.1	Arabidopsis thaliana
Ara_lyr_1	GLR1.3	XP_002863896.1	Arabidopsis lyrata subsp. lyrata
Ara_tha_2	GLR1.4	NP_187408.2	Arabidopsis thaliana
Ara_lyr_2		XP_002863052.1	Arabidopsis lyrata subsp. lyrata
Vit_vin_1		XP_002271013.2	Vitis vinifera
Ara_tha_3	GLR2.7	NP_180476.3	Arabidopsis thaliana
Ric_com_1	GLR2	XP_002515378.1	Ricinus communis
Pop_tri_1	GluR5	XP_002332797.1	Populus trichocarpa
Med_tru_1	GLR2.8	XP_003603256.1	Medicago truncatula
Sor_bic_1		XP_002452948.1	Sorghum bicolor
Bra_dis_1		XP_003572886.1	Brachypodium distachyon
Bra_dis_2		XP_003576552.1	Brachypodium distachyon
Bra_dis_3		XP_003572831.1	Brachypodium distachyon
Bra_dis_4		XP_003566802.1	Brachypodium distachyon
Ara_lyr_3	GLR2.2	XP_002880616.1	Arabidopsis lyrata subsp. lyrata
Bra_dis_5		XP_003560389.1	Brachypodium distachyon
Ory_sat_1		NP_001063236.1	Oryza sativa Japonica Group
Pop_tri_2	GluR5	XP_002324493.1	Populus trichocarpa
Gly_max_1		XP_003528564.1	Glycine max
Vit_vin_2		XP_002282936.1	Vitis vinifera
Ara_lyr_4	GLR2.1	XP_002867285.1	Arabidopsis lyrata subsp. lyrata
Vit_vin_3		XP_002282943.2	Vitis vinifera
Sor_bic_2		XP_002453646.1	Sorghum bicolor
Ara_tha_4	GLR2.5	NP_196682.1	Arabidopsis thaliana
Gly_max_2		XP_003539503.1	Glycine max
Sor_bic_3		XP_002462416.1	Sorghum bicolor
Pop_tri_3	GluR5	XP_002305094.1	Populus trichocarpa
Gly_max_3		XP_003545055.1	Glycine max
Ory_sat_2		NP_001057025.1	Oryza sativa Japonica Group
Pop_tri_4	GluR5	XP_002316843.1	Populus trichocarpa
Vit_vin_4		XP_002273744.2	Vitis vinifera
Phy_pat_1		XP_001779207.1	Physcomitrella patens subsp. patens
Sel_moe_1		XP_002963727.1	Selaginella moellendorffii
Bra_dis_6		XP_003561526.1	Brachypodium distachyon
Vit_vin_5		XP_002276999.1	Vitis vinifera

Med_tru_2	GLR2.7	XP_003593705.1	Medicago truncatula
Gly_max_4		XP_003533407.1	Glycine max
Sor_bic_4		XP_002459199.1	Sorghum bicolor
Bra_dis_7		XP_003580405.1	Brachypodium distachyon
Ara_tha_5	GLR3.6	NP_190716.3	Arabidopsis thaliana
Ara_lyr_5		XP_002869097.1	Arabidopsis lyrata subsp. lyrata
Ory_sat_3		NP_001058372.1	Oryza sativa Japonica Group
Pop_tri_5	GluR5	XP_002306988.1	Populus trichocarpa
Ric_com_2	GLR3	XP_002510703.1	Ricinus communis
Gly_max_5		XP_003540305.1	Glycine max
Ara_tha_6	GLR3.4	NP_172012.2	Arabidopsis thaliana
Vit_vin_6		XP_002273713.1	Vitis vinifera
Med_tru_3	GLR2.9	XP_003593706.1	Medicago truncatula
Med_tru_4	GLR	XP_003629121.1	Medicago truncatula
Sor_bic_5		XP_002459200.1	Sorghum bicolor
Pop_tri_6	GluR5	XP_002316840.1	Populus trichocarpa
Ara_lyr_6		XP_002880613.1	Arabidopsis lyrata subsp. lyrata
Zea_may_1		NP_001169913.1	Zea mays
Bra_dis_8		XP_003560970.1	Brachypodium distachyon
Gly_max_6		XP_003542285.1	Glycine max
Gly_max_7		NP_001242434.1	Glycine max
Dro_wil_1	GK22709	XP_002072179.1	Drosophila willistoni
Ara_lyr_7		XP_002870560.1	Arabidopsis lyrata subsp. lyrata
Dro_moj_1	GI22168	XP_002001083.1	Drosophila mojavensis
Dro_ere_1	GG15269	XP_001979402.1	Drosophila erecta
Hom_sap_1	GRIK2	NP_786944.1	Homo sapiens
Hom_sap_2	GRIK2	NP_068775.1	Homo sapiens
Ail_mel_1	GRIK5	XP_002925279.1	Ailuropoda melanoleuca
Ail_mel_2	GRIK5	XP_002925278.1	Ailuropoda melanoleuca
Lox_afr_1	GRIK2	XP_003404370.1	Loxodonta africana
Ano_gam_1	AGAP000801	XP_003437104.1	Anopheles gambiae str. PEST
Dro_gri_1	GH16102	XP_001994464.1	Drosophila grimshawi
Ano_car_1		XP_003215556.1	Anolis carolinensis
Tae_gut_1		XP_002193226.1	Taeniopygia guttata
Cri_gri_1		XP_003498948.1	Cricetulus griseus
Mac_mul_1		XP_001100677.1	Macaca mulatta
Mus_mus_1	Grid2	NP_032193.1	Mus musculus
Ail_mel_3	GRIK1	XP_002924182.1	Ailuropoda melanoleuca
Acy_pis_1		XP_001945266.2	Acyrthosiphon pisum
Mac_mul_2	GRIK2	XP_001086640.2	Macaca mulatta
Lox_afr_2	GRID2	XP_003414126.1	Loxodonta africana

Gal_gal_1	GRID2	XP_420483.3	Gallus gallus
Dro_gri_2	GH18377	XP_001993929.1	Drosophila grimshawi
Cav_por_1		XP_003467223.1	Cavia porcellus
Dro_ana_1	GF18326	XP_001954551.1	Drosophila ananassae
Bom_imp_1		XP_003486477.1	Bombus impatiens
Dro_gri_3	GH17276	XP_001994492.1	Drosophila grimshawi
Cal_jac_1	GRID2	XP_002745632.1	Callithrix jacchus
Nom_leu_1	GRID2	XP_003257582.1	Nomascus leucogenys
Dro_pse_1	GA17711	XP_001358619.2	Drosophila pseudoobscura pseudoobscura
Hom_sap_3	GRIK1	NP_000821.1	Homo sapiens
Ped_hum_1		XP_002431270.1	Pediculus humanus corporis
Dro_ere_2	GG15279	XP_001979403.1	Drosophila erecta
Pon_abe_1	GRIK1	XP_002830640.1	Pongo abelii
Equ_cab_1	GRIK1	XP_001915295.2	Equus caballus
Dro_ana_2	GF17009	XP_001953893.1	Drosophila ananassae
Dro_sec_1	GM23174	XP_002043454.1	Drosophila sechellia
Ore_nil_1		XP_003447966.1	Oreochromis niloticus
Dro_yak_1	GE11157	XP_002086719.1	Drosophila yakuba
Dro_mel_1	CG5621, isoform B	NP_001036735.1	Drosophila melanogaster
Can_lup_1		XP_544843.3	Canis lupus familiaris
Rat_nor_1	GRIK1	NP_058937.1	Rattus norvegicus
Dan_rer_1		XP_002664816.2	Danio rerio
Dro_mel_2	CG9935, isoform C	NP_001036251.1	Drosophila melanogaster
Dan_rer_2	grik1a	XP_001924038.3	Danio rerio
Equ_cab_2		XP_001501691.2	Equus caballus
Ano_gam_2	AGAP000803	XP_311343.4	Anopheles gambiae str. PEST
Dro_sim_1	GD20025	XP_002102662.1	Drosophila simulans
Cav_por_2		XP_003470472.1	Cavia porcellus
Bos_tau_1	GRIN2B	NP_001179850.1	Bos taurus
Hom_sap_4	GRIN2B	NP_000825.2	Homo sapiens
Cal_jac_2	GRIN2B	XP_002752166.1	Callithrix jacchus
Rat_nor_2	Grik3	NP_001106187.1	Rattus norvegicus
Cri_gri_2		XP_003495563.1	Cricetulus griseus
Xen_tro_1		XP_002937281.1	Xenopus (Silurana) tropicalis
Orn_ana_1		XP_001510480.2	Ornithorhynchus anatinus
Can_lup_2	GRIK5	XP_541594.4	Canis lupus familiaris
Mon_dom_1		XP_003342043.1	Monodelphis domestica
Can_lup_3		XP_850331.3	Canis lupus familiaris
Cav_por_3		XP_003471526.1	Cavia porcellus
Bos_tau_2	GRIA1	XP_002689364.1	Bos taurus
Cav_por_4	Grin1	XP_003473146.1	Cavia porcellus

Hom_sap_5	GRIA1	NP_000818.2	Homo sapiens
Rat_nor_3	Grik5	NP_113696.1	Rattus norvegicus
Hom_sap_6	GRIN1	NP_015566.1	Homo sapiens
Tri_spi_1		XP_003372764.1	Trichinella spiralis
Orn_ana_2	GRID2	XP_001509188.2	Ornithorhynchus anatinus
Dan_rer_3	Grik5	NP_001232890.1	Danio rerio
Mus_mus_2	Grin1	NP_001171127.1	Mus musculus
Acy_pis_2		XP_003242706.1	Acyrthosiphon pisum
Cal_jac_3	GRIA1	XP_002744465.1	Callithrix jacchus
Gal_gal_2	GRIK3	XP_417766.2	Gallus gallus
Bos_tau_3	GRIA1	XP_002689365.1	Bos taurus
Ail_mel_4		XP_002925210.1	Ailuropoda melanoleuca
Lox_afr_3		XP_003404664.1	Loxodonta africana
Dan_rer_4		XP_691754.2	Danio rerio
Pan_tro_1	GRIA2	NP_001171924.2	Pan troglodytes
Tae_gut_2	GRIN2A	XP_002194954.1	Taeniopygia guttata
Sac_kow_1		XP_002730360.1	Saccoglossus kowalevskii
Ano_car_2		XP_003221778.1	Anolis carolinensis
Tri_cas_1		XP_968606.2	Tribolium castaneum
Dan_rer_5	GRIN2AB	XP_699070.5	Danio rerio
Mus_mus_3	GRIA1	NP_001106796.1	Mus musculus
Pan_tro_2	GRIA2	NP_001171923.2	Pan troglodytes
Ail_mel_5	GRIN1	XP_002926176.1	Ailuropoda melanoleuca
Ail_mel_6	GRIN1	XP_002926177.1	Ailuropoda melanoleuca
Ano_gam_3	AGAP002797	XP_312117.5	Anopheles gambiae str. PEST
Orn_ana_3	GRIA2	XP_003428582.1	Ornithorhynchus anatinus
Gal_gal_3	GRIA1	NP_001001774.1	Gallus gallus
Xen_tro_2		XP_002936446.1	Xenopus (Silurana) tropicalis
Rat_nor_4	Grin2A	NP_036705.3	Rattus norvegicus
Hom_sap_7	GRIA2	NP_000817.2	Homo sapiens
Apl_cal_1	GluR5	NP_001191541.1	Aplysia californica
Dan_rer_6	Grin1A	NP_001070182.2	Danio rerio
Ore_nil_2		XP_003440144.1	Oreochromis niloticus
Dro_gri_4	GH16113	XP_001994463.1	Drosophila grimshawi
Ano_car_3		XP_003224461.1	Anolis carolinensis
Mel_gal_1	GRIN2B	XP_003202270.1	Meleagris gallopavo
Mus_mus_4	Gria2	NP_038568.2	Mus musculus
Sac_kow_2		XP_002739876.1	Saccoglossus kowalevskii
Ore_nil_3		XP_003456903.1	Oreochromis niloticus
Mon_dom_2	GRIA4	XP_003341273.1	Monodelphis domestica
Ory_cun_1		XP_002708566.1	Oryctolagus cuniculus

Cav_por_5		XP_003477797.1	Cavia porcellus
Dro_vir_1	GJ14381	XP_002058378.1	Drosophila virilis
Nod_spu_1		ZP_01628414.1	Nodularia spumigena CCY9414
Xen_lae_1	grin1	NP_001081615.1	Xenopus laevis
Xen_lae_2	gria4	NP_001153157.1	Xenopus laevis
Lox_afr_4	GRIK3	XP_003415352.1	Loxodonta africana
Ped_hum_2		XP_002432134.1	Pediculus humanus corporis
Ore_nil_4	NMDAR2A	XP_003454999.1	Oreochromis niloticus
Dan_rer_7	GRIA3A	NP_938153.1	Danio rerio
Dro_vir_2	GJ17530	XP_002052402.1	Drosophila virilis
Mus_mus_5	GRIA4	NP_001106651.1	Mus musculus
Gal_gal_4	GRIA4	NP_990545.1	Gallus gallus
Acy_pis_3		XP_001949860.2	Acyrthosiphon pisum
Equ_cab_3	GRIA1	XP_003362830.1	Equus caballus
Tae_gut_3	GRIA2	NP_001070157.1	Taeniopygia guttata
Nom_leu_2	GRIA2	XP_003257943.1	Nomascus leucogenys
Lox_afr_5		XP_003406444.1	Loxodonta africana
Cio_int_1		XP_002121378.1	Ciona intestinalis
Bra_flo_1		XP_002605553.1	Branchiostoma floridae
Pan_tro_3	GRIK5	XP_524469.3	Pan troglodytes
Dan_rer_8	Gria2a	NP_571969.1	Danio rerio
Nom_leu_3	GRIA4	XP_003253123.1	Nomascus leucogenys
Acy_pis_4		XP_001949419.2	Acyrthosiphon pisum
Dro_yak_2	GE25274	XP_002096067.1	Drosophila yakuba
Mon_dom_3		XP_001366920.1	Monodelphis domestica
Mus_mus_6	GRIA4	NP_062665.3	Mus musculus
Dro_ana_3	GF14315	XP_001962671.1	Drosophila ananassae
Dro_pse_2	GA15505	XP_001359355.1	Drosophila pseudoobscura pseudoobscura
Equ_cab_4		XP_001499518.2	Equus caballus
Cav_por_6		XP_003464694.1	Cavia porcellus
Ano_car_4	GRIA3	XP_003227808.1	Anolis carolinensis
Xen_lae_3	GRIN2B	NP_001106368.1	Xenopus laevis
Equ_cab_5		XP_001917100.2	Equus caballus
Ano_car_5		XP_003228217.1	Anolis carolinensis
Orn_ana_4	GRIA4	XP_001509465.2	Ornithorhynchus anatinus
Ore_nil_5		XP_003450917.1	Oreochromis niloticus
Ore_nil_6	GluR2B	XP_003443499.1	Oreochromis niloticus
Ore_nil_7		XP_003453465.1	Oreochromis niloticus
Pro_mar_1		YP_001017759.1	Prochlorococcus marinus str. MIT 9303
Mon_dom_4	GRID1	XP_001363938.1	Monodelphis domestica
Dro_per_1	GL26648	XP_002021698.1	Drosophila persimilis

Tri_cas_2		XP_971258.2	Tribolium castaneum
Gal_gal_5	GRIA3	NP_001106270.1	Gallus gallus
Dro_vir_3	GJ24560	XP_002054630.1	Drosophila virilis
Cae_ele_1	GLR-6	NP_741822.2	Caenorhabditis elegans
Nom_leu_4		XP_003282100.1	Nomascus leucogenys
Equ_cab_6		XP_001503336.2	Equus caballus
Ory_cun_2		XP_002720316.1	Oryctolagus cuniculus
Ore_nil_8	GluR2A	XP_003452802.1	Oreochromis niloticus
Cav_por_7		XP_003465642.1	Cavia porcellus
Mac_mul_3	GRIK4	XP_001106948.1	Macaca mulatta
Pan_tro_4	GRIK4	NP_001029331.1	Pan troglodytes
Equ_cab_7	GRIA3	XP_001501048.1	Equus caballus
Pon_abe_2	GRIA3	XP_002832117.1	Pongo abelii
Gal_gal_6	GRID1	XP_426488.2	Gallus gallus
Can_lup_4	GRIN2C	XP_540421.4	Canis lupus familiaris
Rat_nor_5	GRIA3	NP_001106213.1	Rattus norvegicus
Gal_gal_7	GRIK4	XP_417889.2	Gallus gallus
Lox_afr_6		XP_003418245.1	Loxodonta africana
Hom_sap_8	GRIA3	NP_015564.4	Homo sapiens
Ail_mel_7		XP_002914121.1	Ailuropoda melanoleuca
Cul_qui_1		XP_001848226.1	Culex quinquefasciatus
Bra_flo_2		XP_002588867.1	Branchiostoma floridae
Tri_ery_1		YP_723930.1	Trichodesmium erythraeum IMS101
Mus_mus_7		NP_034480.2	Mus musculus
Dan_rer_9		NP_991293.1	Danio rerio
Cal_jac_4	GRIN2C	XP_002806915.1	Callithrix jacchus
Apl_cal_2	GluR1	NP_001191539.1	Aplysia californica
Idi_bal_1		ZP_01042624.1	Idiomarina baltica OS145
Tha_sp._1		ZP_05343132.1	Thalassiobium sp. R2A62
Sac_kow_3		XP_002734294.1	Saccoglossus kowalevskii
Biz_arg_1		ZP_08818200.1	Bizionia argentinensis JUB59
Ory_cun_3		XP_002711833.1	Oryctolagus cuniculus
Ano_car_6		XP_003225944.1	Anolis carolinensis
Ail_mel_8	GRID1	XP_002915436.1	Ailuropoda melanoleuca
Dro_yak_3	GE14671	XP_002087966.1	Drosophila yakuba
Ore_nil_9		XP_003438346.1	Oreochromis niloticus
Dro_wil_2	GK12585	XP_002067735.1	Drosophila willistoni
Dro_vir_4	GJ13380	XP_002047341.1	Drosophila virilis
Cae_rem_1	CRE-GLR-3	XP_003091936.1	Caenorhabditis remanei
Tri_adh_1		XP_002108129.1	Trichoplax adhaerens
Syn_sp._1		ZP_01085070.1	Synechococcus sp. WH 5701

Cri_gri_3		XP_003495405.1	Cricetulus griseus
Bom_imp_2		XP_003486640.1	Bombus impatiens
Mel_gal_2		XP_003212259.1	Meleagris gallopavo
Bra_flo_3		XP_002614078.1	Branchiostoma floridae
Bra_flo_4		XP_002600128.1	Branchiostoma floridae
Ano_car_7		XP_003229279.1	Anolis carolinensis
Dro_per_2	GL13273	XP_002026728.1	Drosophila persimilis
Dro_ana_4	GF11879	XP_001953450.1	Drosophila ananassae
Bru_mal_1	GluR2	XP_001900697.1	Brugia malayi
Dro_sec_2	GM18071	XP_002037857.1	Drosophila sechellia
Ped_hum_3		XP_002432650.1	Pediculus humanus corporis
Rho_bac_1		ZP_01740235.1	Rhodobacteraceae bacterium HTCC2150
Mac_mul_4		XP_002802440.1	Macaca mulatta
Bos_tau_4	GRIN2D	XP_875596.2	Bos taurus
Ore_nil_10		XP_003458734.1	Oreochromis niloticus
Mus_mus_8	NMDA2D	NP_032198.2	Mus musculus
Cro_wat_1		ZP_00517290.1	Crocosphaera watsonii WH 8501
Bra_flo_5		XP_002607139.1	Branchiostoma floridae
Lox_afr_7		XP_003418608.1	Loxodonta africana
Beg_sp._1		ZP_02003278.1	Beggiatoa sp. PS
Rue_sp._1		ZP_08861107.1	Ruegeria sp. TW15
Cht_fla_1		ZP_03130928.1	Chthoniobacter flavus Ellin428
Api_flo_1		XP_003694234.1	Apis florea
Bra_bac_1		ZP_08629326.1	Bradyrhizobiaceae bacterium SG-6C
Nos_sp._1		NP_486951.1	Nostoc sp. PCC 7120
Rho_bac_2		ZP_05121772.1	Rhodobacteraceae bacterium KLH11
Dro_sim_2	GD23353	XP_002078252.1	Drosophila simulans
Dro_ere_3	GG15353	XP_001972134.1	Drosophila erecta
Dro_yak_4	GE25526	XP_002089200.1	Drosophila yakuba
Apl_cal_3	GluR8	NP_001191669.1	Aplysia californica
Pon_abe_3	GRIK4	XP_002822654.1	Pongo abelii
Med_tru_5	GLR3.2	XP_003593707.1	Medicago truncatula
Mar_pur_1		ZP_08773888.1	Marichromatium purpuratum 984
Syn_sp._2		YP_730938.1	Synechococcus sp. CC9311
Ore_nil_11		XP_003450662.1	Oreochromis niloticus
Api_flo_2		XP_003697873.1	Apis florea
Cal_jac_5	GRID1	XP_002756209.1	Callithrix jacchus
Adv_kas_1		ZP_09478523.1	Advenella kashmirensis WT001
Dro_mel_3	GluRIIB	NP_523485.3	Drosophila melanogaster
Loa_loa_1	GluR1	XP_003150750.1	Loa loa
Bra_flo_6		XP_002585883.1	Branchiostoma floridae

Oct_ant_1		ZP_05065163.1	Octadecabacter antarcticus 238
Dro_mel_4	GluRIIC	NP_608557.3	Drosophila melanogaster
Api_flo_3		XP_003693148.1	Apis florea
Afi_sp._1		ZP_07028539.1	Afipia sp. 1NLS2
Api_mel_1		XP_396400.3	Apis mellifera
Dro_gri_5	GH23957	XP_001996510.1	Drosophila grimshawi
Bom_imp_3		XP_003489919.1	Bombus impatiens
Mac_mul_5		XP_002808251.1	Macaca mulatta
Owe_hon_1		YP_004990184.1	Owenweeksia hongkongensis DSM 17368
Dro_sim_3	GD23060	XP_002077694.1	Drosophila simulans
Cae_rem_2	CRE-GLR-7	XP_003109814.1	Caenorhabditis remanei
Str_pur_1		XP_796568.2	Strongylocentrotus purpuratus
Gra_for_1		YP_861587.1	Gramella forsetii KT0803
Cae_bri_1	CBR-GLR-7	XP_002643873.1	Caenorhabditis briggsae
Str_pur_2		XP_792639.1	Strongylocentrotus purpuratus
Oli_car_1		YP_002288493.1	Oligotropha carboxidovorans OM5
Ixo_sca_1		XP_002407640.1	Ixodes scapularis
Bra_flo_7		XP_002588581.1	Branchiostoma floridae
Dro_ere_4	GG25084	XP_001968822.1	Drosophila erecta
Bra_flo_8		XP_002613802.1	Branchiostoma floridae
Syn_sp._3		ZP_01124154.1	Synechococcus sp. WH 7805
Chl_pha_1		YP_001960498.1	Chlorobium phaeobacteroides BS1
Dro_wil_3	GK14684	XP_002065406.1	Drosophila willistoni
Cri_gri_4		XP_003504076.1	Cricetulus griseus
Mus_mus_9	Grin3a	NP_001028523.1	Mus musculus
Dro_moj_2	GI17554	XP_002002745.1	Drosophila mojavensis
Dro_gri_6	GH12703	XP_001991512.1	Drosophila grimshawi
Dro_moj_3	GI17553	XP_002002744.1	Drosophila mojavensis
Nem_vec_1		XP_001629614.1	Nematostella vectensis
Cae_bri_2	CBR-NMR-1	XP_002630717.1	Caenorhabditis briggsae
Cae_bri_3	CBR-GLR-2	XP_002641908.1	Caenorhabditis briggsae
Orn_ana_5		XP_001519062.2	Ornithorhynchus anatinus
Syn_sp._4		ZP_01468279.1	Synechococcus sp. BL107
Cul_qui_2		XP_001865374.1	Culex quinquefasciatus
Nas_vit_1		XP_001603675.1	Nasonia vitripennis
Dro_sec_3	GM13027	XP_002044327.1	Drosophila sechellia
Acy_pis_5		XP_001943401.2	Acyrthosiphon pisum
Sch_man_1		XP_002572261.1	Schistosoma mansoni
Syn_sp._5		ZP_05788417.1	Synechococcus sp. WH 8109
Syn_sp._6		1IIT	Synechocystis sp. PCC 6803 substr. Kazusa

LITERATURE CITED

Adl, S. M., A. G. Simpson, M. A. Farmer, R. A. Andersen, O. R. Anderson, J. R. Barta, S. S. Bowser, G. Brugerolle, R. A. Fensome, S. Fredericq, T. Y. James, S. Karpov, P. Kugrens, J. Krug, C. E. Lane, L. A. Lewis, J. Lodge, D. H. Lynn, D. G. Mann, R. M. McCourt, L. Mendoza, O. Moestrup, S. E. Mozley-Standridge, T. A. Nerad, C. A. Shearer, A. V. Smirnov, F. W. Spiegel and M. F. Taylor (2005). "The new higher level classification of eukaryotes with emphasis on the taxonomy of protists." J Eukaryot Microbiol **52**(5): 399-451.

Bergsten, J. (2005). "A review of long branch attraction." Cladistics **21**: 163-193.

Chiu, J., R. DeSalle, H. M. Lam, L. Meisel and G. Coruzzi (1999). "Molecular evolution of glutamate receptors: a primitive signaling mechanism that existed before plants and animals diverged." Mol Biol Evol **16**(6): 826-838.

Chiu, J. C., E. D. Brenner, R. DeSalle, M. N. Nitabach, T. C. Holmes and G. M. Coruzzi (2002). "Phylogenetic and expression analysis of the glutamate-receptor-like gene family in Arabidopsis thaliana." Mol Biol Evol **19**(7): 1066-1082.

Darriba, D., G. L. Taboada, R. Doallo and D. Posada (2011). "ProtTest 3: fast selection of best-fit models of protein evolution." Bioinformatics **27**(8): 1164-1165.

Felsenstein, J. (1978). "Cases in which parsimony or compatibility methods will be positively misleading." Syst Zool **27**: 401-410.

Janovjak, H., G. Sandoz and E. Y. Isacoff (2011). "A modern ionotropic glutamate receptor with a K(+) selectivity signature sequence." Nat Commun **2**: 232.

Jelesko, J. G. (2012). "An expanding role for purine uptake permease-like transporters in plant secondary metabolism." Front Plant Sci **3**: 78.

Katoh, K., K. Kuma, H. Toh and T. Miyata (2005). "MAFFT version 5: improvement in accuracy of multiple sequence alignment." Nucleic Acids Res **33**(2): 511-518.

Keeling, P. J., G. Burger, D. G. Durnford, B. F. Lang, R. W. Lee, R. E. Pearlman, A. J. Roger and M. W. Gray (2005). "The tree of eukaryotes." Trends Ecol Evol **20**(12): 670-676.

Mayer, M. L., R. Olson and E. Gouaux (2001). "Mechanisms for ligand binding to GluR0 ion channels: crystal structures of the glutamate and serine complexes and a closed apo state." J Mol Biol **311**(4): 815-836.

Pearson, W. R. (1996). "Effective protein sequence comparison." Methods Enzymol **266**: 227-258.

Price, M. B., J. Jelesko and S. Okumoto (2012). "Glutamate receptor homologs in plants: functions and evolutionary origins." Front Plant Sci **3**: 235.

Simpson, A. G. and A. J. Roger (2002). "Eukaryotic evolution: getting to the root of the problem." Curr Biol **12**(20): R691-693.

Tapken, D., U. Anschutz, L. H. Liu, T. Huelsken, G. Seebohm, D. Becker and M. Hollmann (2013). "A plant homolog of animal glutamate receptors is an ion channel gated by multiple hydrophobic amino acids." Sci Signal **6**(279): ra47.

Turano, F. J., G. R. Panta, M. W. Allard and P. van Berkum (2001). "The putative glutamate receptors from plants are related to two superfamilies of animal neurotransmitter receptors via distinct evolutionary mechanisms." Mol Biol Evol **18**(7): 1417-1420.

Vincill, E. D., A. M. Bieck and E. P. Spalding (2012). "Ca(2+) conduction by an amino acid-gated ion channel related to glutamate receptors." Plant Physiol **159**(1): 40-46.

Zwickl, D. J. (2006). "Genetic algorithm approaches for the phylogenetic analysis of large biological sequence datasets under the maximum likelihood criterion." Ph.D. Dissertation, The University of Texas.

CHAPTER 3:IDENTIFICATION OF SUBUNITS NECESSARY FOR GLR CHANNEL FUNTIONALITY

INTRODUCTION

Justification

Due to their sessile nature, plants need to sense the availability of minerals to modulate development and maximize fitness. Nitrogen (N) is quantitatively the most important mineral nutrient and its availability has a profound short- and long-term effect on plant growth and development (Marschner 1997). For most plants, nitrate and ammonia are the primary sources of available N, which are converted to amino acids. Amino acids are the predominant form of transported organic N in the plant and are thus considered to be the N currency of the plant body. Considering the critical roles amino acids play in N assimilation and transport, it is not surprising that the change in amino acid levels induce a rapid change in transcriptome and in the activities of key enzymes in the N assimilation pathway (Fritz, Mueller et al. 2006, Gutierrez, Stokes et al. 2008). In fact, amino acids have long been suggested as signals that regulate genes involved in N transport and metabolism in plants, but the exact mechanism of amino acid sensing in plants is not well understood (Vincentz, Moureaux et al. 1993, Forde and Lea 2007).

Some mechanisms for amino acid sensing have been documented in bacteria, yeast, and mammals, and potential homologs of such amino acid sensors from other organisms do exist in plants. One example is Glb1, an Arabidopsis homolog of bacterial PII proteins that are considered N "master regulators" (Arcondeguy, Jack et al. 2001, Coutts, Thomas et al. 2002, Forchhammer 2004, Osanai and Tanaka 2007), although the role of Glb1 seems to be constrained

compared to the bacterial counterparts (Feria Bourrellier, Valot et al. 2010). Likewise, Arabidopsis homolog of Target of Rapamycin (TOR) plays a role in integrating nutrition signals including nitrogen in a similar manner as its yeast and animal counterparts (Ren, Venglat et al. 2012). Lastly, the plant homologs of amino acid gated channels from mammals has recently been established as amino acid gated channels (Tapken, Anschutz et al. 2013, Vincill, Clarin et al. 2013), representing a potential mechanism for amino acid sensing in plants.

Plant GLRs exist in all tracheophytes (vascular plants) and bryophytes (non-vascular plants) sequenced so far. Phylogenetic analyses have revealed that plant GLRs have diverged from metazoan and bacterial iGluRs, which probably happened as early as the last universal common ancestor (Chiu, Brenner et al. 2002, Price, Jelesko et al. 2012). Despite a large evolutionary distance, plant GLRs and mammalian iGluRs share structural similarities with regards to the signature "three plus one" trans- membrane domains M1 to M4 as well as the ligand binding domain (LBD) and amino terminal domain (ATD), which show high amino acid sequence identity (63– 16%), particularly with the M3 domain (63%) of animal NMDA receptor iGluRs.

In animal glutamate receptors, amino terminal domain (ATD) and ligand binding domain (LBD) are responsible for interdomain interactions and ligand-gated conformational change, respectively, and the composition of subunits determines the channel properties (Sobolevsky, Rosconi et al. 2009). The predicted membrane topology and orientation of the protein as a tetramer, with the ATD and LBD exposed to the external side of the membrane, are considered to be conserved in plant GLRs (Lam, Chiu et al. 1998).

Understanding the function of plant GLRs has previously been hampered by gene redundancy and toxicity although genetic, pharmacological, and electrophysiological approaches

suggested diverse physiological roles such as carbon/nitrogen balance regulation (Kang and Turano 2003, Kang, Mehta et al. 2004), stomatal opening (Cho, Kim et al. 2009), pollen tube growth (Michard, Lima et al. 2011), plant-pathogen interaction (Kwaaitaal, Huisman et al. 2011, Kwaaitaal, Maintz et al. 2012, Li, Wang et al. 2013), and lateral root formation (Vincill, Clarin et al. 2013). Recently, two of the Arabidopsis GLRs, *At*GLR3.4 and 1.4, were shown to function as amino acid gated channels when expressed in heterologous systems (Vincill, Bieck et al. 2012, Tapken, Anschutz et al. 2013), further confirming the functional commonality of plant and mammalian glutamate receptors.

So far, most approaches to investigate the roles of GLRs have been centered on understanding the function of one protein through genetic or electrophysiological approaches. We hypothesize that formation of homo- or hetero-tetramers would be required for the formation of the ion-conducting pore (therefore for full function) of plant GLRs, similar to their animal and bacterial counterparts. This level of organization may result in modulation of sensing capabilities in response to multiple ligands, stress, or developmental situations in which plant GLRs may play a role. Recently, it was reported that *At*GLRs 3.2 and 3.4 are capable of physical interactions with one another, and to a lesser extent, with themselves and *At*GLR3.3 in mammalian HEK293 cells as well as *Nicotiana benthamiana* cells (Vincill, Clarin et al. 2013). Despite this, a comprehensive study of inter-domain interaction between plant GLRs has not been reported so far. Such information will allow us to develop hypotheses about possible composition of the channels in a given cell, with particular focus on importance in signaling in different plant tissues and during development.

In this study, we studied two-way interactions between 14 different GLR subunits from Arabidopsis. A modified yeast two-hybrid approach was performed to identify potential

interactors in yeast. In this heterologous expression system, members of all three clades (*At*GLR1, 2, and 3s) interact with each other, which is in contrast with the mammalian iGluRs which only interact with subunits within their own clade. Putative interactors were then confirmed using Förster resonance energy transfer (FRET) in mammalian HEK293 cells and co-immunoprecipitation from *Nicotiana benthamiana*. Data suggests that *At*GLR1.1 and 3.4 preferentially form homomers.

RESULTS

Split Ubiquitin System

A yeast mating-based split ubiquitin system (mbSUS) was used to allow for systematic analyses of GLR protein interactions (Obrdlik, El-Bakkoury et al. 2004). Unlike standard yeast two-hybrid, the method does not require the fusion proteins to travel to the nucleus and is therefore suitable for detecting interactions between membrane proteins (Lehming 2002, Lalonde, Ehrhardt et al. 2008). Fourteen out of 20 GLR cDNAs were successfully isolated, and fused to either a modified N-terminal (NubG) or C-terminal (Cub) half of ubiquitin. Both interaction-dependent auxotrophy and enzymatic activity assays were used to evaluate the interactions between the subunits.

Mating-based SUS of 14 *At*GLRs (listed in Table 3-1) revealed both putative homo- and hetero- GLR subunit interactions. At least three independent experiments were performed for each combination (the results are summarized in Table 3-2). One representative experiment of independent mbSUS experiments with only the strongest interactors is shown in Figure 3-1. Homomeric interactions were consistently observed for GLR1.1NubG/GLR1.1Cub and GLR2.1NubG/GLR2.1Cub. Interestingly, homomeric interaction for GLR1.4NubG/GLR1.4Cub

and GLR3.4NubG/GLR3.4Cub, the subunits capable of acting as homomeric channels in heterologous expression systems (Vincill, Bieck et al. 2012, Tapken, Anschutz et al. 2013), were not among the strongest interactions observed. Heteromeric interactions were also observed between a number of subunits (Table 3-2). In many cases, reciprocal interactions (the same interaction partners with the half-ubiquitin tags swapped) were not observed.

Our experiments identified several subunits (1.1, 2.1, 2.9, 3.2 and 3.4) that consistently interact with multiple other subunits. Both NubG- and Cub- tagged GLR3.6 proteins were capable of auto-activating the transcription of reporters, hence the results were disregarded. None of the other GLR-NubG/Cub fusions interacted with the negative controls NubG or KAT1-NubG, nor promoted growth of yeast on its own. These results were supported using β-galactosidase assays to confirm activity of the *LacZ* reporter gene in interacting yeast (Figure 3-2 and data not shown).

Examination of channel functionality in yeast

As mentioned previously, application of known mammalian glutamate receptor agonists such as glutamate to plant cells results in an increase in cytosolic calcium levels. Further, it has been demonstrated that HEK (human epithelial kidney) cells expressing *At*GLR3.4 are capable of conducting cations in a whole cell patch clamp system, and that exposure to amino acids such as asparagine, serine, and glycine alters this response such that it is desensitized (Vincill, Bieck et al. 2012). In addition, recent evidence shows that the tripeptide glutathione (GSH, γ-Glu-Cys-Gly) is capable of eliciting an increase in cytosolic calcium response that is in part mediated through *At*GLR3.3 (Li, Wang et al. 2013). Thus, yeast cells expressing two positive interactors were further examined to determine if the interacting GLRs form a functional channel capable of

regulating conduction of cations such as calcium, and whether and which amino acids modulate this activity. Unfortunately, despite many attempts, no consistent trend was found for changes in cytosolic calcium concentration in response to different amino acids.

Intra-molecular Förster Resonance Energy Transfer (FRET)

Intra-molecular Förster Resonance Energy Transfer (FRET) was used to analyze interactions between selected GLR subunits found through mbSUS using human epithelial kidney (HEK293) cell culture (Van Munster, Kremers et al. 2005). Two techniques of FRET measurement were applied for determining the FRET efficiency between co-localizing subunits: sensitized emission FRET, which measures the increase in acceptor fluorescence upon donor excitation (Ishikawa-Ankerhold, Ankerhold et al. 2012), and acceptor photobleaching which measures changes in donor emission upon destruction of the acceptor molecule (Van Munster, Kremers et al. 2005).

Among the GLRs that interacted with multiple other GLRs in the mbSUS experiments, *At*GLRs 1.1, 2.9, 3.2, and 3.4 were successfully expressed in mammalian HEK293 cells. Each construct was fused to either monomeric Venus (mVenus)(Nagai, Ibata et al. 2002) or enhanced CFP (ECFP, Clontech Laboratories), and FRET efficiency between the two subunits were measured using either epifluorescent or confocal microscopy. The cells co-expressing ECFP- and mVenus-tagged constructs are shown in Figure 3-3. All of the constructs localized to the plasma membrane, although in many cases internal membranes were also visible. Co-transfection efficiency varied between constructs, with reduced efficiency for 1.1mVenus expression when co-transfected with 3.2 or 3.4 ECFP, and those combinations including 2.9 with 3.2 or 3.4 (regardless of which fluorescent tag) producing no or minimal co-localization.

Of 16 possible combinations, 12 two-way interactions were successfully examined and homomeric interactions were identified between GLRs 1.1 and 3.4 using sensitized emission FRET (Figure 3-3). No other homomeric or heteromeric combinations resulted in detectable FRET, regardless of apparent co-localization on the plasma membrane (Figure 3-3C). Homomeric interaction of GLR1.1 and 3.4 were further confirmed using a YFP acceptor photobleaching strategy (Figure 3-4). Both of the homomeric interactions produced positive FRET values with 77.8±30.0 and 47.6±29.5 for GLR1.1 and 26.2±16.1 and 40.4±23.9 for GLR3.4 using sensitized emission and YFP acceptor photobleaching, respectively, whereas no detectable FRET was observed with GLR1.1/3.4 combinations. From these results, we concluded that GLR1.1 and 3.4 are capable of forming monomeric channels.

DISCUSSION

Understanding the stoichiometry and assembly of plant GLR subunits can give insight into the overall function of the plant glutamate receptor homologs. Systematic analysis of 14 GLR cDNA clones in yeast revealed both homo- and hetero-meric GLR subunit interactions (Figure 3-1). These interactions were also confirmed by using β-galactosidase assays (Figure 3-2). Interestingly, interaction between the subunits did not correlate with the similarity within clades. Rather, the studies identified several subunits (GLRs 1.1, 2.1, 2.9, 3.2 and 3.4) that more frequently interacted with other subunits in different clades. In contrast, animal glutamate receptors form homo-/hetero-tetramers only within their own group (e.g. NMDA receptors only interacts with subunits that also belong to the NMDA family)(Dingledine, Borges et al. 1999). In animals, inter-subunit interaction is mainly determined by the amino-terminal domains (Ayalon and Stern-Bach 2001, Ayalon, Segev et al. 2005). Although the amino-terminal domains are

conserved in plant glutamate receptors, the mechanism through which the subunit composition is determined can be different in plants.

Among the subunits identified through yeast mbSUS assay, interactions among GLRs 1.1, 2.9, 3.2, and 3.4 were further studied using heterologous expression in mammalian cell lines. Two separate approaches using Förster Resonance Energy Transfer (FRET) identified homomeric interactions for GLR1.1 and GLR3.4. GLR3.4 has been shown to function as a channel when expressed in HEK293 cells in a previous work (Vincill, Bieck et al. 2012), corroborating the finding in this study. In contrast to the results published from the same group, we did not observe consistent interactions between GLR3.2 and GLR3.4 (Vincill, Clarin et al. 2013). The difference could be due to subtle differences in the constructs used, since FRET is sensitive to both the distance and relative dipole orientations of the fluorophores, and the linker regions between the subunit and the fluorescent proteins could have a large effect on FRET efficiency (Okumoto, Jones et al. 2012). Therefore, the results need to be interpreted with caution; the lack of apparent energy transfer does not exclude the inter-subunit interactions, nor can FRET efficiency be used as a measure of the strength of interactions. Both of the techniques used in this study employed heterologous expression systems. Ideally another approach such as co-immunoprecipitation should be applied to examine the interactions in plant cells. However, we were not successful in expressing epitope-tagged GLRs in plant tissues at the levels necessary for such experiments (data not shown), potentially due to the toxicity of GLRs when present at higher concentration. Therefore, further examination of individual interactions might require other approaches such as electrophysiological studies of cells expressing multiple subunits, or examining genetic interactions (Vincill 2013).

In conclusion, our study identified multiple potentially interacting *At*GLRs in heterologous expression systems. Utilization of high-resolution transcriptome and proteome data (Brady, Orlando et al. 2007, Gifford, Dean et al. 2008, Petricka, Schauer et al. 2012) can be used to further examine coexpression of GLR subunits. Such analyses along with this data will guide identification of potential GLR subunits that could comprise a channel in a given cell type.

METHODS AND MATERIALS

Split Ubiquitin System

GLR cDNA clones 1.1 (AT3G04110), 1.3 (AT5G48410), 2.2 (AT2G24720), 2.9 (AT2G29100), 3.2 (AT4G35290), 3.3 (AT1G42540), 3.4 (AT1G05200), and 3.7 (AT2G32400) were isolated through a high-throughput membrane protein interactome project (http://www.associomics.org/index.php) and were amplified from *Arabidopsis* cDNA and cloned into either pDONR221 (GLR1.1, 2.2, and 3.7) or pCR8/GW/TOPO (GLR1.3, 2.2, 3.2, 3.3, 3.4, and 3.7)(courtesy of Dr. Wolf Frommer, Carnegie Institution). GLRs 1.4 (AT3G07520), 2.1 (AT5G27100), 2.7 (AT2G29120), 3.1 (AT2G17260), and 3.6 (AT3G51480) genes were successfully amplified using reverse transcriptase PCR from *Arabidopsis thaliana* ecotype Columbia leaf-derived cDNA and cloned into pENTR1A vector (Invitrogen). GLR3.5 (AT2G32390) was amplified from a pENTR clone generously provided by Dr. June Kwak (University of Maryland). Multiple attempts to amplify GLRs 1.2 (AT5G48400), 2.3 (AT2G24710), 2.4 (AT4G31710), 2.5 (AT5G11210), 2.6 (AT5G11180), and 2.8 (AT2G29110) were unsuccessful. A series of controls including WT Nub, KAT1-NubG, KAT1-Cub, KEA3-Cub, NIP7.1-Cub, and ETR1-Cub were kindly provided by Dr. Guillaume Pilot (Virginia Tech).

N-terminal (Nub) or C-terminal (Cub) split ubiquitin were fused to the C-terminus of GLR cDNA entry clones using GATEWAY cloning and then used to examine interaction between different combinations of subunits. NubG, a modified N-terminal ubiquitin with a decreased affinity for its counterpart, Cub, was used to reduce the possibility of a false-positive interaction resulting from spontaneous reunion between ubiquitin halves. N-terminal ubiquitin (Nub) constructs were transformed into the yeast mating strain THY.AP5, genotype MATα leu2-3, 112 trp1-289 his3-Δ1 loxP::ade2 URA3, phenotype *leu- trp- his- ade- ura-*. C-terminal ubiquitin (Cub) constructs were transformed into the yeast mating strain THY.AP4, genotype MATa leu2-3, 112 ura3-52 lexA::HIS3 lexA::ADE2 lexA::lacZ::trp1, phenotype *leu- trp- his- ade- ura- lexA:: lacZ/ ADE2/ HIS3*. The yeast mating strain was cultured to an OD600nm of 0.6 and cells were harvested by centrifugation. Transformation medium containing the following components was added to the cell suspension at a final concentration of 35% w/v PEG 3350 (Sigma), 80mM lithium acetate (Acros), 1.6mM ethylenediamine tetraacetic acid (EDTA) disodium salt dihydrate, 8mM Tris-HCl, pH7.5 (Fisher Scientific), and 300µg salmon sperm DNA. Approximately 200ng of plasmid DNA was added to 98µL cells suspended in transformation medium, then heat shocked by exposing cells to 28°C for 30 minutes, 42°C for 13 minutes. Cells were harvested and plated on a selective media plate (SC *+trp +met +ade +his –leu* for THY.AP4 and SC *+leu +met +ade +his –trp*for THY.AP5) and allowed to grow over 2 nights at 28°C.

Transformants of AP4 and AP5 expressing Cub and Nub constructs, respectively, were mated by mixing 10µL of each cell suspension in micro-titer plates then spotted on YPAD media and allowed to grow at 28°C. Once visible growth was observed (overnight to 20 hours) cells were scraped and re-suspended in 200µL H_2O and 5µL of each suspension was spotted on SC –

leu –trp +ade +his +met for selection of mated yeasts and allowed to grow over 2 nights at 28°C. Interaction between Nub and Cub fusion proteins were observed by growing diploids on SC *–leu –trp –ade –his*, and growth of yeast was recorded as a positive indicator of interaction between Nub and Cub fusion constructs. In order to exclude growth effect independent of the interaction between the two constructs, cell suspensions were spotted on SC *–leu –trp –ade –his +met* (125µM and 250µM) to increase the repression of the Cub expression cassette, which is repressed by methionine. In addition, *Arabidopsis* KAT1 NubG/Cub fusions served as positive controls for interaction (Schachtman 2000), and the well-characterized membrane proteins ETR1, NIP7.1 and KEA3 were used as negative controls.

β-Galactosidase Assay in Yeast

β-galactosidase activity of yeast interactors was measured following the manufacturer's protocol (Clontech, manual no. PT3024-1) to confirm interaction between NubG and Cub GLR fusion constructs. Briefly, diploid yeast were spotted onto Hybond C-Extra nitrocellulose membrane (Amersham Biosciences) atop SC *–leu –trp –ade –his* agar media and grown for 2 days at 28°C. The nitrocellulose sheet was freeze-thawed 3 times in liquid nitrogen and warmed to room temperature to lyse the cells. B-galactosidase activity was monitored by placing the nitrocellulose membrane on Whatman 3M filter paper soaked with Z-buffer (100 mM Na_2HPO_4, pH 7, 10 mM KCl, 1 mM $MgSO_4$, and 5 mM β-mercaptoethanol) and incubated at 37°C until blue color developed.

Calcium Conductance in Yeast

Cytosolic Ca^{2+} measurements were conducted as follows. Yeasts transformed with both NubG- and Cub- GLR fusions were incubated in the presence of cell permeable Fluo-3 AM ester (Invitrogen), in the dark for 2 hours, washed with PBS 3 times, and re-suspended in 50µL PBS in 96-well round bottom plates. Fluorescence measurements were taken at 526nm following excitation at 500nm over a time course. To determine whether addition of extracellular calcium was taken-up by putative GLR cation channels, Fluo-3 fluorescence was monitored upon addition of 5mM Ca^{2+}, as well as 25mM Ca^{2+}. Additionally, the response of cytosolic Ca^{2+} to 1mM of amino acid was examined.

Transfection of HEK293 Cells

GLR 1.1, 2.9, 3.2, and 3.4 cDNA clones were digested with SalI and SmaI and ligated to SalI/AfeI site of pENTR-mVenus or pENTR-ECFP (Altaf Ahmad, unpublished results) to produce Gateway-compatible C-terminal fusion entry constructs. The mVenus and ECFP fusion constructs were then Gateway recombined into the mammalian expression vector pCDNA 3.2 V5 DEST. HEK293 cells were grown to 80% confluency in Dulbecco's modified eagle medium containing 10% cosmic calf serum and 100U penicillin/streptomycin (DMEM, HyClone, ThermoScientific), trypsinated and split into glass-bottom 8-well chamber (Lab-Tek). At 50% confluency, cells were transfected using Opti-MEM I Reduced serum media (Invitrogen) containing 1µL Lipofectamine 2000 (Invitrogen) and 400ng of plasmid and allowed to transfect 24hours and then exchanged back to DMEM media for one day prior to imaging, cells approximately 80-100% confluency.

Sensitized Emission FRET using Wide-field Microscopy

Cells were imaged using an epi-fluorescence microscope (IX81, Olympus) with appropriate filters for excitation: YFP 500/20 nm and CFP 430/24 nm; dichroic beam splitter: YFP 535/30 nm and CFP 470/24 nm; and emission: YFP 535/30 nm and CFP 470/24 nm (Chroma). Images were taken with a microscope equipped with a 40x oil-immersion objective and a Lamda-XL filter wheel (Sutter) that allows for rapid exchange of filters and captured with an EMCCD Rolera-MGI FAST 1394 monochromatic camera (Olympus). Regions of cells were selected and the pixels quantified for each channel using the appropriate software (Slidebook, 3I) and then corrected for spectral cross-talk, non-specific photobleaching, and relative abundance of fluorophores to give a normalized FRET efficiency, N_{FRET}, using the following equation (Youvan 1997):

$$N_{FRET} = \frac{I_{FRET} - I_{YFP} \times a - I_{CFP} \times b}{\sqrt{I_{YFP}} \times \sqrt{I_{CFP}}}$$

Where I_{FRET}, I_{CFP}, and I_{YFP} are the intensities under FRET, CFP, and YFP filter sets, respectively, in each region of interest (ROI), and *a* and *b* are the normalization of percentage of CFP- or YFP-bleed-through, respectively, under the FRET filter set. The normalizations for *a* and *b* varied between experiments and thus were calculated for each individual experiment by analyzing images of cells expressing only CFP or YFP and quantifying the relative intensity ratio under the FRET/CFP or FRET/YFP filter sets (Xia and Liu 2001).

YFP Acceptor Photobleaching Using Confocal Microscopy

Cells were imaged on a Zeiss LSM510 confocal microscope using a plan-apo 63x oil immersion objective. CFP and YFP fluorophores were excited using 458 nm and 514 nm light, respectively. Colocalization was determined by using the RG2B colocalization plugin with

autothresholding (Christopher Mauer, Northwestern University) in Image J software (NIH). For FRET the cells were imaged and bleached for 16 iterations of 100% 514 nm laser intensity on selected ROIs to 30% or less of initial YFP intensity. CFP fluorescence intensity was determined using fluorescence intensity (FI) NIH Image J software. FRET efficiency was calculated as follows:

$$E_{FRET} = \frac{YFP_{POST}^{*} - YFP_{PRE}}{YFP_{PRE}}$$

Where FRET efficiency, E_{FRET}, is determine by correcting fluorescence intensity for the donor (YFP) after YFP bleaching for nonspecific bleaching using an ROI outside of the bleached area to determine amount of fluorescence change over time. A minimum of 16 cells were analyzed for each construct from at least two separate transfections.

FIGURES

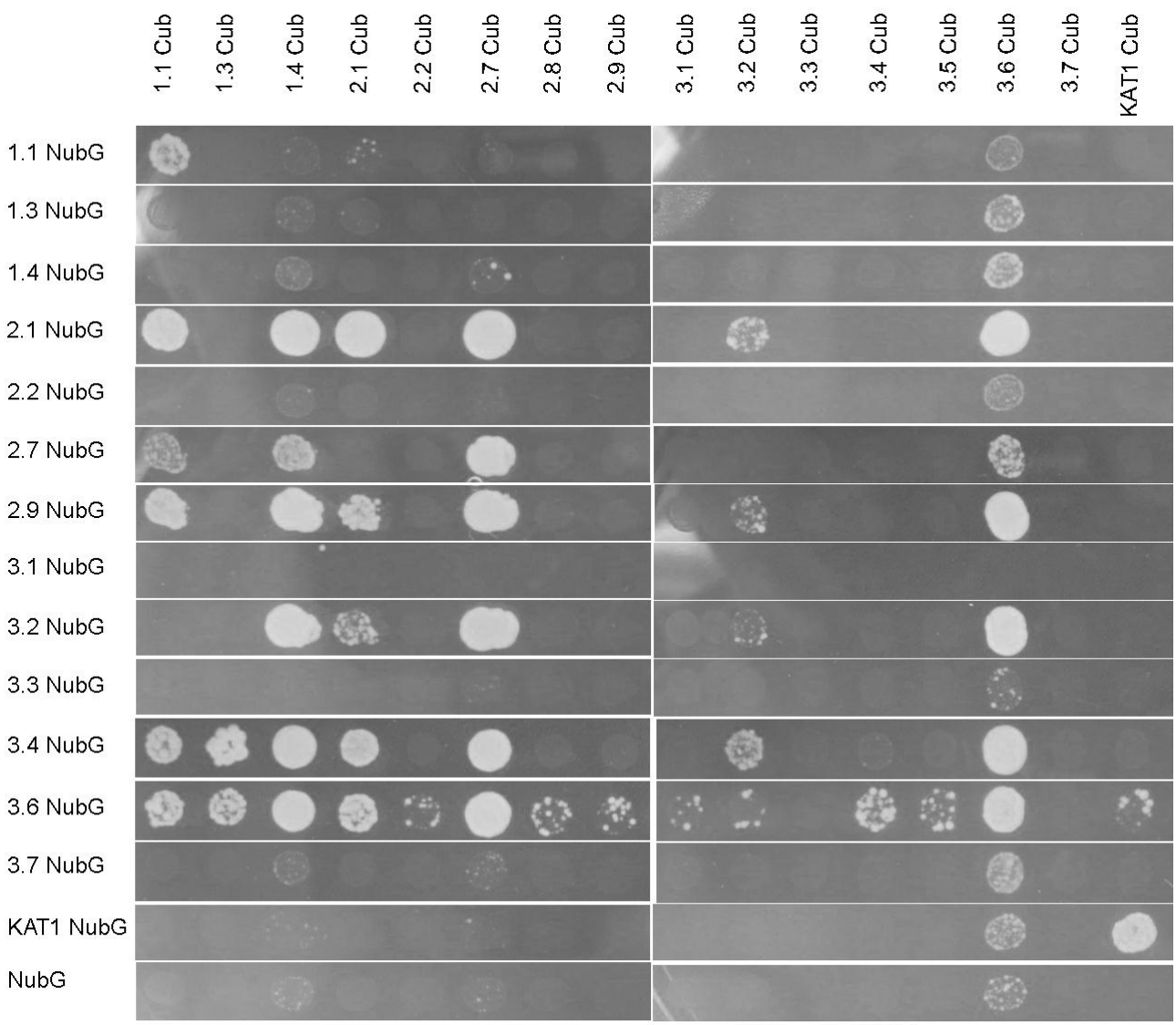

Figure 3-1. Results of split ubiquitin assay demonstrating interaction between GLR subunits.

Representation of one experiment demonstrating a number of putative interactors, where the growth on interaction-selective media indicates a potential interaction.

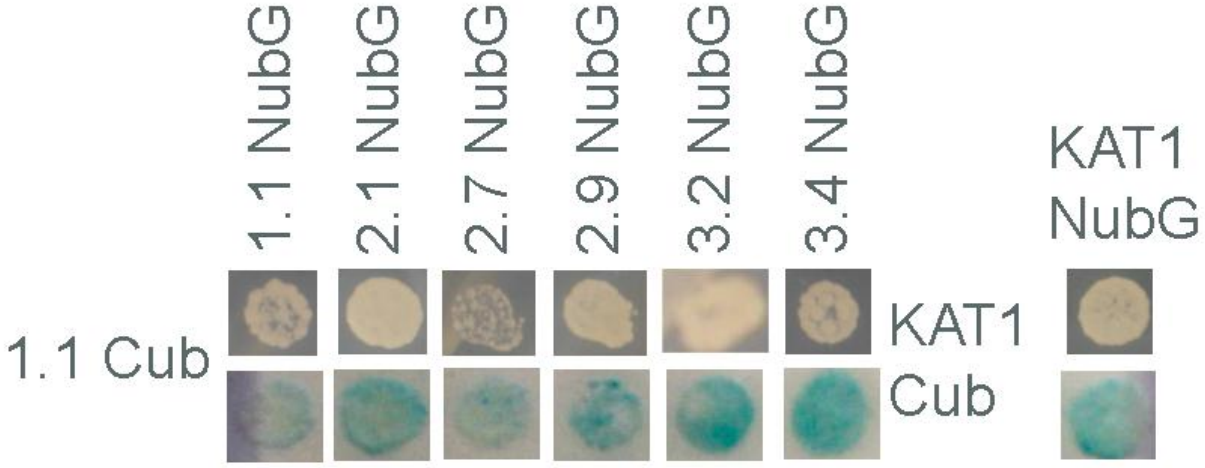

Figure 3-2. Results of split ubiquitin assay demonstrating interaction between GLR subunits and corresponding β-galactosidase activity.

Interaction between GLR1.1-CUB and a number of GLR-NUBG fusion proteins are shown with potassium channel KAT1 serving as a positive interaction. The top panels are growth of yeast on interaction-selective media, with bottom panels showing blue coloration are indicative of β-galactosidase activity to confirm interaction.

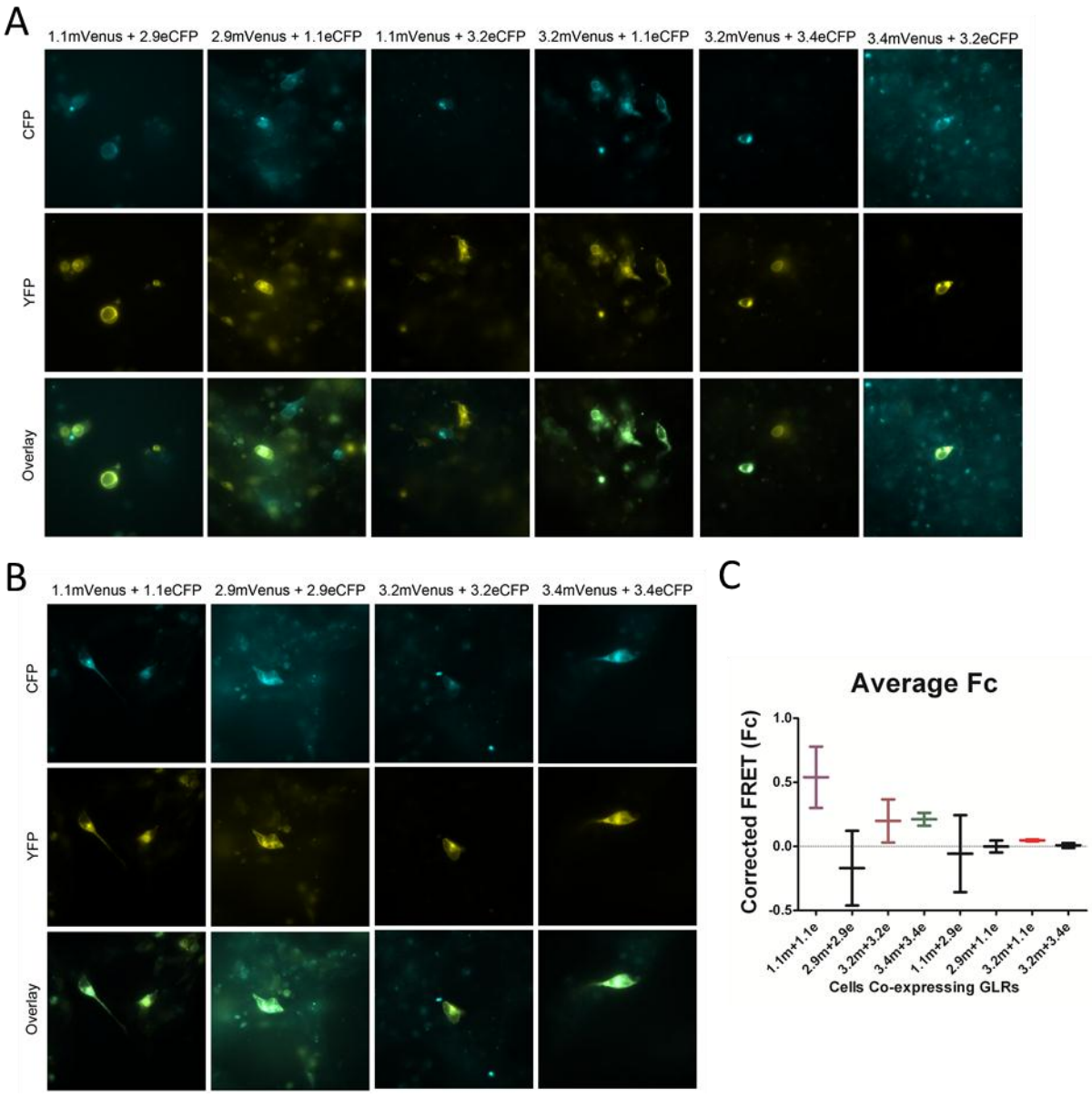

Figure 3-3. Co-localization of co-expressed GLR ECFP/mVenus fusion proteins in mammalian HEK293 cells imaged using wide-field microscopy.

A) Cells expressing two different subunits tagged with either ECFP or mVenus B) Cells co-expressing one GLR subunit tagged with either ECFP or mVenus, C) Average corrected FRET (F_C) of HEK293 cells co-expressing GLR subunits using wide-field sensitized emission FRET microscopy. The error bars indicated standard deviations.

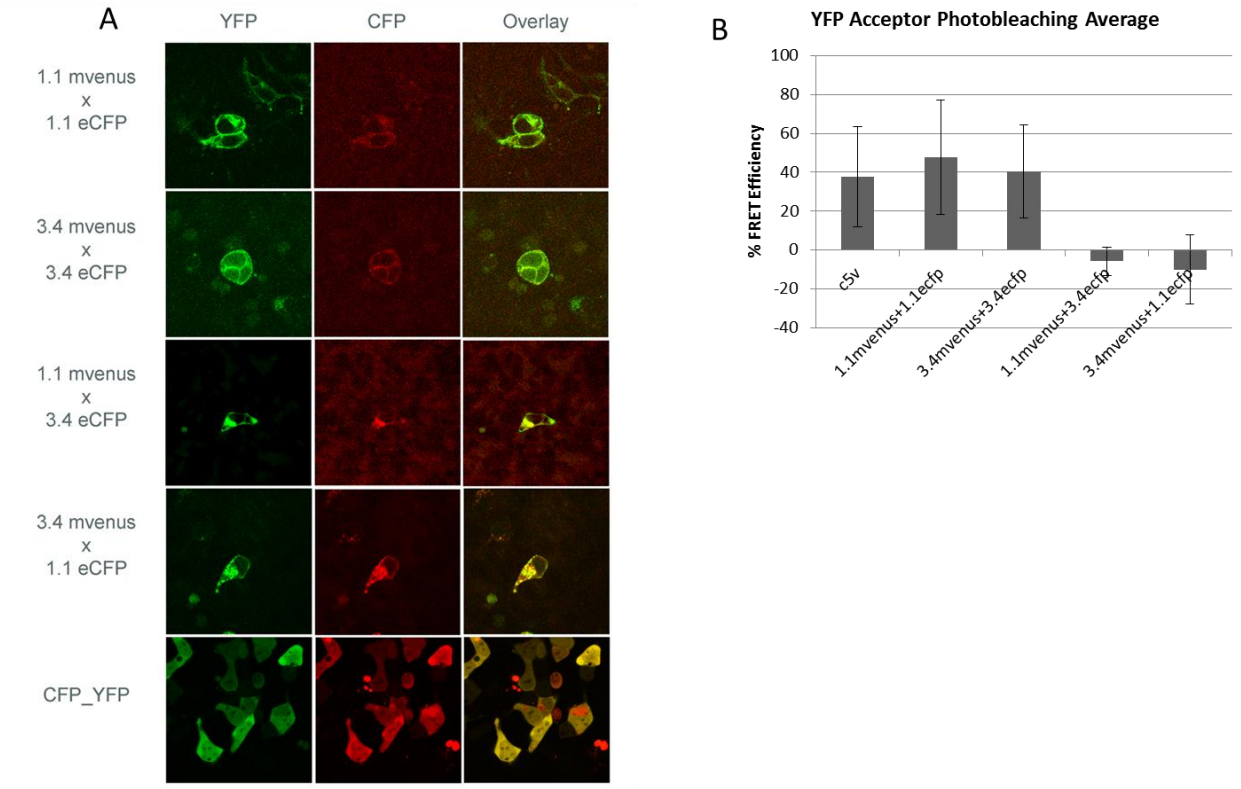

Figure 3-4. Co-expressed GLR 1.1 and 3.4 ECFP/mVenus proteins in mammalian HEK293 cells imaged using confocal microscopy.

A) ECFP, mVenus, and overlay images from HEK cells co-expressing tagged subunits. B) % FRET Efficiency between the two subunits expressed in HEK293 cells, using photobleaching method. The results from 3 independent experiments are summarized. C5V, a positive control for FRET was also included in the experiment (Chen, Mauldin et al. 2007).

TABLES

Table 3-1. AGI Number of Arabidopsis glutamate-like receptors (GLRs).

GLR	OTHER	AGI NUMBER
1.1		AT3G04110
1.2		AT5G48400
1.3		AT5G48410
1.4		AT3G07520
2.1		AT5G27100
2.2		AT2G24720
2.3		AT2G24710
2.4		AT4G31710
2.5		AT5G11210
2.6		AT5G11180
2.7		AT2G29120
2.8		AT2G29110
2.9		AT2G29100
3.1	GLR2	AT2G17260
3.2	GLUR2	AT4G35290
3.3		AT1G42540
3.4		AT1G05200
3.5		AT2G32390
3.6		AT3G51480
3.7	GLR5	AT2G32400

Arabidopsis glutamate receptor (GLR) numbers along with alternative nomenclature and their corresponding Arabidopsis genome initiative (AGI) identification number.

Table 3-2. Summary of split ubiquitin interactions from all experiments.

	1.1-Cub	1.3-Cub	1.4-Cub	2.1-Cub	2.2-Cub	2.7-Cub	2.9-Cub	3.1-Cub	3.2-Cub	3.4-Cub	3.6-Cub
1.1-NubG	**0.78**	0.00	0.00	0.00	0.00	0.00	0.00	0.00	0.11	0.00	0.20
1.3-NubG	**0.67**	0.00	0.20	0.00	0.00	0.20	0.11	0.00	0.22	0.00	**0.80**
1.4-NubG	0.40	0.00	0.20	0.00	0.00	0.20	0.00	0.20	0.17	0.00	**0.60**
2.1-NubG	**0.60**	0.00	0.33	**1.00**	0.00	0.33	0.00	0.20	0.40	0.00	**0.67**
2.2-NubG	0.22	0.00	0.00	0.00	0.00	0.00	0.00	0.00	0.22	0.00	0.20
2.7-NubG	0.25	0.00	0.25	0.00	0.00	0.33	0.20	0.00	0.00	0.00	**0.60**
2.9-NubG	**0.88**	0.00	0.33	**1.00**	0.22	0.33	0.33	0.00	**0.75**	0.22	**1.00**
3.1-NubG	0.00	0.00	0.00	0.00	0.00	0.00	0.00	0.00	0.00	0.00	0.33
3.2-NubG	**0.75**	0.00	0.33	**1.00**	0.33	0.25	0.38	0.00	0.44	0.11	**1.00**
3.3-NubG	0.13	0.11	0.00	0.00	0.00	0.00	0.00	0.00	0.00	0.00	0.00
3.4-NubG	**1.00**	0.13	0.33	**1.00**	0.22	0.33	0.33	0.00	**0.67**	0.33	**1.00**
3.5-NubG	0.00	0.00	0.00	0.00	0.00	0.00	0.00	0.00	0.00	0.00	0.00
3.6-NubG	**0.75**	0.25	0.33	0.50	0.00	0.33	0.00	0.40	0.40	0.20	**0.75**
3.7-NubG	0.00	0.00	0.00	0.00	0.00	0.00	0.00	0.00	0.11	0.00	0.20
KAT1-NubG	0.00	0.00	0.00	0.00	0.00	0.00	0.00	0.00	0.00	0.00	0.20
WT-Nub	0.11	0.00	0.00	0.00	0.00	0.00	0.00	0.00	0.11	0.00	0.40
NubG	0.00	0.00	0.00	0.00	0.00	0.00	0.00	0.00	0.00	0.00	0.00

Summary of all experiments performed on split ubiquitin-GLR fusion proteins with the rate of interaction for each combination tested. Values listed in red are equal to or above a threshold of 0.60 (60% or greater) incident of occurrence and represent “consistent” interactions.

LITERATURE CITED

Arcondeguy, T., R. Jack and M. Merrick (2001). "P(II) signal transduction proteins, pivotal players in microbial nitrogen control." Microbiol Mol Biol Rev **65**(1): 80-105.

Ayalon, G., E. Segev, S. Elgavish and Y. Stern-Bach (2005). "Two regions in the N-terminal domain of ionotropic glutamate receptor 3 form the subunit oligomerization interfaces that control subtype-specific receptor assembly." J Biol Chem **280**(15): 15053-15060.

Ayalon, G. and Y. Stern-Bach (2001). "Functional assembly of AMPA and kainate receptors is mediated by several discrete protein-protein interactions." Neuron **31**(1): 103-113.

Brady, S. M., D. A. Orlando, J. Y. Lee, J. Y. Wang, J. Koch, J. R. Dinneny, D. Mace, U. Ohler and P. N. Benfey (2007). "A high-resolution root spatiotemporal map reveals dominant expression patterns." Science **318**(5851): 801-806.

Chen, Y., J. P. Mauldin, R. N. Day and A. Periasamy (2007). "Characterization of spectral FRET imaging microscopy for monitoring nuclear protein interactions." J Microsc **228**(Pt 2): 139-152.

Chiu, J. C., E. D. Brenner, R. DeSalle, M. N. Nitabach, T. C. Holmes and G. M. Coruzzi (2002). "Phylogenetic and expression analysis of the glutamate-receptor-like gene family in Arabidopsis thaliana." Mol Biol Evol **19**(7): 1066-1082.

Cho, D., S. A. Kim, Y. Murata, S. Lee, S. K. Jae, H. G. Nam and J. M. Kwak (2009). "De-regulated expression of the plant glutamate receptor homolog AtGLR3.1 impairs long-term Ca2+-programmed stomatal closure." Plant J **58**(3): 437-449.

Coutts, G., G. Thomas, D. Blakey and M. Merrick (2002). "Membrane sequestration of the signal transduction protein GlnK by the ammonium transporter AmtB." EMBO J **21**(4): 536-545.

Dingledine, R., K. Borges, D. Bowie and S. F. Traynelis (1999). "The glutamate receptor ion channels." Pharmacol Rev **51**(1): 7-61.

Feria Bourrellier, A. B., B. Valot, A. Guillot, F. Ambard-Bretteville, J. Vidal and M. Hodges (2010). "Chloroplast acetyl-CoA carboxylase activity is 2-oxoglutarate-regulated by interaction of PII with the biotin carboxyl carrier subunit." Proc Natl Acad Sci U S A **107**(1): 502-507.

Forchhammer, K. (2004). "Global carbon/nitrogen control by PII signal transduction in cyanobacteria: from signals to targets." FEMS Microbiol Rev **28**(3): 319-333.

Forde, B. G. and P. J. Lea (2007). "Glutamate in plants: metabolism, regulation, and signalling." J Exp Bot **58**(9): 2339-2358.

Fritz, C., C. Mueller, P. Matt, R. Feil and M. Stitt (2006). "Impact of the C-N status on the amino acid profile in tobacco source leaves." Plant Cell Environ **29**(11): 2055-2076.

Gifford, M. L., A. Dean, R. A. Gutierrez, G. M. Coruzzi and K. D. Birnbaum (2008). "Cell-specific nitrogen responses mediate developmental plasticity." Proc Natl Acad Sci U S A **105**(2): 803-808.

Gutierrez, R. A., T. L. Stokes, K. Thum, X. Xu, M. Obertello, M. S. Katari, M. Tanurdzic, A. Dean, D. C. Nero, C. R. McClung and G. M. Coruzzi (2008). "Systems approach identifies an organic nitrogen-responsive gene network that is regulated by the master clock control gene CCA1." Proc Natl Acad Sci U S A **105**(12): 4939-4944.

Ishikawa-Ankerhold, H. C., R. Ankerhold and G. P. Drummen (2012). "Advanced fluorescence microscopy techniques--FRAP, FLIP, FLAP, FRET and FLIM." Molecules **17**(4): 4047-4132.

Kang, J., S. Mehta and F. J. Turano (2004). "The putative glutamate receptor 1.1 (AtGLR1.1) in Arabidopsis thaliana regulates abscisic acid biosynthesis and signaling to control development and water loss." Plant Cell Physiol **45**(10): 1380-1389.

Kang, J. and F. J. Turano (2003). "The putative glutamate receptor 1.1 (AtGLR1.1) functions as a regulator of carbon and nitrogen metabolism in Arabidopsis thaliana." Proc Natl Acad Sci U S A **100**(11): 6872-6877.

Kwaaitaal, M., R. Huisman, J. Maintz, A. Reinstadler and R. Panstruga (2011). "Ionotropic glutamate receptor (iGluR)-like channels mediate MAMP-induced calcium influx in Arabidopsis thaliana." Biochem J **440**(3): 355-365.

Kwaaitaal, M., J. Maintz, M. Cavdar and R. Panstruga (2012). "On the ligand binding profile and desensitization of plant ionotropic glutamate receptor (iGluR)-like channels functioning in MAMP-triggered Ca(2)(+) influx." Plant Signal Behav **7**(11): 1373-1377.

Lalonde, S., D. W. Ehrhardt, D. Loque, J. Chen, S. Y. Rhee and W. B. Frommer (2008). "Molecular and cellular approaches for the detection of protein-protein interactions: latest techniques and current limitations." Plant Journal **53**(4): 610-635.

Lam, H. M., J. Chiu, M. H. Hsieh, L. Meisel, I. C. Oliveira, M. Shin and G. Coruzzi (1998). "Glutamate-receptor genes in plants." Nature **396**(6707): 125-126.

Lehming, N. (2002). "Analysis of protein-protein proximities using the split-ubiquitin system." Brief Funct Genomic Proteomic **1**(3): 230-238.

Li, F., J. Wang, C. Ma, Y. Zhao, Y. Wang, A. Hasi and Z. Qi (2013). "Glutamate receptor-like channel3.3 is involved in mediating glutathione-triggered cytosolic calcium transients, transcriptional changes, and innate immunity responses in Arabidopsis." Plant Physiol **162**(3): 1497-1509.

Li, F., J. Wang, C. Ma, Y. Zhao, Y. Wang, A. Hasi and Z. Qi (2013). "Glutamate Receptor Like Channel 3.3 is involved in mediating glutathione-triggered cytosolic Ca2+ transients, transcriptional changes and innate immunity responses in Arabidopsis." Plant Physiol.

Marschner, H. (1997). Functions of Mineral Nutrients: Macronutrients. Mineral Nutrition of Higher Plants. San Diego, CA, Academic Press Inc**:** 231-254.

Michard, E., P. T. Lima, F. Borges, A. C. Silva, M. T. Portes, J. E. Carvalho, M. Gilliham, L. H. Liu, G. Obermeyer and J. A. Feijo (2011). "Glutamate receptor-like genes form Ca2+ channels in pollen tubes and are regulated by pistil D-serine." Science **332**(6028): 434-437.

Nagai, T., K. Ibata, E. S. Park, M. Kubota, K. Mikoshiba and A. Miyawaki (2002). "A variant of yellow fluorescent protein with fast and efficient maturation for cell-biological applications." Nat Biotechnol **20**(1): 87-90.

Obrdlik, P., M. El-Bakkoury, T. Hamacher, C. Cappellaro, C. Vilarino, C. Fleischer, H. Ellerbrok, R. Kamuzinzi, V. Ledent, D. Blaudez, D. Sanders, J. L. Revuelta, E. Boles, B. Andre and W. B. Frommer (2004). "K+ channel interactions detected by a genetic system optimized for systematic studies of membrane protein interactions." Proc Natl Acad Sci U S A **101**(33): 12242-12247.

Okumoto, S., A. Jones and W. B. Frommer (2012). "Quantitative imaging with fluorescent biosensors." Annu Rev Plant Biol **63**: 663-706.

Osanai, T. and K. Tanaka (2007). "Keeping in touch with PII: PII-interacting proteins in unicellular cyanobacteria." Plant Cell Physiol **48**(7): 908-914.

Petricka, J. J., M. A. Schauer, M. Megraw, N. W. Breakfield, J. W. Thompson, S. Georgiev, E. J. Soderblom, U. Ohler, M. A. Moseley, U. Grossniklaus and P. N. Benfey (2012). "The protein expression landscape of the Arabidopsis root." Proc Natl Acad Sci U S A **109**(18): 6811-6818.

Price, M. B., J. Jelesko and S. Okumoto (2012). "Glutamate receptor homologs in plants: functions and evolutionary origins." Front Plant Sci **3**: 235.

Ren, M., P. Venglat, S. Qiu, L. Feng, Y. Cao, E. Wang, D. Xiang, J. Wang, D. Alexander, S. Chalivendra, D. Logan, A. Mattoo, G. Selvaraj and R. Datla (2012). "Target of rapamycin signaling regulates metabolism, growth, and life span in Arabidopsis." Plant Cell **24**(12): 4850-4874.

Schachtman, D. P. (2000). "Molecular insights into the structure and function of plant K(+) transport mechanisms." Biochim Biophys Acta **1465**(1-2): 127-139.

Sobolevsky, A. I., M. P. Rosconi and E. Gouaux (2009). "X-ray structure, symmetry and mechanism of an AMPA-subtype glutamate receptor." Nature **462**(7274): 745-756.

Tapken, D., U. Anschutz, L. H. Liu, T. Huelsken, G. Seebohm, D. Becker and M. Hollmann (2013). "A plant homolog of animal glutamate receptors is an ion channel gated by multiple hydrophobic amino acids." Sci Signal **6**(279): ra47.

Van Munster, E. B., G. J. Kremers, M. J. Adjobo-Hermans and T. W. Gadella, Jr. (2005). "Fluorescence resonance energy transfer (FRET) measurement by gradual acceptor photobleaching." J Microsc **218**(Pt 3): 253-262.

Vincentz, M., T. Moureaux, M. T. Leydecker, H. Vaucheret and M. Caboche (1993). "Regulation of nitrate and nitrite reductase expression in Nicotiana plumbaginifolia leaves by nitrogen and carbon metabolites." Plant J **3**(2): 315-324.

Vincill, E. D., A. M. Bieck and E. P. Spalding (2012). "Ca2+ conduction by an amino Acid-gated ion channel related to glutamate receptors." Plant Physiol **159**(1): 40-46.

Vincill, E. D., A. M. Bieck and E. P. Spalding (2012). "Ca(2+) conduction by an amino acid-gated ion channel related to glutamate receptors." Plant Physiol **159**(1): 40-46.

Vincill, E. D., A. E. Clarin, J. N. Molenda and E. P. Spalding (2013). "Interacting Glutamate Receptor-Like Proteins in Phloem Regulate Lateral Root Initiation in Arabidopsis." Plant Cell.

Xia, Z. and Y. Liu (2001). "Reliable and global measurement of fluorescence resonance energy transfer using fluorescence microscopes." Biophys J **81**(4): 2395-2402.

Youvan, D. C., C. M. Silva, E. J. Bylina, W. J. Coleman, M. R. Dilworth, and M. M. Yang (1997). "Calibration of fluorescence resonance energy transfer in microscopy using genetically engineered GFP derivatives on nickel chelating beads." Biotechnology (Faisalābād, Pakistan) **3**: 1-18.

CHAPTER 4:EXAMINATION OF SUBCELLULAR LOCALIZATION AND INTER-SUBUNIT INTERACTION OF GLRS IN PLANTS

INTRODUCTION

Project Justification

In animal cells, subcellular localization of glutamate receptors (GLRs) are highly regulated by subunit compositions and interactions with other cellular proteins, and the regulation of receptor density at the plasma membrane is critical for neuronal plasticity (Malinow and Malenka 2002, McGee and Bredt 2003). Much less is known about GLRs in plants; to date, the only GLRs with reported subcellular localization are *At*GLRs 3.2, 3.3, and 3.4 (Teardo, Formentin et al. 2011, Vincill, Bieck et al. 2012, Vincill, Clarin et al. 2013). All of them are reported to be localized at the plasma membrane, with one study reporting GLR3.4 localization in the plastid (Teardo, Formentin et al. 2011). Localization of GLRs belonging to other GLR clades 1 and 2, however, has not been reported so far.

Examination of expression of GLRs in HEK293 cells has shown plasma membrane localization for GLRs 1.1, 2.9, 3.2, and 3.4 (Vincill, Bieck et al. 2012)(Chapter 3). Using heterologous expression systems, however, sometimes results in mis-localization of internal membrane proteins to the plasma membrane (Reinders, Sivitz et al. 2008, Dundar and Bush 2009). Since subcellular localization would have apparent implications for the functions of the channels, we wished to determine native subcellular localization of GLRs in plants. Moreover, we identified potential interactors of GLRs using heterologous expression systems (Chapter 3). Confirmation of interactions *in planta* is desired, however, because there could be some

endogenous factors that might interfere with interaction. The aim of this research was to determine subcellular localization of GLRs and examine the inter-subunit interaction *in planta*.

RESULTS

Subcellular Localization of Plant GLRs

To determine subcellular localizations of *Arabidopsis* GLRs, the cDNA or genomic sequences were tagged with sequences encoding fluorescent proteins (ECFP or mVenus).GLRs 1.1, 2.9, 3.2, and 3.4 were selected since these subunits were found to interact with multiple other GLRs through mbSUS studies (Chapter 3). In addition, localization of GLR3.3 was also examined because of the apparent genetic interaction between *glr3.3 and 3.4* mutants (Stephens, Qi et al. 2008).These constructs were expressed transiently in *Nicotiana benthamiana* plant leaves using *Agrobacterium*-mediated plant transformation (Voinnet, Rivas et al. 2003).

Single and co-expression of the cDNA clones for GLRs 1.1, 3.2, and 3.4 mVenus and ECFP fusions show plasma membrane localization (Figure 4-1). Expression of GLR2.9 fusion proteins was undetectable, therefore was not analyzed further (data not shown). On the other hand, GLR3.3-ECFP or Venus fusions did not exclusively localize to the plasma membrane; in addition to the plasma membrane localization, punctate intracellular structures were observed (Figure 4-2). Interestingly, examination of singly- and co-expressed full-length gene-fluorescent protein fusions for GLRs 3.3 and 3.4 show altered expression profiles. This is witnessed by the localization of the fluorescent protein fusions of each gene, where GLR 3.3 localizes to the endomembrane when GLR3.3-ECFP and GLR3.3-mVenus are co-expressed; and GLR 3.4 localizes to the plasma membrane when GLR3.4-ECFP and GLR3.4-mVenus are co-expressed (Figures 4-2 and 4-3). When GLR3.4-ECFP and GLR3.3-mVenus are co-expressed, the

localization of GLR 3.3 is seen at the plasma membrane (Figure 4-2). This evidence suggested that localization of GLR3.3 is altered in the presence of GLR 3.4. To quantify such change of localization of GLR3.3 when co-expressed with GLR3.4, the number of plant cells with endomembrane localization versus plasma membrane localization was examined for the level of fluorescent intensities while keeping imaging parameters constant. This approach revealed that when the ratio of GLR3.3: 3.4 is high, there is a high amount of endomembrane localization for GLR3.3-venus, and as that ratio decreases the number of cells with plasma membrane localization increases (Figure 4-3).

Stable Overexpression of GLR-Fluorescent Protein Fusions in Arabidopsis

In order to examine whether the localization pattern observed for GLR3.3 and 3.4 represent that of the native system (i.e. Arabidopsis), Arabidopsis plants stably expressing the full-length GLR3.3-ECFP or GLR3.4-mVenus gene were examined for protein localization. As expected, GLR3.4-mVenus exhibited plasma membrane localization (Figure 4-4). Quite unexpectedly, GLR3.3-ECFP expression was localized to the nuclei in root cells with no plasma membrane expression (Figure 4-5) in at least three independent transgenic lines. The nucleic acid stain Syto82 was used to highlight the nucleus and demonstrate co-localization with GLR3.3-ECFP (Figure 4-5). A western blot was performed using antibody against the fluorescent protein tag to ensure that fluorescence was not coming from degraded products (Figure 4-7).

Quantification of FRET between GLR subunits in plant cells

In order to examine the inter-subunit interactions between GLRs, FRET efficiency was quantified in the plant cells co-expressing ECFP-and mVenus-fusion of GLRs. *Nicotiana*

benthamiana plants transiently expressing the two fusion constructs were examined through sensitized FRET and acceptor photobleaching as discussed in Chapter 3. However, auto-fluorescence from the cell wall was prohibitively high for such quantification.

In an attempt to decrease the amount of auto-fluorescence in the samples, protoplasts obtained from 10 day-old *Arabidopsis* roots were used to examine localization of GLRs 1.1, 2.9, 3.2, and 3.4 with C-terminal mVenus tags (Figure 4-6). Unfortunately, despite achieving a high transformation efficiency with the control GFP construct, only a small percentage of protoplasts transformed with GLRs could be visualized. Localization of protein fusions was very grainy and not uniformly to the plasma membrane, likely as a result of increased stress due to over-expression of a potential cation channel which may be leaky without necessary additional components such as interacting proteins (Figure 4-6).

DISCUSSION

Localization of GLR-Fluorescent Protein Fusions

Fluorescent protein tags are often utilized to gain insight into protein function through understanding where the proteins are localized. The plant glutamate receptors are hypothesized to function as membrane-bound cation channels capable of sensing amino acids in the extracellular environment. As expected, examination of fluorescent-tagged GLR proteins revealed plasma membrane localization for GLRs 1.1, 3.2, and 3.4 in *Nicotiana* and *Arabidopsis* expression systems (Figures 4-1, 4-2, and 4-4). Interestingly, however, there also appears to be subcellular localization in the endomembrane for GLR3.3 when expressed in *Nicotiana* (Figures 4-2 and 4-3). The endomembrane localization is relocated to the membrane when GLR3.4 is co-expressed along with GLR3.3 in *Nicotiana* (Figures 4-2 and 4-3). It is tempting to speculate that

some GLRs require specific interactions with other subunits for plasma membrane localization, as it is with well documented cases in animal cells (Malinow and Malenka 2002, McGee and Bredt 2003, Marrus, Portman et al. 2004).

Quite surprisingly, the subcellular localization of GLR3.3-ECFP was largely different between two expression systems used, even though the exact same expression vector was used for both experiments. The GLR3.3-ECFP fusion apparently did not localize to nuclear membrane, since the fluorescence was not confined to the periphery of nuclei (Figure 4-5). It seems quite unlikely that a membrane protein would not associate with an obvious subcellular membrane structure. Since size of the chimeric protein did not show an apparent truncation by Western blot, whether the localization pattern we have observed indeed reflects that of the endogenous protein remains unclear. Thus, it is still important to determine whether this phenomenon is true or is an artifact of our system and what the biological significance of GLR3.3 localization to nuclear bodies is, if confirmed true.

Interestingly, it seemed that over-expression of GLR3.4-venus fusion in Arabidopsis roots seemed to induce swelling of root hairs, although quantitative imaging has not been performed to demonstrate whether there was a significant change from wild-type. Given the ability of GLR3.4 to conduct cations including calcium (Vincill, Bieck et al. 2012), and the role of calcium in root hair elongation (Tominaga-Wada, Ishida et al. 2011), the swelling of root hairs in GLR3.4 over-expression plants can be due to the disruption of calcium gradient. In analogy to the role of GLR1.2 in pollen tube elongation, it is tempting to speculate that some GLRs might be involved in the Ca^{2+} signaling in root hair cells. Gene expression analyses have shown that Clade 3 GLRs are expressed more highly in roots than shoots of Arabidopsis (Chiu, DeSalle et al. 1999, Roy, Gilliham et al. 2008). High resolution transcriptome analysis (Bruex, Kainkaryam

et al. 2012) combined with genetic and pharmacological approaches can be used to examine such possibilities.

METHODS AND MATERIALS

Overexpression of Fluorescent-tagged GLR proteins in Arabidopsis

GLR cDNA clones 1.1 (AT3G04110), 2.9 (AT2G29100), 3.2 (AT4G35290), and 3.4 (AT1G05200) were isolated through a high-throughput membrane protein interactome project (NSF 0618402, http://www.associomics.org/index.php) and were amplified from cDNA and Gateway cloned into either pDONR221 (GLR1.1) or pCR8/GW/TOPO (GLRs 2.9, 3.2, and 3.4)(Dr. Wolf Frommer, Carnegie Institution). GLR 1.1, 2.9, 3.2, and 3.4 cDNA entry clones were restriction digested with *SalI* and *SmaI* and ligated to pENTR-mVenus or pENTR-ECFP vectors restriction digested with *SalI* and *AfeI* to produce Gateway-compatible C-terminal fusion entry constructs. In addition, full-length GLR 3.3 (AT1G42540) and 3.4 (AT1G05200) genes were amplified from cDNA and restriction cloned into pENTR-mVenus or pENTR-ECFP vectors to generate C-terminal fusion proteins by Altaf Ahmad.

The mVenus and ECFP fusion constructs were then Gateway recombined into the agro-bacterium/plant estradiol-inducible binary expression vector pMDC7 (Karimi, Inze et al. 2002, Curtis and Grossniklaus 2003). Stable transformation was performed by floral dip of *Arabidopsis thaliana* ecotype Columbia-0 with *Agrobacterium tumefaciens* strain GV3101 transformed with pMDC7 constructs expressing either the mVenus or ECFP GLR-fusion clones.

Another approach to look at localization of GLR1.1, 2.9, 3.2, and 3.4 mVenus or ECFP protein fusions involved generation of *Arabidopsis* root protoplasts (Birnbaum, Shasha et al. 2003). Briefly, approximately 200 seedlings were grown on vertical plates for 10 days post-

germination prior to harvesting root tissue. Dissected roots were finely chopped and placed in a protoplasting solution (Solution B= Solution A [(600mM Mannitol, 2mM $MgCl_2$, 0.1% BSA 2mM CaCl, 2mM MES, 10mM KCl, pH 5.5] + 1.5% cellulase, 0.1% pectolyase) and incubated on an orbital shaker at room temperature for 60 min. Cells were aspirated and then strained through a 70μm cell strainer and harvested by centrifugation at 500x*g* for 5-10 minutes at 4°C and very gently resuspended in 500μL Solution A. PEG-mediated transformation was performed as previously described (Negrutiu 1987).

Nucleic Acid Staining of Arabidopsis Roots Using Syto82

Two week-old seedlings grown axenically on MS+ sucrose solid medium were harvested and the roots incubated in 1μM Syto82 (Invitrogen Catalog No. S11363) for 30 minutes prior to imaging. Cells were imaged using an epifluorescence microscope (Olympus IX81) with 40x oil objective and excitation/emission of approximately 541/560.

Overexpression of Fluorescent-tagged GLR proteins in Tobacco

Fusions of full-length GLRs 3.3 and 3.4 (AT1G42540 and AT1G05200, respectively) to enhanced cyan fluorescent protein (ECFP) or yellow fluorescent protein variant (mVenus) in the binary plant vector pMDC7 were created by Altaf Ahmad. In addition, GLR 1.1, 3.2, and 3.4 cDNA clones were restriction digested with SalI and SmaI and ligated to pENTR-mVenus or pENTR-ECFP vectors restriction digested with SalI and AfeI to produce Gateway-compatible C-terminal fusion entry constructs. The mVenus and ECFP fusion constructs were then Gateway recombined into the binary plant vector pMDC7. These constructs are under control of the estradiol-inducible promoter G10-90 (Curtis and Grossniklaus 2003). *Agrobacterium*-mediated

transfection of *Nicotiana benthamiana* has been performed as previously described, where constructs are co-infiltrated with the post-transcriptional gene silencing inhibitor p19 in order to increase the expression level of GLR fusion proteins (Lindbo 2007). Fluorescent protein fusions of GLR3.3 or GLR3.4 full-length proteins were infiltrated singly, as well as together (i.e., GLR3.3 ECFP + GLR3.3 mVenus), and between genes (i.e., GLR3.4 ECFP + GLR3.3 mVenus). 1.1, 3.2, and 3.4 cDNA fusion proteins were infiltrated singly, as well as together and between genes as well. Proteins were allowed to mature 2 or 3 days prior to imaging.

Imaging of Fluorescent-tagged GLR proteins using Wide-field Microscopy

Cells were imaged using an epi-fluorescence microscope (IX81, Olympus) with appropriate filters for excitation: YFP 500/20 nm and CFP 430/24 nm; dichroic beam splitter: YFP 535/30 nm and CFP 470/24 nm; and emission: YFP 535/30 nm and CFP 470/24 nm (Chroma). Images were taken with a microscope equipped with a 20x air objective or 40x oil-immersion objective and a Lamda-XL filter wheel (Sutter) that allows for rapid exchange of filters and captured with an EMCCD Rolera-MGI FAST 1394 monochromatic camera (Olympus).

FIGURES

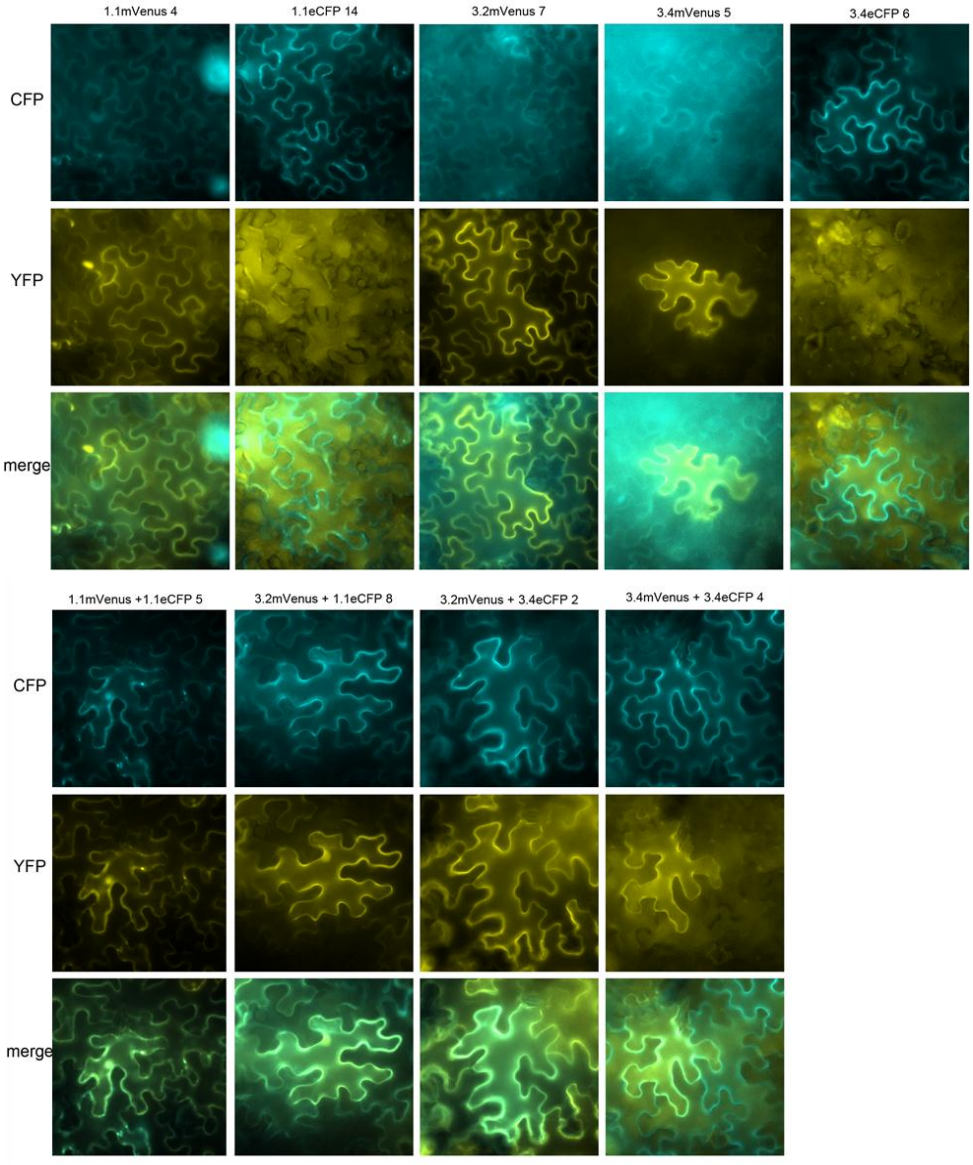

Figure 4-1.Single and Co-expression of GLR-fluorescent protein fusions in Nicotiana benthamiana.

Abaxial view of leaf epidermal cells expressing proteins captured under YFP (mVenus-fusions) or CFP (ECFP-fusions) with merge representing cells present in both conditions.

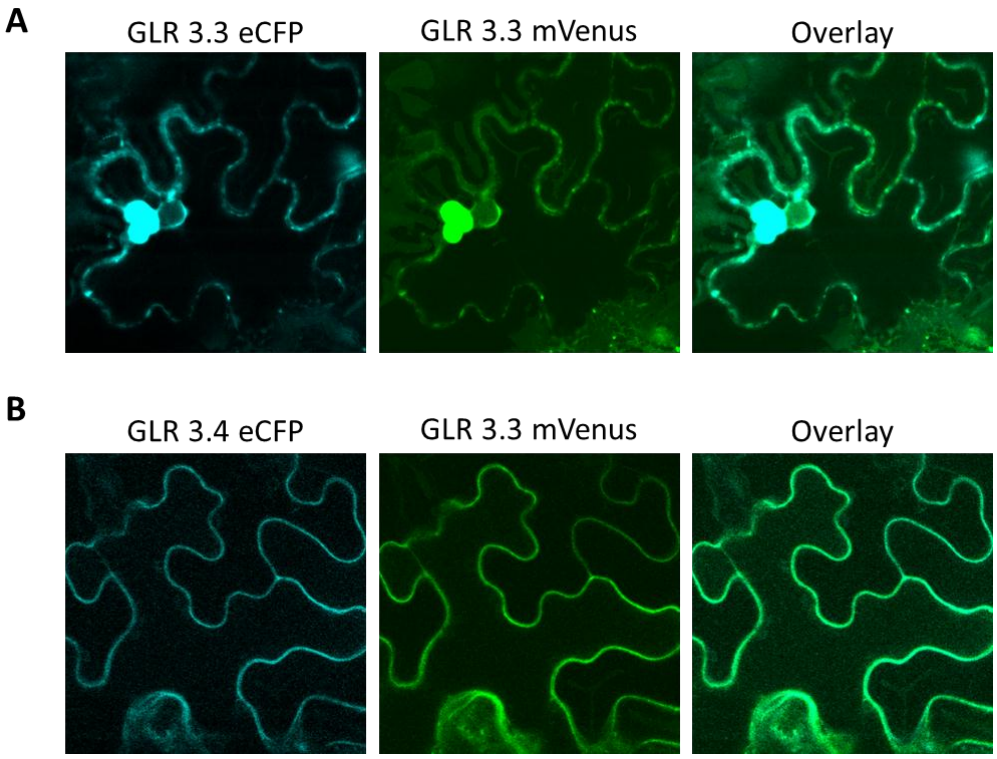

Figure 4-2. Co-expression of GLR-fluorescent protein fusions in Nicotiana benthamiana. Abaxial view of leaf epidermal cells where A) GLR3.3 localizes to the endomembrane in punctae; and B) GLR3.3 localization appears to be stabilized in the plasma membrane by co-expression with GLR3.4.

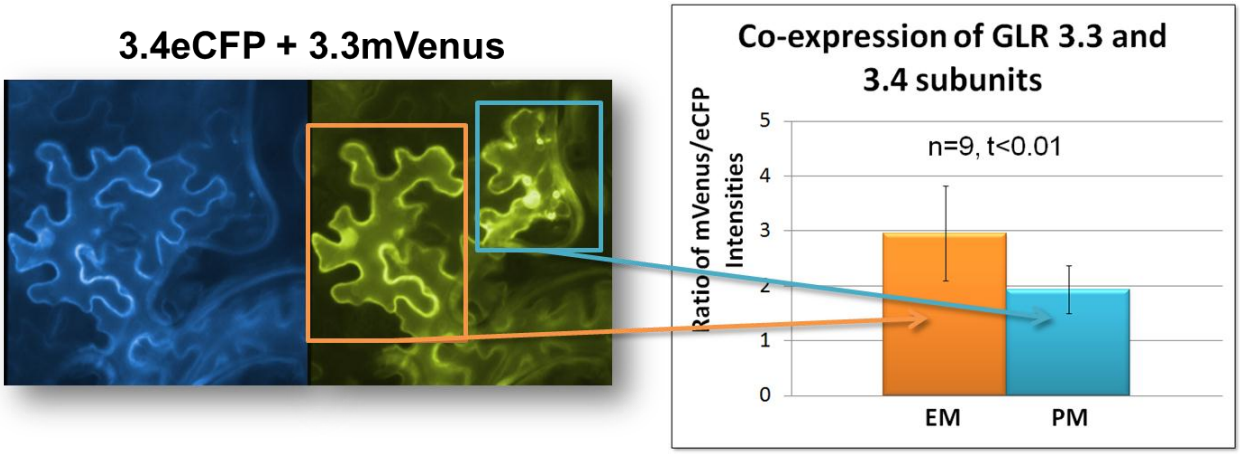

Figure 4-3. Co-expression of GLR 3.3 and 3.4- fluorescent proteins in Nicotiana benthamiana.

Expression of 3.4ECFP (blue) and 3.3mVenus (yellow) demonstrating a higher level of co-expression of both subunits in plasma membrane (PM) localized protein compared to cells singly expressing GLR3.3 showing "grainy" localization in the endomembrane (EM).

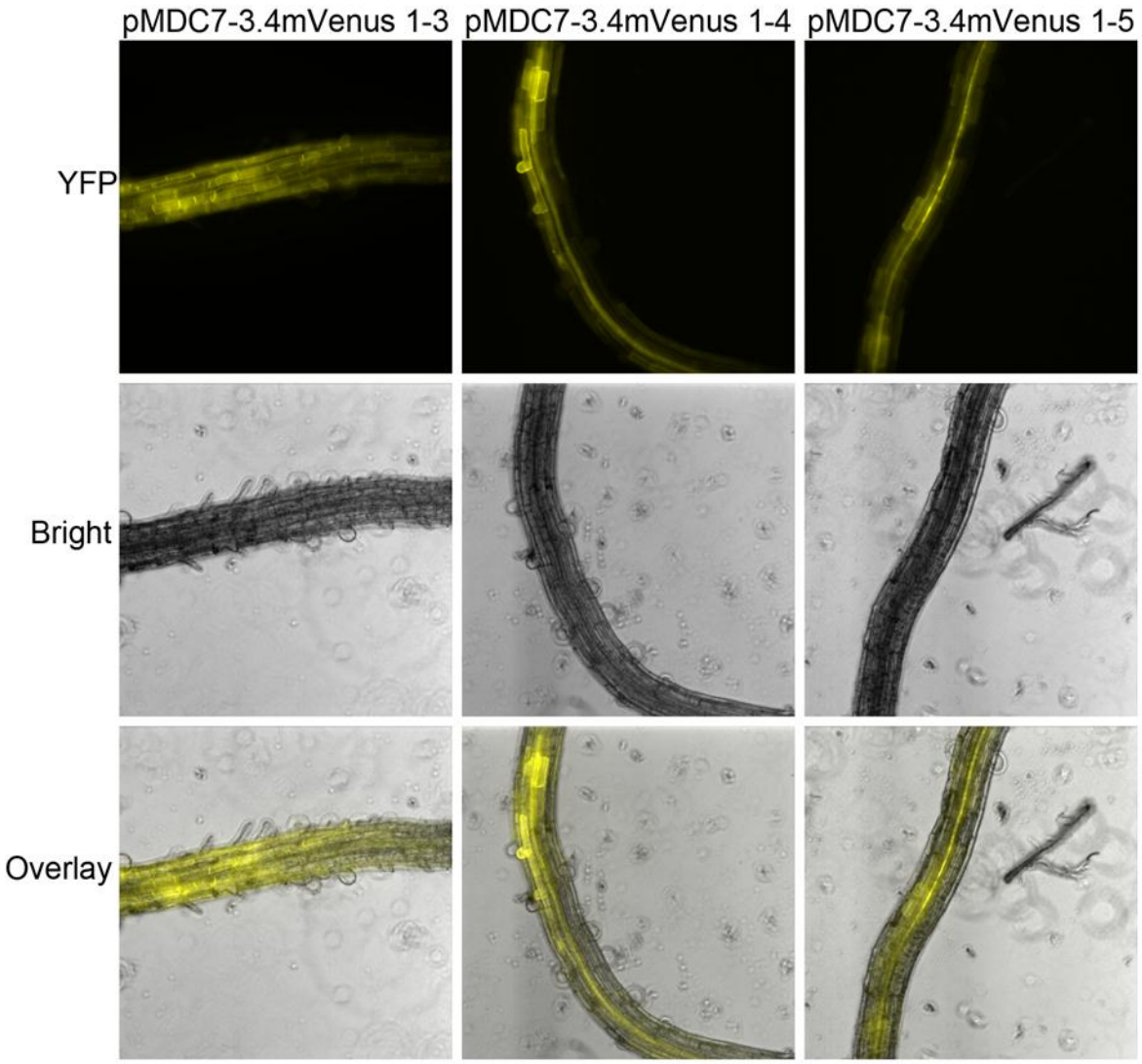

Figure 4-4. Transgenic Arabidopsis seedlings overexpressing GLR3.4.

Fluorescence and brightfield images of 2 week old Arabidopsis roots expressing GLR3.4-mVenus are nicely expressed in plasma membrane and along vascular tissue.

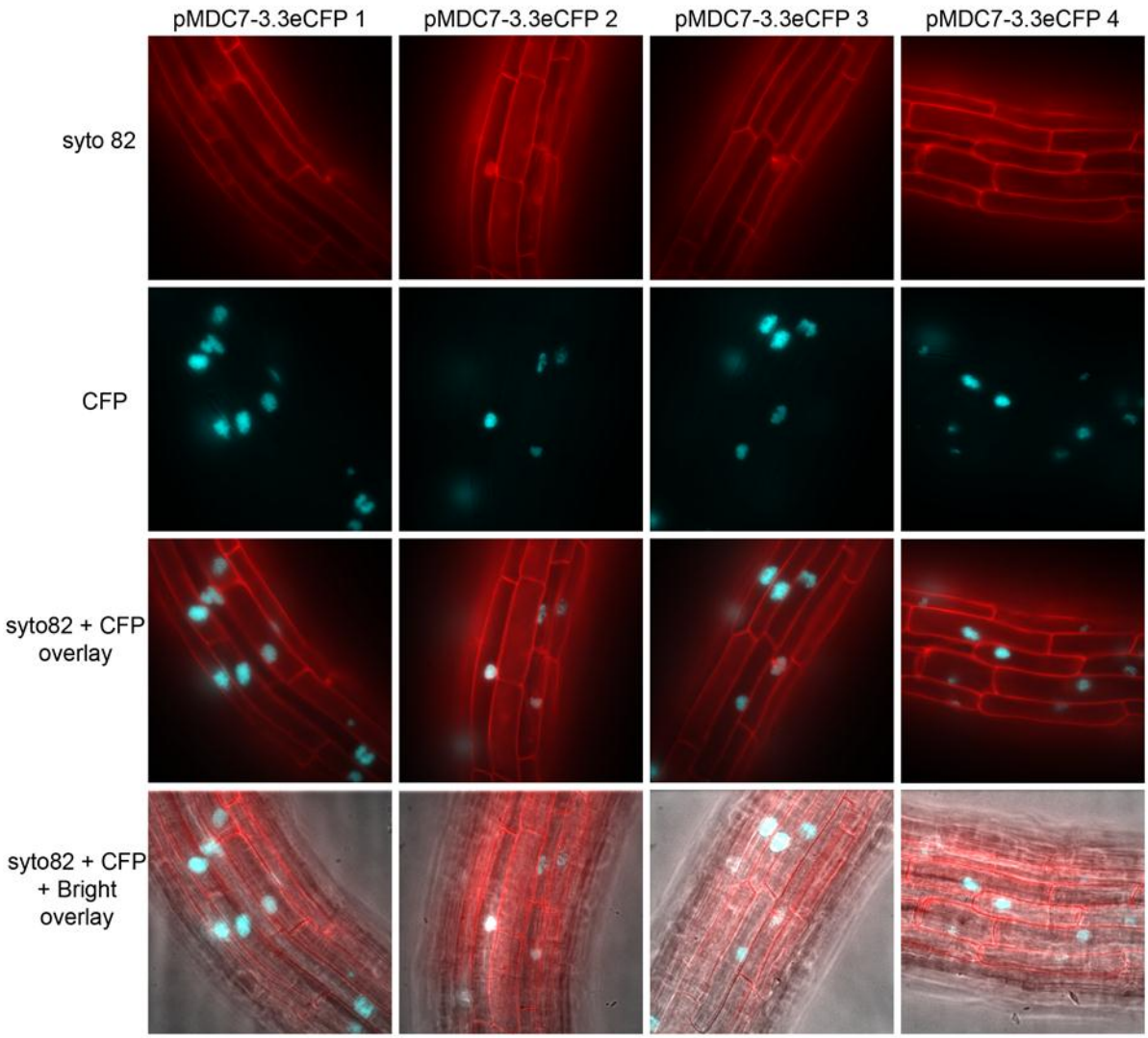

Figure 4-5. Transgenic Arabidopsis seedlings overexpressing GLR3.3.

Fluorescence and brightfield images of 2 week old Arabidopsis roots expressing GLR3.3-ECFP and Syto82 are both expressed in the nucleus.

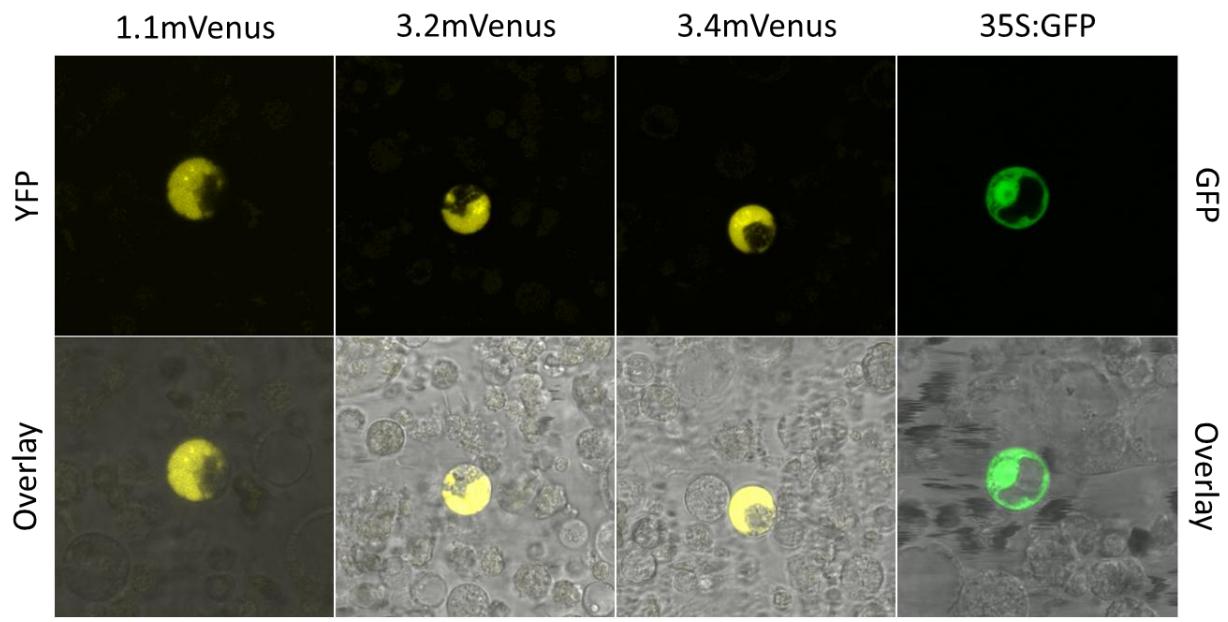

Figure 4-6. Expression of GLR-fluorescent protein fusions in Arabidopsis root protoplasts. Estradiol-inducible pMDC7-GLR-mVenus fusion proteins were transformed into 10 day old *Arabidopsis* root protoplasts and imaged using YFP for mVenus fusions and GFP for positive control and overlayed with bright field image.

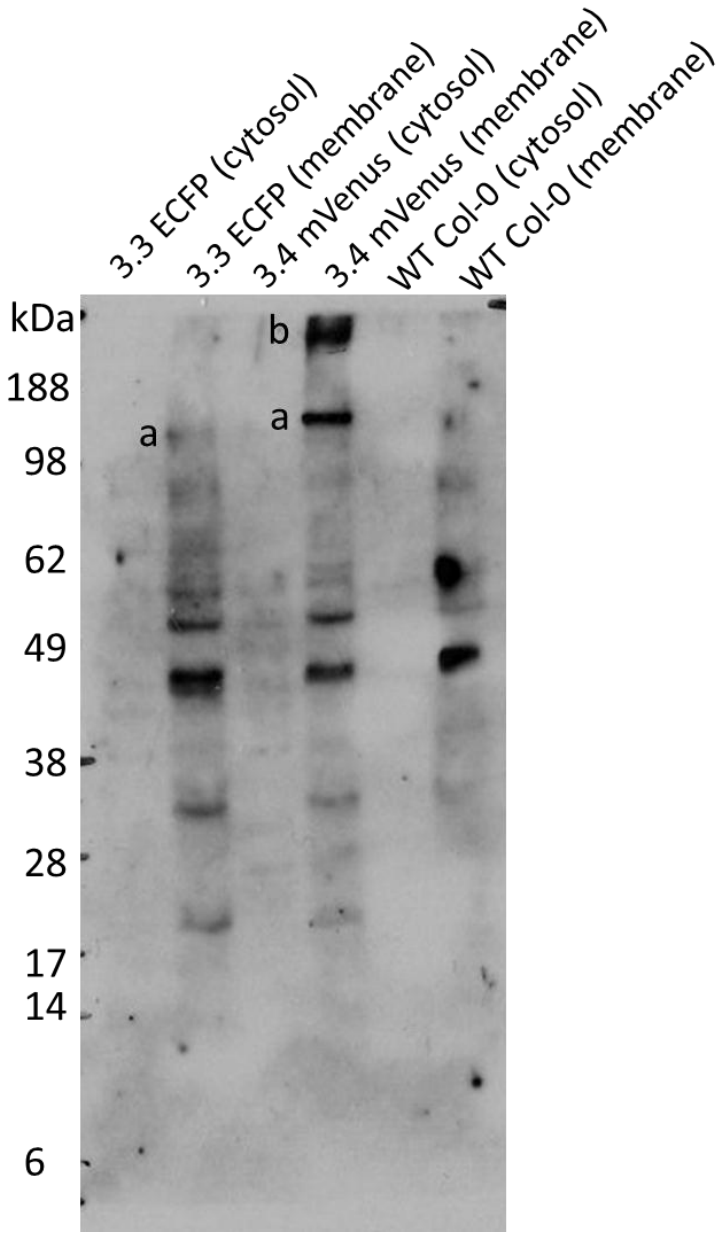

Figure 4-7. Western blot of GLR3.3-ECFP and 3.4-mVenus proteins in *Arabidopsis* seedlings.

Cytosolic and membrane protein fractions of *Arabidopsis* seedlings expressing GLR3.3-ECFP or GLR3.4-mVenus fusion proteins detected with α-GFP polyclonal antibody. Individual proteins are denoted by "a" and suspected multimers are denoted by "b".

LITERATURE CITED

Birnbaum, K., D. E. Shasha, J. Y. Wang, J. W. Jung, G. M. Lambert, D. W. Galbraith and P. N. Benfey (2003). "A gene expression map of the Arabidopsis root." Science **302**(5652): 1956-1960.

Bruex, A., R. M. Kainkaryam, Y. Wieckowski, Y. H. Kang, C. Bernhardt, Y. Xia, X. Zheng, J. Y. Wang, M. M. Lee, P. Benfey, P. J. Woolf and J. Schiefelbein (2012). "A gene regulatory network for root epidermis cell differentiation in Arabidopsis." PLoS Genet **8**(1): e1002446.

Chiu, J., R. DeSalle, H. M. Lam, L. Meisel and G. Coruzzi (1999). "Molecular evolution of glutamate receptors: a primitive signaling mechanism that existed before plants and animals diverged." Mol Biol Evol **16**(6): 826-838.

Curtis, M. D. and U. Grossniklaus (2003). "A gateway cloning vector set for high-throughput functional analysis of genes in planta." Plant Physiol **133**(2): 462-469.

Dundar, E. and D. R. Bush (2009). "BAT1, a bidirectional amino acid transporter in Arabidopsis." Planta **229**(5): 1047-1056.

Karimi, M., D. Inze and A. Depicker (2002). "GATEWAY vectors for Agrobacterium-mediated plant transformation." Trends Plant Sci **7**(5): 193-195.

Lindbo, J. A. (2007). "High-efficiency protein expression in plants from agroinfection-compatible Tobacco mosaic virus expression vectors." BMC Biotechnol **7**: 52.

Malinow, R. and R. C. Malenka (2002). "AMPA receptor trafficking and synaptic plasticity." Annu Rev Neurosci **25**: 103-126.

Marrus, S. B., S. L. Portman, M. J. Allen, K. G. Moffat and A. DiAntonio (2004). "Differential localization of glutamate receptor subunits at the Drosophila neuromuscular junction." J Neurosci **24**(6): 1406-1415.

McGee, A. W. and D. S. Bredt (2003). "Assembly and plasticity of the glutamatergic postsynaptic specialization." Curr Opin Neurobiol **13**(1): 111-118.

Negrutiu, I., Shillito, R.D., Potrykus, I., Biasini, G. and Sala, F. (1987). "Hybrid genes in the analysis of transformation conditions I. Setting up a simple method for direct gene transfer in plant protoplasts." Plant Mol. Biol. **8**: 363-373.

Reinders, A., A. B. Sivitz, C. G. Starker, J. S. Gantt and J. M. Ward (2008). "Functional analysis of LjSUT4, a vacuolar sucrose transporter from Lotus japonicus." Plant Mol Biol **68**(3): 289-299.

Roy, S. J., M. Gilliham, B. Berger, P. A. Essah, C. Cheffings, A. J. Miller, R. J. Davenport, L. H. Liu, M. J. Skynner, J. M. Davies, P. Richardson, R. A. Leigh and M. Tester (2008).

"Investigating glutamate receptor-like gene co-expression in Arabidopsis thaliana." Plant Cell Environ **31**(6): 861-871.

Stephens, N. R., Z. Qi and E. P. Spalding (2008). "Glutamate receptor subtypes evidenced by differences in desensitization and dependence on the GLR3.3 and GLR3.4 genes." Plant Physiol **146**(2): 529-538.

Teardo, E., E. Formentin, A. Segalla, G. M. Giacometti, O. Marin, M. Zanetti, F. Lo Schiavo, M. Zoratti and I. Szabo (2011). "Dual localization of plant glutamate receptor AtGLR3.4 to plastids and plasmamembrane." Biochim Biophys Acta **1807**(3): 359-367.

Tominaga-Wada, R., T. Ishida and T. Wada (2011). "New insights into the mechanism of development of Arabidopsis root hairs and trichomes." Int Rev Cell Mol Biol **286**: 67-106.

Vincill, E. D., A. M. Bieck and E. P. Spalding (2012). "Ca(2+) conduction by an amino acid-gated ion channel related to glutamate receptors." Plant Physiol **159**(1): 40-46.

Vincill, E. D., A. E. Clarin, J. N. Molenda and E. P. Spalding (2013). "Interacting Glutamate Receptor-Like Proteins in Phloem Regulate Lateral Root Initiation in Arabidopsis." Plant Cell.

Voinnet, O., S. Rivas, P. Mestre and D. Baulcombe (2003). "An enhanced transient expression system in plants based on suppression of gene silencing by the p19 protein of tomato bushy stunt virus." Plant J **33**(5): 949-956.

CHAPTER 5:DETERMINATION OF THE ROLE OF PLANT GLUTAMATE RECEPTORS (GLRs) IN RESPONSE TO PATHOGEN INFECTION

INTRODUCTION

Plant Immunity Overview

The lack of mobile immune cells and a so-called circulatory system in plants, compared with mammals, has prompted the plant to develop an efficient immune system. In such a system, each cell is capable of mounting an immune response that is highly specific and capable of reacting to a multitude of stressors. Thusly, a successful plant pathogen must be highly adapted to overcoming these sensory systems. Despite this, the lack of genetic diversity in most major crop species in tandem with pathogen evolution of several unique virulence strategies, as well as other factors such as contamination of irrigation water sources, has enabled plant pathogens to achieve a level of success which is quite devastating to agricultural yield and thus global food security (Steele and Odumeru 2004, Strange and Scott 2005, Dodds and Rathjen 2010).

Most plant pathogens must be able to evade or suppress plant immune defenses as well as acquire nutrients and water in order to successfully colonize plant host tissue. This requires the pathogen to develop mechanisms to modulate the physiology of the host such that it becomes a compatible niche for the pathogen. Depending on the specific plant pathogen, the apoplastic space between plant cells is often the location for this niche despite the fact that it is unfavorable due to presence of several antimicrobial compounds in a relatively nutrient-poor environment (Kunkel 2006, Rico and Preston 2008). Further, a barrier of plant defenses are localized to this extracellular space because of the epiphytic nature of some plant pathogens (Rico and Preston

2008). Thus, successful plant pathogens are capable of modulating the apoplastic environment by suppressing defense responses as well as eliciting nutrients and water from plant cells (Kunkel 2006, Rico and Preston 2008).

Phytopathogenic bacteria utilize an array of virulence strategies to successfully infect hosts which can be both broadly conserved (such as cell wall degrading enzymes) as well as highly specialized (such as virulence proteins or effector molecules) to specific hosts. In most cases, genetic incompatibility is predominant, consisting of 1) lack of ability of host to support life-strategy requirements of pathogen, including availability of nutrients, 2) preformed structural barriers or toxic compounds (such as saponins or glucosinolates) which limit infection to only specialized pathogens that are able to detoxify or resist these compounds, or 3) recognition of pathogen upon attack, resulting in growth inhibition of the invading pathogen (Hammond-Kosack and Jones 2000). Bacterial virulence is defined by the ability of bacteria to increase in growth or population size and disease symptoms which facilitate the release of the bacteria from the plant into the environment (Hammond-Kosack and Jones 2000, Abramovitch, Anderson et al. 2006).

For the purpose of this chapter, focus will be on two types of innate immunity in *Arabidopsis* to the model plant pathogen Pto DC3000 caused either by 1) sensing of conserved pathogen traits known as pathogen-associated molecular patterns (PAMPs) by pattern recognition receptors (PRRs) resulting in PAMP-triggered immunity (PTI) , or 2) effector molecules, which are capable of modulating defense signaling on hosts but may be sensed by disease-resistant plants, resulting in effector-triggered immunity (ETI) (Abramovitch, Anderson et al. 2006, Aslam, Erbs et al. 2009, Boller and Felix 2009).

PTI occurs when bacterial pathogens are betrayed by conserved components known as PAMPs (Darvill and Albersheim 1984, Boller 1995). The most well established PAMPs (pathogen-associated molecular patterns) include flagellin epitope, flg22, which is sensed by the FLS2 (flagellin-sensitive 2) receptor, the elongation factor Tu (EF-Tu) epitope, elf18, which is recognized by the receptor EFR, as well as lipopolysaccharide (LPS), which is the glycolipid component of gram-negative outer membranes (Newman, Daniels et al. 1995, Felix, Duran et al. 1999, Gomez-Gomez and Boller 2000, Felix and Boller 2003, Zipfel, Kunze et al. 2006). A typical defense response elicited by these molecules involves Ca^{2+} and H^{+} influx, and generation of reactive oxygen species (ROS), nitric oxide (NO), and ethylene, as a result of transcriptional changes initiated by calcium-dependent protein cascades (CDPK/KK) and mitogen-activated protein kinase (MAPK/KK) cascades resulting in defense-gene activation (Hammond-Kosack and Jones 2000, Boller and Felix 2009, Newman, Sundelin et al. 2013).

ETI (R-gene-mediated resistance) occurs as a result of direct or indirect interactions of pathogen effector molecules and the products of plant resistance (R) genes (Jones and Dangl 2006). One example is the avirulence gene avrRpt2, a virulence-promoting *P. syringae* type III effector, which is recognized by the plant R-protein RPS2 (resistance to *P. syringae*) and also targets RIN4 (RPM1-interacting protein 4) in *Arabidopsis* to promote virulence (Chen, Kloek et al. 2004, Kim, da Cunha et al. 2005, Chen, Agnew et al. 2007, Cui, Wu et al. 2013). With ETI, recognition leads to a stronger defense reaction called the hypersensitive response which results in localized tissue necrosis due to rapid apoptosis (Martin, Bogdanove et al. 2003, Nimchuk, Eulgem et al. 2003).

Potential Role of GLRs in Calcium-Mediated Defense Signaling

One of the earliest responses to PAMPs consists of an influx of Ca^{2+} leading to an increase in cytosolic Ca^{2+} concentrations causing membrane depolarization and potentially serving as a second messenger to open other membrane channels or activate CDPKs. However the ion channels or transporters responsible are not very well understood. Calcium is known to act as a second messenger in many biotic and abiotic stress responses, including responses to microbial attack, temperature, oxidative stress, and plant hormones (Lecourieux, Ranjeva et al. 2006, Aslam, Erbs et al. 2009, Boller and Felix 2009, Batistic and Kudla 2012). While some orthologs of mammalian calcium channels are lacking in plants, there are a number of potential candidates for calcium-mediated defense signaling in plants. These include cyclic nucleotide gated channels (CNGCs), voltage-gated channels, and plant homologs of ionotropic glutamate receptors (iGluRs) known as glutamate receptor-like proteins (GLRs) (Very and Sentenac 2002, Lecourieux, Ranjeva et al. 2006, Batistic and Kudla 2012).

Investigation of publicly available microarray data shows differential regulation of clade 1 GLRs in response to bacterial elicitors and effectors (Hruz T, Laule O et al. 2008). A recent examination of transgenic *Arabidopsis* seedlings expressing the Ca^{2+} sensor aequorin using specific calcium channel blockers to determine where and how intracellular Ca^{2+} increases in response to PAMPs flg22 and elf18 was undertaken (Kwaaitaal, Huisman et al. 2011). In this study, it was demonstrated that known antagonists of mammalian iGluRs were capable of diminishing the transient Ca^{2+} response elicited by flg22 and elf18, but not chitin (Kwaaitaal, Huisman et al. 2011). Further, the known iGluR-agonists, glutamate and kynurenic acid, are capable of modulating transcription of PAMP-triggered defense genes downstream of CDPK and MAPK cascades (Kwaaitaal, Huisman et al. 2011).

Thus, it is likely that plant glutamate receptors are capable of modulating defense signaling induced as a result of PTI. This research aims to explore this possibility by 1) examining growth of Pto DC3000 on plants deficient in clade 1 GLRs; 2) characterize the response of GLR-deficient plants to PAMP elicitors flg22 and elf18; and 3) elucidate which clade 1 GLRs are responsible for immune response to *P. syringae* pv. tomato DC3000.

RESULTS

Identification of T-DNA insertion lines

In order to test whether GLR1 genes indeed are involved in plant-pathogen interactions, we isolated T-DNA insertion lines. Multiple insertion lines were found in publicly available seed stocks (Figure 5-1A). All of the lines listed in Table 1 were tested for T-DNA insertion by PCR using insertion-specific primers. Among those lines, two insertion lines for *GLR1.1*, one for *GLR1.2*, and one for *GLR1.4* were confirmed and were successfully made homozygous by self-pollination. The insertion lines, designated *glr1.1-1, glr1.1-3, glr1.2-1, and glr1.4-1,* are indicated in Figure 5-1B. Transcript abundance of respective genes was examined using quantitative reverse transcriptase (qRT)-PCR (Figure 5-2). The results indicated that the transcript levels were decreased to nearly undetectable level for *glr1.1-1 and glr1.1-3*, and less than 10% and 20% of wild-type for *glr1.2-1, and glr1.4-1* (Figure 5-2). Interestingly, examination of Clade 1 GLRs in single gene knock-outs revealed an increase in 1.2 and 1.3 transcript abundance for *glr1.1-1* and a decrease in 1.3 transcript for *glr1.2* alleles, suggesting that expression of certain GLRs may regulate the expression of other GLRs (Figure 5-3).

Multi-gene knock-down lines using artificial microRNA (amiRNA)

In addition to the T-DNA insertion lines, we attempted to create transgenic plants expressing artificial microRNA (Schwab, Ossowski et al. 2006), in order to suppress expression of multiple genes. Four independent target sequences were chosen, which are predicted to target multiple GLR1 genes (Table 5-1). Plants carrying the homozygous amiRNA transgene were obtained for two (amiRNA II, which is predicted to target *GLRs 1.2, 1.3*; and *1.4* , and amiRNA VI, which target *GLRs 1.2* and *1.3*) of the four constructs. For amiRNA II-expressing lines, there appears to be no effect on *GLR1.3* and *1.4* transcript abundance whereas the expression of *GLR1.2* and off-target *GLR1.1* were reduced in all lines (Figure 5-4A). For amiRNA VI lines, three independent lines were identified based on RT-PCR showing a decrease in 1.2 and/or 1.3 transcript abundance (Figure 5-4B). However, subsequent qRT-PCR using gene specific primers showed variable levels of *GLR1.2* and *1.3* transcripts among independent experiments (data not shown). We hypothesized that the primers used for qRT-PCR may have detected partially degraded products along with the full-length mRNAs. To examine such possibility, primers which are located on either sides of predicted target region conserved among *GLRs 1.2* and *1.3* were designed. qRT-PCR using these primers revealed that at least one line shows a reduction in *1.2/1.3* transcript abundance (Figure 5-4C).

Phenotypical examination of single gene knock-out and artificial microRNA II plants did not show any differences between mutants and wild-type. AmiRNA-VI plants, however, do tend to be larger and flower later than wild-type plants when well-fertilized, with stress or low-nutrient conditions alleviating this difference (data not shown).

Expression of Clade 1 GLRs is Altered in Response to Pathogen Infection

In order to examine whether expression levels of GLR1 genes are indeed induced by pathogen infection, transcript abundance of GLR1.1, 1.2, 1.3 and 1.4 were analyzed. Transcript levels were determined by qRT-PCR on cDNA isolated from either mock- or *P. syringae* pv. tomato DC3000- inoculated wild-type *Arabidopsis thaliana* ecotype Columbia-0 10 day-old seedlings grown in liquid. The results showed that the transcript abundance of GLRs 1.2, 1.3 and 1.4 were increased by 44-, 12-, and 18-fold, respectively (Figure 5-5). No significant change were observed for GLR1.1 expression levels under the condition tested.

Because of the similarities in GLR genes, the potential for altered transcript abundance of Clade 1 GLRs as a result of functional compensation was examined using qRT-PCR. Interestingly, the two alleles of GLR1.1, *glr1.1-1* and *glr1.1-3* which are in different backgrounds (Columbia-0 and Wassilewskija, respectively) differ in compensation by other GLRs, where *glr1.1-1* has an increase in GLR1.2 expression not found in the *glr1.1-3* allele (Figure 5-3A). Of further interest, there is a decrease in GLR1.3 transcripts in knock-out alleles of GLR1.2 (Figure 5-3B). No significant changes were observed for GLR Clade 1 genes in *glr1.4-5* alleles (Figure 5-3C).

Decrease in Pathogen Growth in GLR-Deficient Seedlings Grown in Liquid Culture

Two-week old T-DNA insertion lines deficient in GLRs 1.1 or 1.4 (Figure 5-3) grown in liquid culture and challenged with *P. syringae* pv. tomato DC3000 had a decrease in pathogen growth response (Figure 5-6). On the other hand, bacterial growth in plants deficient in GLR1.2 gene expression (Figure 5-3), was not significantly different from wild-type (Figure 5-6).

Examination of artificial microRNA-II plants targeting GLRs 1.2, 1.3, and 1.4 showed a decrease in transcript abundance for 1.1 and 1.2 in all three independent lines, with variable

transcript abundances for 1.3 and 1.4 (Figure 5-4A). A decrease in pathogen growth in all three independent artificial microRNA-II lines was observed in this system (Figure 5-7). Artificial microRNA-VI (referred to as Kunkel 6) targeting GLRs 1.2 and 1.3 only show a decrease in transcript abundance for GLR1.3 in one of three independent lines (Figure 5-4C). However, the induction of GLR1.2/ 1.3 expression by challenge with DC3000 was decreased in all three independent lines (Figure 5-8). Plants expressing amiRNA-VI (Kunkel 6) did not show an altered ability for pathogen growth in liquid culture (Figure 5-7).

Pathogen Growth in Soil-Grown GLR-Deficient Plants Infiltrated with P. syringae pv. Tomato DC3000

Pathogen growth in *glr* mutants was further investigated in plants grown on soil. Leaves of four-week old, soil-grown plants carrying T-DNA insertions in GLR1.1, 1.2, and 1.4 (Figure 5-2A) were infiltrated with *P. syringae* pv. tomato DC3000. Representative results are summarized in Figure 5-9. From these results, it was concluded that the growth of *P. syringae* pv. tomato DC3000 is not different under this condition in any of the insertion lines tested.

Plants expressing artificial microRNA-VI were also tested for the growth of DC3000. Slight, but statistically significant, increases in pathogen growth were detected in multiple experiments (Figure 5-10).

DISCUSSION

Phenotypic Analysis of GLR-Deficient Plants

Examination of knock-down or knock-out mutants of genes help identifying protein functions *in planta*. In this study, both T-DNA insertion lines and artificial microRNA engineered lines were utilized to examine the resultant phenotypic changes when expression of single or multiple GLRs is minimized or abolished. T-DNA insertion lines of *GLRs* 1.1, 1.2 and 1.4 did not have any obvious phenotypic changes with regards to their respective wild-type ecotypes. Changes in gene expression of other GLR family members were observed using qRT-PCR.Abolished GLR1.1 expression resulted in a concomitant increase in GLRs 1.2 ($p=0.043$) and 1.3 ($p=0.036$) transcript abundance compared with wild-type Columbia-0 (Figure 5-3A).A slight decrease in GLR1.3 expression was observed in knock-outs of GLR1.2 ($p=0.066$). No changes in Clade 1 GLR transcripts were seen in knock-outs of GLR1.4 (Figure 5-3). Artificial microRNAs designed to target multiple GLRs for knock-down were also utilized. The only physiological changes observed were amiRNA-VI lines, where plants were larger compared to their wild-type ecotype when nutrient conditions were favorable. There is a decrease in the off-target GLR1.1 for the amiRNA-II lines (targeting 1.2, 1.3, and 1.4), with variable changes in the remaining Clade 1 GLRs. Whether and which GLR gene expression changes are responsible for differences in growth remains to be investigated.

Bacterial growth in glr knockout plants

We have investigated the growth of Pto DC3000 in multiple lines of plants deficient in *glr* Clade 1 gene expression. We utilized two systems (i.e. liquid cultures and soil-grown plants) to evaluate bacterial growth. Interestingly, the two systems produced very different results; for example, the bacterial growth measured in liquid culture for *glr1.1* plants were very consistently decreased compared to the wild-type, whereas no such effect was observed when plants were

grown on soil. Such disconnect can be due to a number of factors. For example, the age of plant used for each experiment differed greatly, which may play a significant role in their response to pathogens, where 10 day-old seedlings were used in liquid culture assays and four-week old plants were used for soil assays (Peters 1999, Korves and Bergelson 2003). The high-humidity environment of liquid cultures, compared to the relatively dry soil conditions most likely plays a significant role in pathogen success due to their requirement for open stomata for invasion (Zeng, Brutus et al. 2011). Notably, ethylene may have been produced as a result of the flood-like growth conditions; two transcription factors regulating ethylene biosynthesis, EIN3 (ethylene-insensitive 3) and EIL1 (ethylene-insensitive-like 1), have been shown to repress plant immunity by negatively regulating SA (salicylic acid) biosynthesis (Chen, Xue et al. 2009) .

While we did not observe any bacterial growth difference between soil-grown *glr* mutants and WT, we did observe a mild increase in susceptibility for one of the amiRNA plants. Since many of the GLRs, including GLR1.2 and 1.3 tested here are in tandem location, the approach of using amiRNA to target multiple genes is valuable. At this point, we cannot exclude that the phenotypic change we observed is due to a secondary effect of off-target genes. The results need to be confirmed through compensation (native-promoter driven expression) of individual and multiple GLRs to restore wild-type phenotype, as well as examination of protein abundance changes.

Very recently, it was demonstrated that a T-DNA insertion mutant in *glr3.3* had enhanced susceptibility to pathogens such as Pto DC3000 and *Hyaloperonospora* in *Arabidopsis*. Moreover, it was also suggested to play a role in wounding-induced long distance signaling (Mousavi, Chauvin et al. 2013). These data collectively suggest that GLR3.3 is involved in a very early step of biotic and abiotic stress recognition. Surprisingly, we did not see any evidence

for the induction of GLR3.3 expression in any of the publically available transcriptome data, whereas a number of other GLRs, including GLR1 clade genes, were induced by a number of biotic and abiotic stresses. Considering the fact that GLR3.3 does interact with some of the other GLRs (see Chapter 3), some of which are induced by biotic stresses, it is tempting to speculate that pathogen-induced GLR subunits would modulate the function of GLR3.3, and lead to the change in channel properties. Such plasticity is well documented as long-term potentiation in animal neurons (Bliss and Collingridge 2013, Moreau and Kullmann 2013). It would be very interesting to investigate whether the induction of GLRs results in such modification of channel properties.

Role of GLRs in Plant Defense

Evidence of a role for plant glutamate receptors in response to plant-pathogen interaction is now of major interest due to several recent reports discussed previously. Currently, however, the exact mechanism for GLR involvement is unclear and likely to be quite complex. The decrease in pathogen growth of single gene knock-outs for GLRs 1.1 and 1.4 in liquid cultures when challenged with Pto DC3000 suggests that these proteins may be negative regulators of plant immunity. Conversely, targeted disruption of multiple GLRs using artificial microRNAs resulting in an increase in pathogen susceptibility suggests that these proteins may be positive regulators. It is possible that even through these genes belong to the same family they play opposite roles in defense against Pto DC3000. Alternatively, functional compensation caused by one gene knockout (Fig. 5-3) might be causing the difference in the respective phenotypes.

Several scenarios are possible, and given the diversity of apparent physiological roles of this large protein family, quite probable that one or more are occurring simultaneously. First,

GLR cation channels may be directly involved in sensing of molecules in the extracellular environment (either specifically released through transporter proteins or non-specifically released from cellular damages) as a direct result of pathogen-elicited release. In such a case, ligands could be acting to agonize the channel and promote calcium-mediated defense signaling. Alternatively, change in extracellular metabolites upon infection might decrease the conductivity of GLRs by antagonizing the channels, resulting in an altered calcium signature in the cells. Calcium signaling is indispensable for response to SA-mediated response against biotrophic pathogens(Levine, Pennell et al. 1996, Ma and Berkowitz 2007). At the same time, calcium has been indicated in responses to other hormones, including ethylene that generally is considered as antagonizing to SA. Therefore activation of GLR could result in both an increase or decrease in growth of biotrophic pathogens. Cellular calcium signatures are very complex, both amplitude and frequency playing major roles in the output (Swanson, Choi et al. 2011). It would therefore be very interesting to investigate how calcium signatures are affected in GLR mutants, and how such change influences the outputs of various defense hormone signaling. Whichever the case, the role of plant GLRs in immunity is becoming more apparent and is quite novel compared to their bacterial and mammalian counterparts.

MATERIALS AND METHODS

T-DNA Insertion Lines

Multiple T-DNA insertion lines for individual GLR genes from Clade 1 were obtained from the Arabidopsis Biological Resource Center (ABRC, (Reiser and Rhee 2005)) and are listed in Figure 5-1. These genes were selected based on the following criteria: availability from ABRC (Reiser and Rhee 2005) and potential for ligand-gated cation conductance as determined by

similarity in amino acid sequence identity of plant glutamate receptors (GLRs) and animal ionotropic glutamate receptors (iGluRs) (Davenport 2002). For each gene, attempts were made to obtain more than one independent T-DNA insertion allele, however for GLRs 1.2 and 1.4 this was not possible, so 3 different plant lines were examined to demonstrate consistency. Using this approach, homozygous lines were obtained for *glr1.1-1, glr1.1-3, glr1.2, glr1.4-1,* and *glr1.4-5* (Figure 5-1). A combination of genomic DNA PCR and quantitative real-time PCR was used to confirm a decrease in transcript abundance as described below.

Generation of Artificial MicroRNA Gene Knock-down Lines

Artificial microRNAs (amiRNAs) targeting conserved sequences between GLR genes 1.1, 1.2, 1.3, and 1.4 have been designed using Web-MicroRNA Designer2 (Schwab, Ossowski et al. 2006). These structures form a secondary structure known as a hairpin RNA which is then chopped into approximately 21mer single stranded- RNA units that target specific mRNA sequences and lead to degradation of transcript, thus "knocking-down" the available transcript (Ossowski, Schwab et al. 2008). Site-directed mutagenesis (Kunkel 1985) and PCR stitching (Schwab, Ossowski et al. 2006, Ossowski, Schwab et al. 2008) was performed to replace microRNA sequences on the pRS300 template (obtained from Dr. Weigel, Max Planck Institute for Developmental Biology, Tübingen, Germany) with the designed artificial microRNAs (listed in Table 3-1). Using this strategy, homozygous amiRNAs were obtained which target GLRs 1.2 and 1.3 (Kunkel 6) as well as GLRs 1.2, 1.3, and 1.4 (amiRNA II). A combination of genomic DNA PCR and quantitative real-time PCR was used to confirm a decrease in transcript abundance as described below.

Antibiotic Segregation for Homozygous Lines

Each T1 line was segregated for resistance to the appropriate antibiotic selection marker on Murashige and Skoog (MS) basal salt media (Phytotechnology Labs Catalog # M524) supplemented with 2% (w/v) sucrose and 0.8% (w/v) plant agar (Phytotechnology Labs Catalog # A181) adjusted to pH5.8. Seeds were vernalized at 4°C in the dark for 2 days prior to growth under long day conditions (16 hour light/ 8 hour dark) at light intensity between 120-150 μmol/m^2sec at 22°C for approximately 2 weeks before transplanting to soil (for kanamycin selectivity at 50μg/mL) or growth under 24 hour continuous light at light intensity between 100-120 μmol/m^2sec at room temperature for 1 week prior to transplanting to soil (for hygromycin selectivity at 20μg/mL). Plants were selfed to produce T2 seeds which were then segregated in the same manner to confirm homozygosity through antibiotic resistance.

Genomic DNA PCR to Identify Homozygous Lines

Leaf tissue excised from 2-3 week old plants were homogenized in 50μL TE (10mM Tris-HCl and 1mM EDTA, pH8.0) using one 3mm glass bead in a 1.5mL eppendorf tube in a tissue amalgamator at room temperature for approximately 20 seconds, and immediately transferred to ice. Total cellular DNA was isolated using the cetyltrimethylammonium bromide method (Murray and Thompson 1980). PCR amplification of amplicons flanking the T-DNA insertion site, as well as gene-specific regions was performed where the presence of a gene-specific amplicon and absence of a T-DNA flanking amplicons were indication of potential homozygosity, and seeds from those plants were harvested for further characterization.

In Planta Pathogen Growth Response

Four week old leaves from *Arabidopsis* were infiltrated with OD_{600} of 0.001 using a 1-mL needless syringe, using water as a mock-wounding control. Following inoculation, plants were placed in a high humidity environment for 24 hours and allowed to recover for 24 hours. The infected leaf samples were collected at 2 and 3 days post infection (dpi), ground in sterilized low-salt LB (Luria-Bertani Lennox) broth, plated onto LB agar media containing the appropriate antibiotics, and allowed to grow at 28°C for 2 days. At least 3 independent experiments were performed by counting colony forming units for a minimum of 4 biological replicates per experiment.

Alternatively, a liquid-growth assay was performed on 2 week old *Arabidopsis* seedlings. In this method, seeds were surface sterilized by incubating in 1.2% NaHClO (bleach) and 50% ethanol for 20 minutes, rinsing 3 times with 100% ethanol, and air-drying. Approximately 20 seeds per chamber of 12-well sterile microtiter plate were vernalized 2 days in the dark in 1mL of 1x Murashige and Skoog basal media (PhytoTech Labs) supplemented with 0.5% sucrose, pH5.7, then grown for 8 days under 16h light/8h dark, 100 µE.m-2.s-1 of irradiance, and 22°C constant temperature. Growth media was then refreshed and plants allowed to grow 2 days prior to challenge with Pto DC3000 bacteria inoculated at OD_{600} 0.00002. 36 hours post-infection, seedlings were harvested and blotted to remove excess media, ground in sterile low-salt LB, plated onto LB agar media containing the appropriate antibiotics, and allowed to grow at 28°C for 2 days. At least 2 independent experiments were performed bycounting colony forming units for a minimum of 2 biological replicates per experiment.

Quantitative Real-Time PCR of GLR Genes

Leaf tissue from 2-3 weekold plants were harvested and immediately flash frozen in liquid nitrogen in 1.5mL eppendorf tubes containing one 3mm glass bead and homogenized using a tissue amalgamator for 20-30 seconds and immediately transferred to ice. Total RNA isolation was performed using Qiagen RNeasy mini kit (Qiagen 74104) with on-column DNaseI digestion (Qiagen Catalog # 79254). cDNA synthesis was performed on total RNA to make a final concentration of 40 ng/μL cDNA using High Capacity cDNA Reverse Transcription Kit (Applied Biosystems Catalog # 4374966). Relative quantitative real-time PCR (qRT-PCR) was performed on 100ng cDNA using DyNAmo HS SYBR Green qPCR Kit (Thermo Scientific Catalog # F-410L) on ABI7300 Instrument, with at least two biological replicates and two technical replicates per sample and primer combination. Data was analyzed using the Pfaffl method, where the ratio of target gene: control gene (ubiquitin, UBQ10) was calculated from relative PCR efficiencies of both the target and reference gene for treated (mutant) and non-treated (wild-type) samples (Pfaffl 2001).

FIGURES

A

Gene	AGI number	line	allele	insertion	marker gene	background
AtGLR1.1	AT3G04110	SALK_057748C	*glr1.1-1*	4th exon	Kan	col-0
		SALK_117347	*glr1.1-2*	4th exon	Kan	col-0
		FLAG_526D10	*glr1.1-3*	3rd exon	Kan+BASTA	WS
AtGLR1.2	AT5G48400	FLAG_558C03	*glr1.2-1*	1st exon	Kan+BASTA	WS
		SALK_053535C	*glr1.2-2*	4th exon	Kan	col-0
		SALK_114821	*glr1.2-3*	2nd exon	Kan	col-0
AtGLR1.3	AT5g48410	SAIL_791_A03	*glr1.3-1*	1st exon	Basta	col-0
		FLAG_481E08	*glr1.3-2*	4th exon	Kan+BASTA	WS
AtGLR1.4	AT3G07520	SALK_129955C	*glr1.4-1*	5'UTR?	Kan	col-0
		FLAG_340G04	*glr1.4-2*	2nd exon	Kan+BASTA	WS
		SALK_124603	*glr1.4-3*	1st intron	Kan	col-0
		SALK 021986C	*glr1.4-4*	5th exon	KAN	col-0
		SAIL 398-E07	*glr1.4-5*	1st exon	BASTA	col-0

B

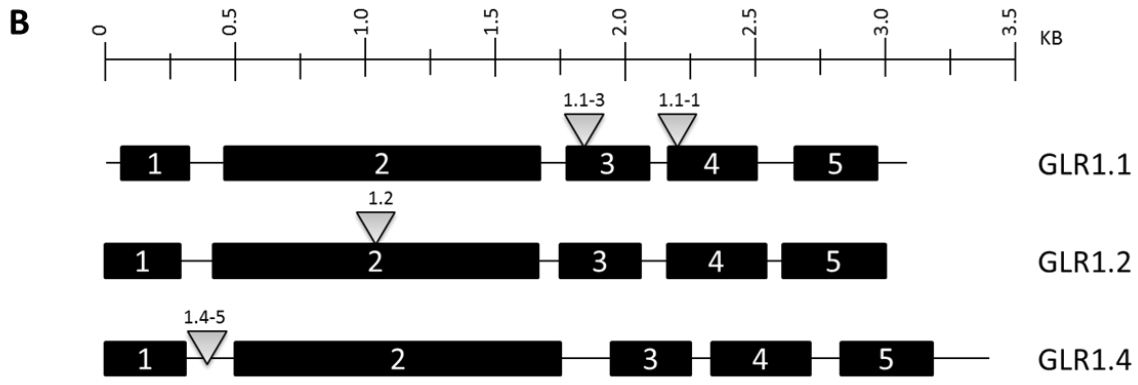

Figure 5-1. T-DNA insertion lines for Clade 1 GLRs.

A) Complete list of Clade 1 GLR germplasms from Arabidopsis Biological Resource Center obtained to attempt to identify homozygous insertion lines disrupting individual GLR gene expression. B) Successful T-DNA insertion lines characterized with alleles for each of the GLR Clade 1 genes.

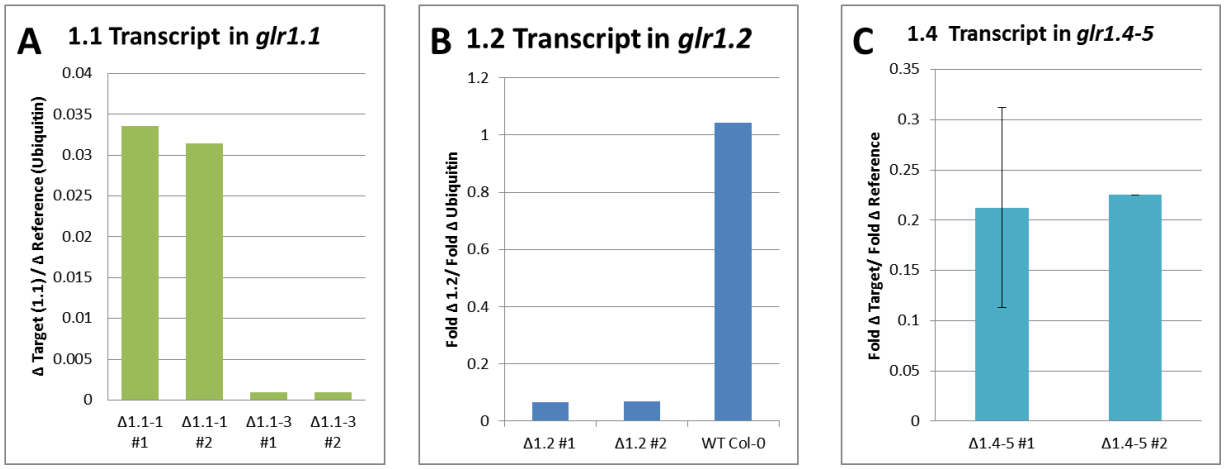

Figure 5-2. Relative transcript abundance of GLR genes in T-DNA insertion lines.

Fold change in target gene expression compared to wildtype ubiquitin abundance in A) *glr1.1* alleles, B) *glr1.2* alleles, and C) *glr1.4* alleles. Each bar represents independent plant lines examined using qRT-PCR.

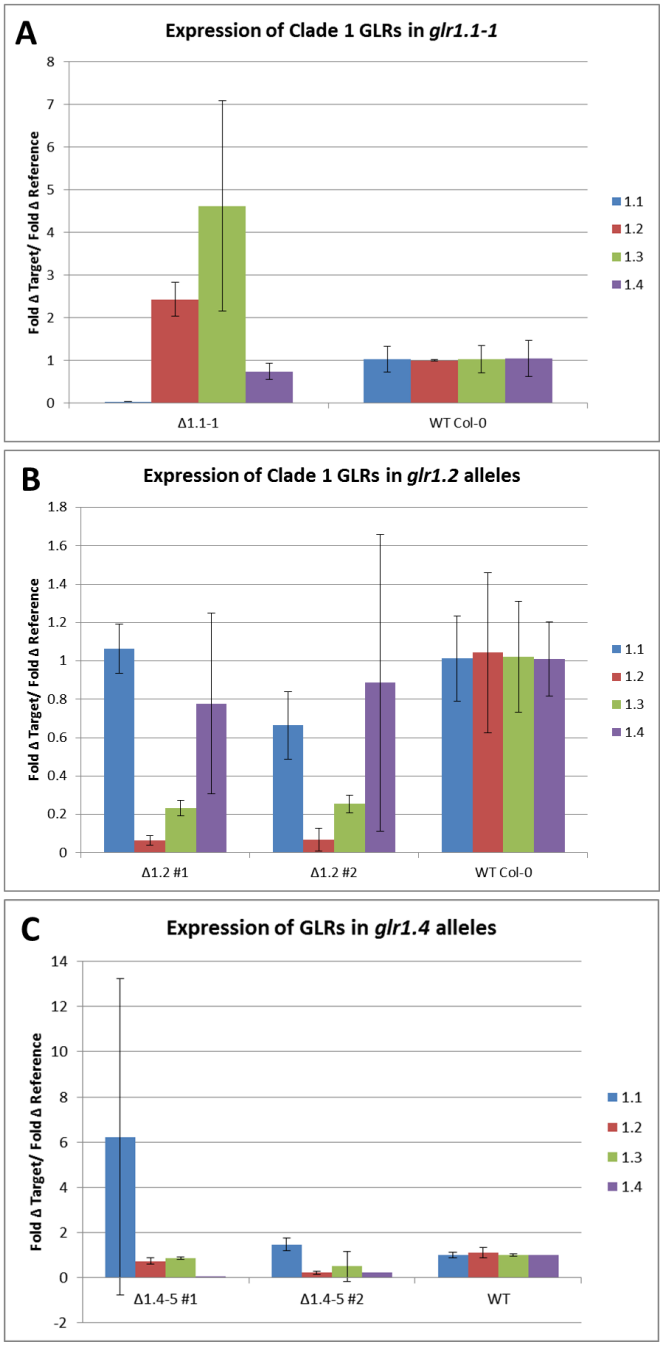

Figure 5-3. Relative transcript abundance of GLR Clade 1 genes in GLR T-DNA insertion lines.

Transcript abundance for GLRs 1.1, 1.2, 1.3, and 1.4 genes relative to wild-type ubiquitin abundance for A) *glr1.1-1*, B) *glr1.2*, and C) *glr1.4* homozygous T-DNA insertion knock-out seedlings.

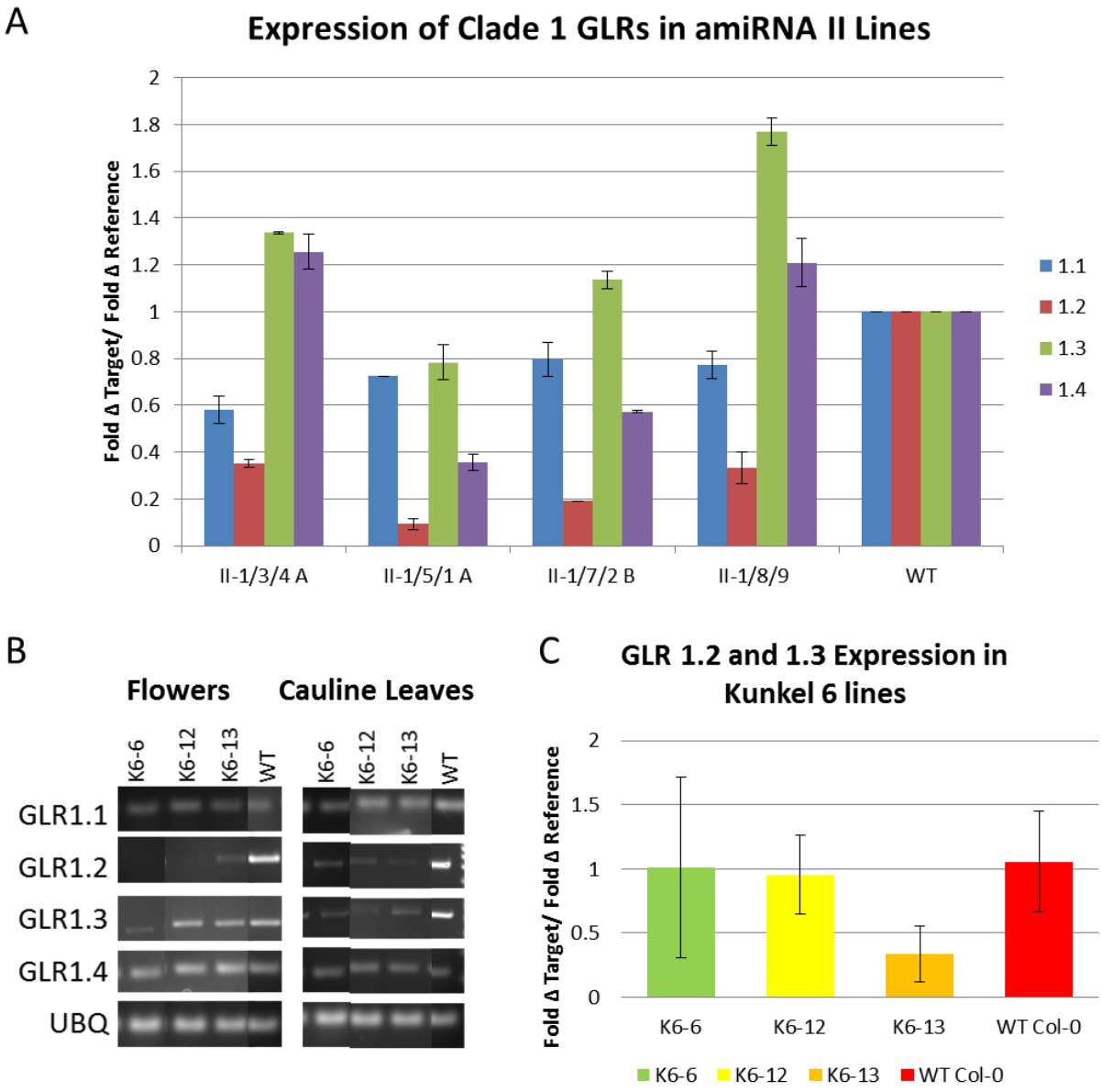

Figure 5-4. Relative transcript abundance of GLR genes in artificial microRNA lines.

Transcript abundance relative to wild-type ubiquitin abundance for A) microRNA-II independent lines, B) reverse-time PCR result for GLR1.2 and 1.3 transcripts in flowers and cauline leaves of artificial microRNA-VI (Kunkel 6) independent lines, and C) qRT-PCR transcript abundances of conserved target regions between 1.2 and 1.3 for Kunkel 6 plants.

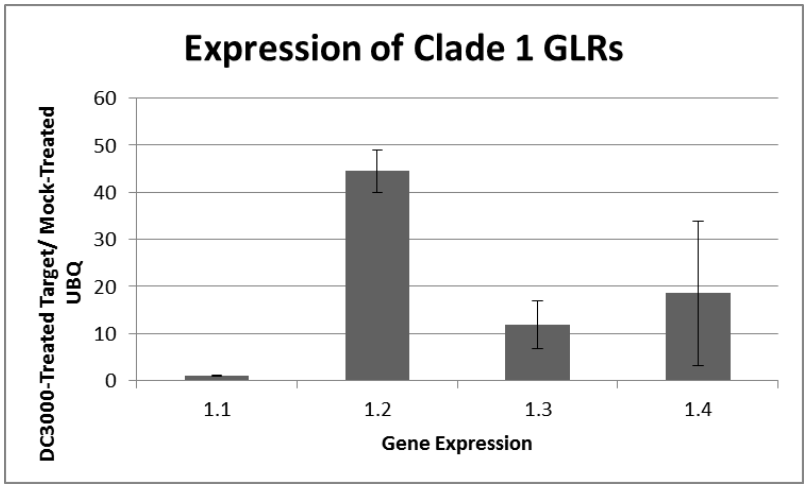

Figure 5-5. Expression of GLRs 1.2 and 1.3 is induced upon pathogen challenge in wildtype *Arabidopsis* seedlings grown in liquid culture.

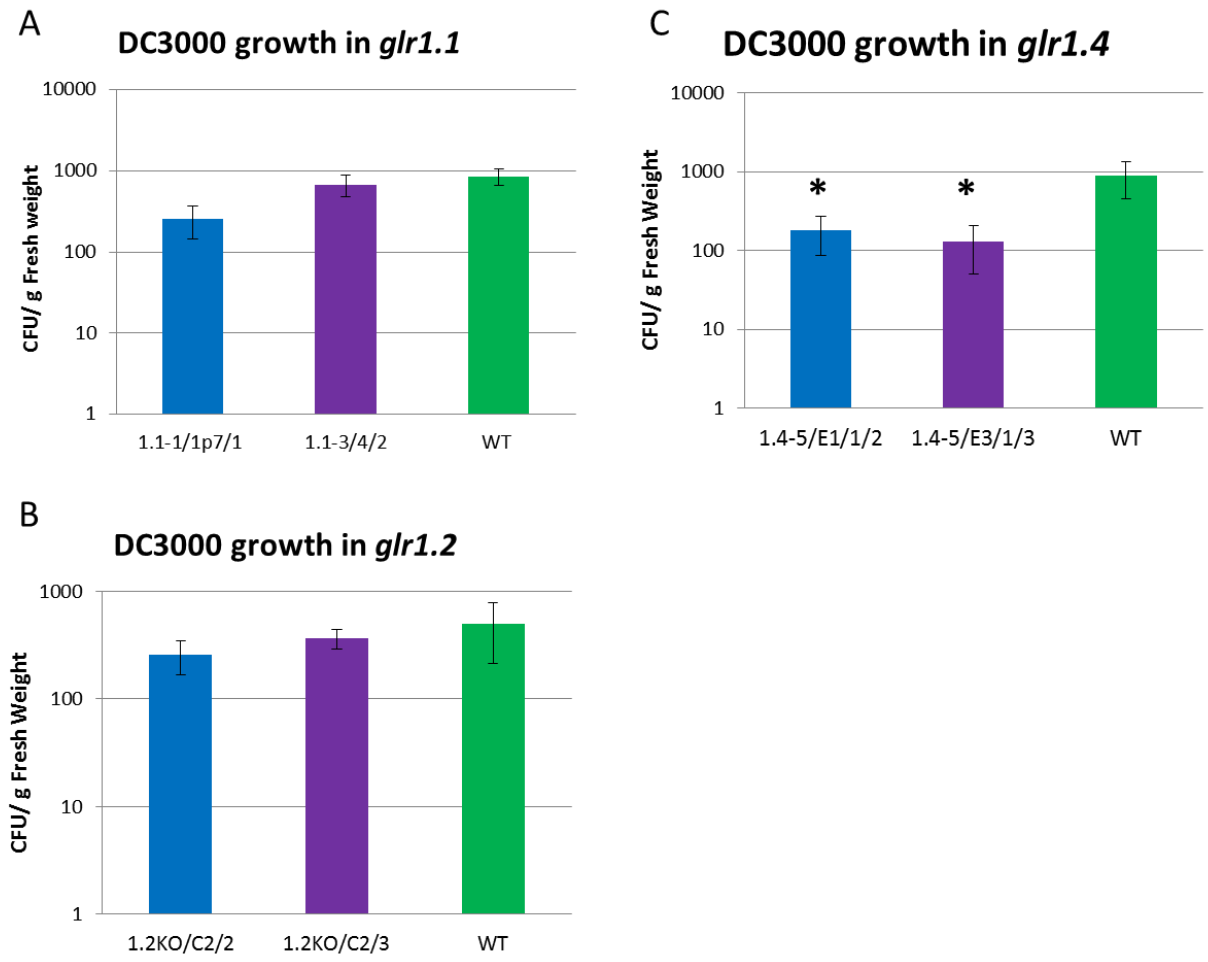

Figure 5-6. Bacterial growth responses in T-DNA insertion lines grown in liquid culture.

Growth of *P. syringae* pv. Tomato DC3000 shown in colony forming units (CFU) per gram fresh weight tissue for A) *glr1.1* alleles, B) *glr1.2* alleles, and C) *glr1.4* alleles.

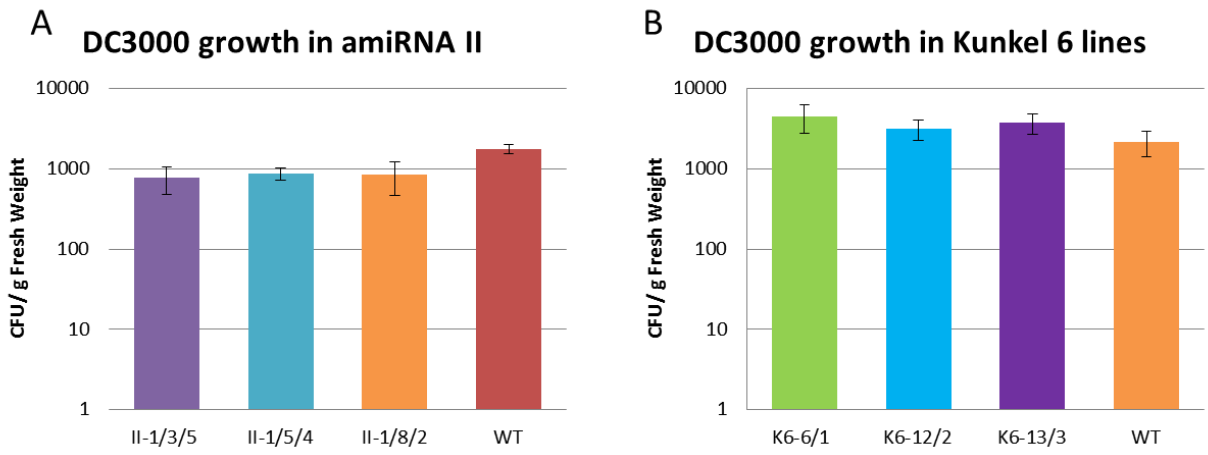

Figure 5-7. Bacterial growth responses in artificial microRNA lines grown in liquid culture. Growth of *P. syringae* pv. Tomato DC3000 shown in colony forming units (CFU) per gram fresh weight tissue for A) artificial microRNA-II and B) artificial microRNA-VI (Kunkel 6, K6).

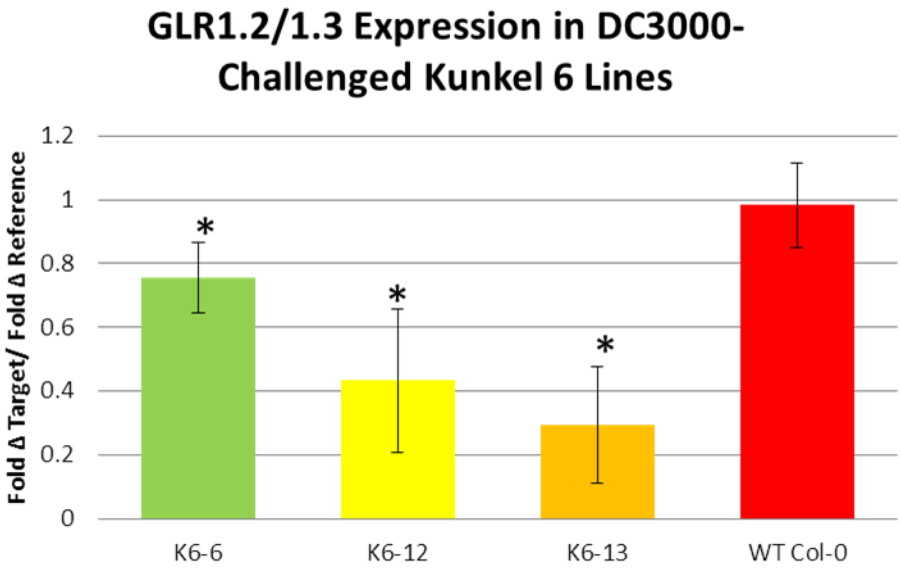

Figure 5-8. Relative transcript abundance for GLR1.2/1.3 transcripts in artificial microRNA VI lines challenged with P. syringae pv. Tomato DC3000 in liquid culture.

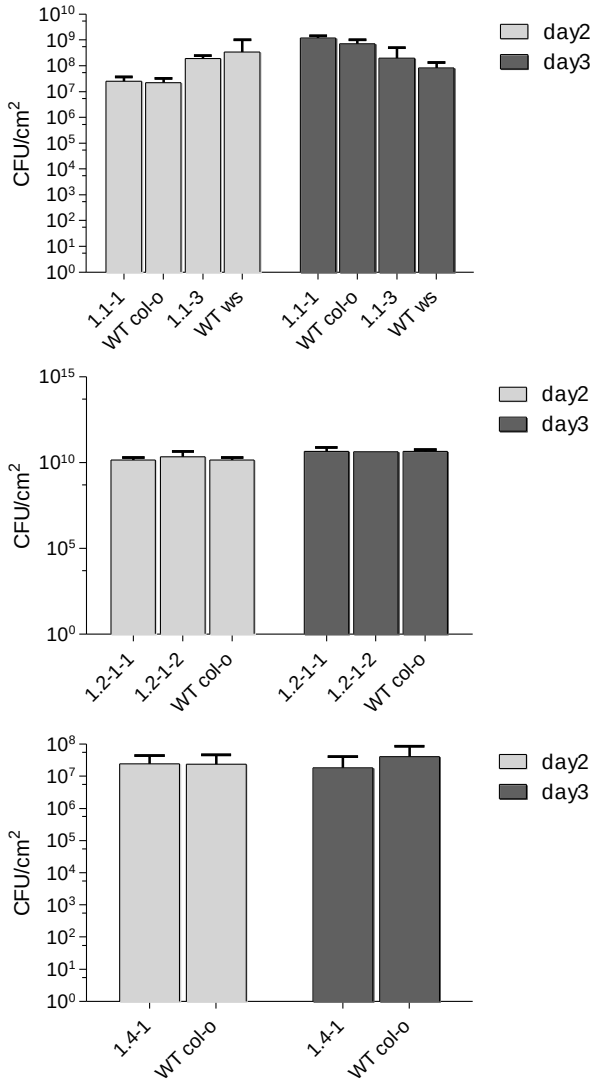

Figure 5-9. Bacterial growth responses in T-DNA insertion lines syringe-infiltrated with P. syringae pv. Tomato DC3000.

Bacterial growth shown in colony forming units (CFU)/cm^2 for A) *glr1.1*, B) *glr1.2*, and C) *glr1.4* plants.

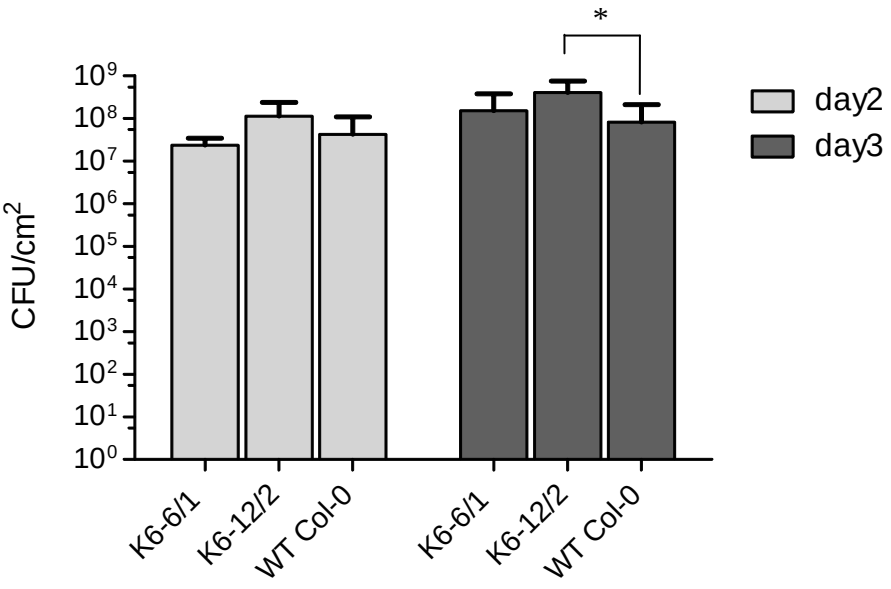

Figure 5-10. Bacterial growth responses in plants expressing amiRNA-VI (K6).

Plants were infiltrated with *P. syringae* pv. Tomato DC3000 OD600=0.001. Statistically significant differences are marked with asterisks ($p<0.05$).

TABLES

Table 5-1. Artificial microRNAs designed to target multiple Clade 1 GLR genes.

Name	Gene Targets	Target Sequence	amiRNA	amiRNA*
amiRNA I	1.1, 1.3, 1.4	TCAGTGAGGATCCAAGCGAAC	TCAGTGAGGATCCAAGCGAAC	GTCCGCTTGGATCGTCACTGT
amiRNA II	1.2, 1.3, 1.4	TTTGCATACTCTCTCTCCGGT	TTTGCATACTCTCTCTCCGGT	ACAGGAGAGAGAGAATGCAAT
amiRNA IV	1.1, 1.4	TCAGTGAGGATCCAAGCGCAC	TCAGTGAGGATCCAAGCGCAC	GTACGCTTGGATCGTCACTGT
Kunkel 6	1.2, 1.3	TGCAAGAAGAGGCTCTCCGTG	TGCAAGAAGAGGCTCTCCGTG	CAAGGAGAGCCTCATCTTGCT

Each line represents an attempt to target more than one gene for transcript reduction using microRNA 319a as a template to generate an artificial gene target sequence where amiRNA and amiRNA* are the sequences of the oligonucleotides used to generate the hairpin loop essential for cleavage of target site.

LITERATURE CITED

Abramovitch, R. B., J. C. Anderson and G. B. Martin (2006). "Bacterial elicitation and evasion of plant innate immunity." Nat Rev Mol Cell Biol **7**(8): 601-611.

Aslam, S. N., G. Erbs, K. L. Morrissey, M. A. Newman, D. Chinchilla, T. Boller, A. Molinaro, R. W. Jackson and R. M. Cooper (2009). "Microbe-associated molecular pattern (MAMP) signatures, synergy, size and charge: influences on perception or mobility and host defence responses." Mol Plant Pathol **10**(3): 375-387.

Batistic, O. and J. Kudla (2012). "Analysis of calcium signaling pathways in plants." Biochim Biophys Acta **1820**(8): 1283-1293.

Bliss, T. V. and G. L. Collingridge (2013). "Expression of NMDA receptor-dependent LTP in the hippocampus: bridging the divide." Mol Brain **6**: 5.

Boller, T. (1995). "Chemoperception of Microbial Signals in Plant-Cells." Annual Review of Plant Physiology and Plant Molecular Biology **46**: 189-214.

Boller, T. and G. Felix (2009). "A renaissance of elicitors: perception of microbe-associated molecular patterns and danger signals by pattern-recognition receptors." Annu Rev Plant Biol **60**: 379-406.

Chen, H., L. Xue, S. Chintamanani, H. Germain, H. Lin, H. Cui, R. Cai, J. Zuo, X. Tang, X. Li, H. Guo and J. M. Zhou (2009). "ETHYLENE INSENSITIVE3 and ETHYLENE INSENSITIVE3-LIKE1 repress SALICYLIC ACID INDUCTION DEFICIENT2 expression to negatively regulate plant innate immunity in Arabidopsis." Plant Cell **21**(8): 2527-2540.

Chen, Z., J. L. Agnew, J. D. Cohen, P. He, L. Shan, J. Sheen and B. N. Kunkel (2007). "Pseudomonas syringae type III effector AvrRpt2 alters Arabidopsis thaliana auxin physiology." Proc Natl Acad Sci U S A **104**(50): 20131-20136.

Chen, Z., A. P. Kloek, A. Cuzick, W. Moeder, D. Tang, R. W. Innes, D. F. Klessig, J. M. McDowell and B. N. Kunkel (2004). "The Pseudomonas syringae type III effector AvrRpt2 functions downstream or independently of SA to promote virulence on Arabidopsis thaliana." Plant J **37**(4): 494-504.

Cui, F., S. Wu, W. Sun, G. Coaker, B. Kunkel, P. He and L. Shan (2013). "The Pseudomonas syringae Type III Effector AvrRpt2 Promotes Pathogen Virulence via Stimulating Arabidopsis Auxin/Indole Acetic Acid Protein Turnover." Plant Physiol **162**(2): 1018-1029.

Darvill, A. G. and P. Albersheim (1984). "Phytoalexins and Their Elicitors - a Defense against Microbial Infection in Plants." Annual Review of Plant Physiology and Plant Molecular Biology **35**: 243-275.

Davenport, R. (2002). "Glutamate receptors in plants." Ann Bot **90**(5): 549-557.

Dodds, P. N. and J. P. Rathjen (2010). "Plant immunity: towards an integrated view of plant-pathogen interactions." Nat Rev Genet **11**(8): 539-548.

Felix, G. and T. Boller (2003). "Molecular sensing of bacteria in plants. The highly conserved RNA-binding motif RNP-1 of bacterial cold shock proteins is recognized as an elicitor signal in tobacco." J Biol Chem **278**(8): 6201-6208.

Felix, G., J. D. Duran, S. Volko and T. Boller (1999). "Plants have a sensitive perception system for the most conserved domain of bacterial flagellin." Plant Journal **18**(3): 265-276.

Gomez-Gomez, L. and T. Boller (2000). "FLS2: an LRR receptor-like kinase involved in the perception of the bacterial elicitor flagellin in Arabidopsis." Mol Cell **5**(6): 1003-1011.

Hammond-Kosack, K. and J. D. G. Jones (2000). Responses to Plant Pathogens. Biochemistry and Molecular Biology of Plants. B. Buchanan, W. Gruissem and R. Jones. Rockville, Maryland, American Society of Plant Biologists.

Hruz T, Laule O, Szabo G, Wessendorp F, Bleuler S, Oertle L, Widmayer P, Gruissem W and Z. P (2008). "Genevestigator V3: a reference expression database for the meta-analysis of transcriptomes. ." Advances in Bioinformatics.

Jones, J. D. and J. L. Dangl (2006). "The plant immune system." Nature **444**(7117): 323-329.

Kim, M. G., L. da Cunha, A. J. McFall, Y. Belkhadir, S. DebRoy, J. L. Dangl and D. Mackey (2005). "Two Pseudomonas syringae type III effectors inhibit RIN4-regulated basal defense in Arabidopsis." Cell **121**(5): 749-759.

Korves, T. M. and J. Bergelson (2003). "A developmental response to pathogen infection in Arabidopsis." Plant Physiol **133**(1): 339-347.

Kunkel, B. N., Chen, Z. (2006). "Virulence Strategies of Plant Pathogenic Bacteria." Prokaryotes **2**: 421-440.

Kunkel, T. A. (1985). "Rapid and efficient site-specific mutagenesis without phenotypic selection." Proc Natl Acad Sci U S A **82**(2): 488-492.

Kwaaitaal, M., R. Huisman, J. Maintz, A. Reinstadler and R. Panstruga (2011). "Ionotropic glutamate receptor (iGluR)-like channels mediate MAMP-induced calcium influx in Arabidopsis thaliana." Biochem J **440**(3): 355-365.

Lecourieux, D., R. Ranjeva and A. Pugin (2006). "Calcium in plant defence-signalling pathways." New Phytol **171**(2): 249-269.

Levine, A., R. I. Pennell, M. E. Alvarez, R. Palmer and C. Lamb (1996). "Calcium-mediated apoptosis in a plant hypersensitive disease resistance response." Curr Biol **6**(4): 427-437.

Ma, W. and G. A. Berkowitz (2007). "The grateful dead: calcium and cell death in plant innate immunity." Cell Microbiol **9**(11): 2571-2585.

Martin, G. B., A. J. Bogdanove and G. Sessa (2003). "Understanding the functions of plant disease resistance proteins." Annu Rev Plant Biol **54**: 23-61.

Moreau, A. W. and D. M. Kullmann (2013). "NMDA receptor-dependent function and plasticity in inhibitory circuits." Neuropharmacology **74**: 23-31.

Mousavi, S. A., A. Chauvin, F. Pascaud, S. Kellenberger and E. E. Farmer (2013). "GLUTAMATE RECEPTOR-LIKE genes mediate leaf-to-leaf wound signalling." Nature **500**(7463): 422-426.

Murray, M. G. and W. F. Thompson (1980). "Rapid isolation of high molecular weight plant DNA." Nucleic Acids Res **8**(19): 4321-4325.

Newman, M. A., M. J. Daniels and J. M. Dow (1995). "Lipopolysaccharide from Xanthomonas-Campestris Induces Defense-Related Gene-Expression in Brassica-Campestris." Molecular Plant-Microbe Interactions **8**(5): 778-780.

Newman, M. A., T. Sundelin, J. T. Nielsen and G. Erbs (2013). "MAMP (microbe-associated molecular pattern) triggered immunity in plants." Front Plant Sci **4**: 139.

Nimchuk, Z., T. Eulgem, B. F. Holt, 3rd and J. L. Dangl (2003). "Recognition and response in the plant immune system." Annu Rev Genet **37**: 579-609.

Ossowski, S., R. Schwab and D. Weigel (2008). "Gene silencing in plants using artificial microRNAs and other small RNAs." Plant J **53**(4): 674-690.

Peters, A. (1999). "The effects of pathogen infection and mutation on life-history characters in Arabidopsis thaliana." J Evol Biol **12**(3): 460-470.

Pfaffl, M. W. (2001). "A new mathematical model for relative quantification in real-time RT-PCR." Nucleic Acids Res **29**(9): e45.

Reiser, L. and S. Y. Rhee (2005). "Using the Arabidopsis Information Resource (TAIR) to find information about Arabidopsis genes." Curr Protoc Bioinformatics **Chapter 1**: Unit 1 11.

Rico, A. and G. M. Preston (2008). "Pseudomonas syringae pv. tomato DC3000 uses constitutive and apoplast-induced nutrient assimilation pathways to catabolize nutrients that are abundant in the tomato apoplast." Mol Plant Microbe Interact **21**(2): 269-282.

Schwab, R., S. Ossowski, M. Riester, N. Warthmann and D. Weigel (2006). "Highly specific gene silencing by artificial microRNAs in Arabidopsis." Plant Cell **18**(5): 1121-1133.

Steele, M. and J. Odumeru (2004). "Irrigation water as source of foodborne pathogens on fruit and vegetables." J Food Prot **67**(12): 2839-2849.

Strange, R. N. and P. R. Scott (2005). "Plant disease: a threat to global food security." Annu Rev Phytopathol **43**: 83-116.

Swanson, S. J., W. G. Choi, A. Chanoca and S. Gilroy (2011). "In vivo imaging of Ca2+, pH, and reactive oxygen species using fluorescent probes in plants." Annu Rev Plant Biol **62**: 273-297.

Very, A. A. and H. Sentenac (2002). "Cation channels in the Arabidopsis plasma membrane." Trends Plant Sci **7**(4): 168-175.

Zeng, W., A. Brutus, J. M. Kremer, J. C. Withers, X. Gao, A. D. Jones and S. Y. He (2011). "A genetic screen reveals Arabidopsis stomatal and/or apoplastic defenses against Pseudomonas syringae pv. tomato DC3000." PLoS Pathog **7**(10): e1002291.

Zipfel, C., G. Kunze, D. Chinchilla, A. Caniard, J. D. Jones, T. Boller and G. Felix (2006). "Perception of the bacterial PAMP EF-Tu by the receptor EFR restricts Agrobacterium-mediated transformation." Cell **125**(4): 749-760.

CHAPTER 6:CHARACTERIZATION OF A NOVEL MUTANT PHENOTYPE

INTRODUCTION

Background Information

Upon analysis of *Arabidopsis* mutants that carry T-DNA insertion in a gene encoding glutamate receptor homolog GLR1.3 (Davenport 2002), we identified a line with a strong defect in cell expansion. The mutant plants, tentatively named *camp1,* are severely dwarfed, less than 2cm tall as compared to the wild-type *Arabidopsis* that usually grow to ~20cm in height (Figure 6-1). Leaf epidermal cells fail to expand properly compared to the wild-type, and leaf cells are significantly smaller. Also, the leaves show epinastic growth (i.e. the upper side of the leaf epidermis grows faster than the lower side, resulting in leaf curling/folding (Figure 6-1). In addition, the "bolts" of these plants are present though not visible, in most cases curled under the leaf mass, and examination of stem cross-sections show an abnormal arrangement of irregularly shaped cells with individual cell types difficult to distinguish (Figure 6-2). In some ways, the dwarf phenotype of *camp1* mutant resembles plants defective in perception of the plant hormones, auxin, gibberellin, and brassinosteroid, which are important in cell expansion and division (Figure 6-3)(Lincoln, Britton et al. 1990, Clouse, Langford et al. 1996, Ross, Murfet et al. 1997, Cowling and Harberd 1999). However, there are some crucial differences. For example, strong alleles of gibberellin and brassinosteroid mutants are both male sterile, which is not the case in our mutant. Additionally, the complete lack of inflorescence stem growth that is observed in our mutants is not observed in viable auxin signaling mutants.

This study aims to identify the mutation(s) responsible for the *camp1* phenotype obtained from GLR1.3-1 seed lines (SAIL_791_A03), using a combination of tail-PCR, plasmid rescue, and map-based approaches. Additionally, *camp1* responses to the plant hormones auxin, gibberellin, and brassinosteroid, will be examined. Typically, such mutants are associated with a deficiency in one or more hormone signaling or biosynthetic pathways. However, comparison to auxin, gibberellin, and brassinosteroid mutants revealed unique differences indicating that this is a novel mutant phenotype. The outcome of this research will contribute to discovering new components that control cell division/expansion process in plants.

Project Justification

The *camp* phenotype is not likely to be caused by the T-DNA insertion into GLR1.3 (SAIL_793_A03), due to the following: 1) a plant that carries homozygous T-DNA insertion in GLR1.3 gene and shows no obvious phenotype has been identified; 2) plants that carry homozygous T-DNA insertion at another position in GLR1.3 do not show the *camp1* phenotype; and 3) a plant that does not carry a T-DNA insertion in GLR1.3 and shows *camp1* phenotype has been isolated from the same stock. Unfortunately, seeds from *glr1.3* homozygous plants were not obtained due to a detrimental fungus gnat infestation and failure to recover additional lines from the parent obtained from Arabidopsis Biological Resource Center (ABRC). Whether the phenotype is a result of a secondary independent T-DNA insertion or is the result of a point mutation remains to be discovered. Identification of the causative mutation for this unusual phenotype may lend insight into the biological processes important for cell expansion and the role of hormones in this process.

RESULTS

Determination of Dominant or Recessive Mutation

Among plants grown from SAIL_793_A03 stock obtained from the ABRC, a plant that 1) showed the *camp1* phenotype, 2) carries no T-DNA insertion in GLR1.3 gene, and 3) carries at least another copy of T-DNA insertion (i.e. resistant to the BASTA) was isolated. Using this plant as the starting material, multiple strategies for determining the mutation responsible for *camp1* phenotype was utilized. Low frequency of appearance (~10%) of plants that shows *camp1* phenotype in SAIL_793_A03 seed stock suggested that the mutation is recessive. All 16 analyzed F1 plants from *camp1* – wild-type (Col-0) cross were phenotypically identical to wild-type, confirming that the mutation is indeed recessive. BASTA resistance was used as the marker for T-DNA insertion.

Plasmid Rescue and TAIL-PCR to Identify Additional T-DNA Insertions

The F1 plant stated above was self-fertilized, and some of the F2 progenies showed *camp* phenotype, as expected for recessive mutations. After another round of back-crossing and self-fertilization with *Arabidopsis thaliana* ecotype Col-0, and progenies showing *camp* phenotype were identified. These plants were found to be resistant to BASTA, suggesting the possibility that the mutation is linked to another T-DNA insertion on the genome.

Two independent strategies to identify additional T-DNA insertion were carried out. The first strategy, plasmid rescue, was made possible due to the pBluescript backbone included in the T-DNA cassette used for creating SAIL lines (McElver, Tzafrir et al. 2001)(Figure 6-4). Using this method, we isolated three distinct plasmids showing distinct restriction digestion patterns

(data not shown). However, none of these plasmids included Arabidopsis-derived sections, hence we were unable to identify the location of the T-DNA insertion through this method.

Another method used was TAIL-PCR which identified an insertion in AT3G26160, a putative cytochrome P450 oxidase. However, further linkage analyses showed that this insertion is not linked to the *camp* phenotype (data not shown).

Illumina Sequencing to Identify Mutation Candidates

High-throughput sequencing can accelerate the identification of mutations responsible for a phenotype. In *Arabidopsis*, the small, well-annotated genome makes it possible to map the mutations from a small, pooled F2 population without prior genetic analysis (Austin, Vidaurre et al. 2011). Therefore we performed multiparallel sequencing of a library prepared from a pool of plants showing *camp* phenotype.

The c*amp* mutant plant (Col-0 background) was out-crossed with another ecotype (Landsberg *erecta*) to obtain recombinant lines. Plants showing the *camp* phenotype (89 lines total) were identified in the F2 population and their genomic DNA was pooled for the construction of a paired-end TruSeq library. One run on Illumina Miseq produced 5,763,306 paired end reads on a paired-end 100 cycle. After removal of primer sequence, 4,704,512 reads (81.63%) concordantly mapped to the Arabidopsis genome (TAIR10) on a single location.

Figure 6-5 shows the distribution of fixed SNPs (i.e. nucleotides that differed from TAIR10 genomic sequence) on all five chromosomes. Since *camp* phenotype is apparently a recessive mutation, it is expected that the chromosomal region adjacent to the causative mutation will be solely coming from the parent with *camp* phenotype, causing loss of SNPs. Indeed, the upper arm of chromosome 2 showed much higher representation of fixed SNPs compared to

other regions. To further narrow down the region of interest, we utilized a web-interfaced program (http://bar.utoronto.ca/NGM/) that is designed to predict the region of mutation in F2 mapping population (Austin, Vidaurre et al. 2011). In this algorithm, the degree of variations within a given SNP compared to the reference genome is calculated (termed discordant chastity, ChD). As shown in Figure 6-6, heterozygous SNP (i.e. not purified by the phenotypic selection) will have ChD values close to 0.5, whereas "purified SNP" in the F2 mapping population will have ChD values close to 1.0. Average ChD value over sliding windows on each chromosome is plotted, then homozygous/heterozygous signal ratio is calculated. Using this method, we further narrowed down the region of interest to ~ 2Mb section on the upper arm of chromosome 2 (Figure 6-6). Potential causative SNPs in this region are listed in Table 6-1.

Metabolite Profiling to Identify Changes in Metabolite Levels

The stunted nature of *camp1* plants led us to examine whether there is an altered abundance of metabolites which might cause the deficiency and irregular cell division seen in the mutant (Figures 6-1 and 6-2). Polar and non-polar metabolites and amino acids were examined in lyophilized callus tissue of *camp1* and wild-type Columbia-0 plants. Two independent experiments were performed with 4 biological replicates each to determine whether any differences in metabolite profiles were present between *camp1* and Col-0, with one experiment shown in Figure 6-7. Interestingly, the only clear difference lies with the long-chain polyunsaturated fatty acids C18:1, C18:2, and C18:3 derived from membrane lipids were significantly reduced ($p<0.05$) compared to wild-type (Figure 6-7A).

Characterization of Hormone Response

Although there are significant differences between the *camp1* phenotype and the previously described plant hormone mutants, it is possible that the mutation in *camp1* disturbs a sub-network of signaling pathways mediated by plant hormones. To evaluate this possibility, we examined responses of *camp1* to auxin, gibberellin, and brassinosteroid. Figure 6-8 shows the response of both light- and dark- grown 10 day old seedlings to differing concentrations of the plant hormones gibberellin and brassinosteroid. There is clearly a difference in hypocotyl length of etiolated seedlings of *camp1* compared with wild-type Columbia-0 (Figure 6-8B and C), which is partially rescued by low concentrations (1μM) of GA_3 (Figure 6-8). The response to epibrassinolide (EBR) was not significantly different from the wild-type, except for the decreased germination efficiency of *camp1* plants in etiolated seedlings in response to 1μM 24-epibrassinolide (Figure 6-8B). The inhibition of root growth to the plant hormone auxin (0.1μM L-2,4-D) was not significantly different between wild-type and *camp1* mutant (data not shown).

DISCUSSION

The discovery of the *camp1*mutant that does not carry GLR1.3 T-DNA insertion suggests that there could be a second-site T-DNA insertion or a point mutation responsible for the phenotype. Therefore, other T-DNA insertions in the *camp1* plant were investigated using a combination of plasmid rescue and tail PCR. Only one T-DNA insertion was identified in the parent line, which later was found not to be linked to the phenotype.

While metabolite profiles were not significantly different between *camp1* and the wildtype plants, there was a substantial decrease in C16 saturated and C18 polyunsaturated fatty acids (Figure 6-7A). Examination of cross-section of *camp1* mutant stem also revealed a decrease in overall cuticle thickness as well as irregularly shaped epidermal cells compared to

the wildtype (Figure 6-2C and D). There is a connection between these two phenomena because these fatty acids serve as templates for the production of very long chain fatty acids (VLCFAs), which are important for the production of cuticle in epidermal cells (Raffaele, Leger et al. 2009). Thus, it is possible that the mutation responsible for the *camp1* phenotype is disrupting some component of VLCFA biosynthesis either directly or indirectly.

Camp1, gibberellin, and brassinosteroid mutants are reminiscent of one another, although there are notable differences. For example, etiolated GA mutants exhibit a decrease in hypocotyl length (Cowling and Harberd 1999), while EBR mutants have short, thickened hypocotyls with opened cotyledons (Clouse, Langford et al. 1996) compared to the wildtype. To determine whether the *camp1* phenotype is a result of disruption (signaling or biosynthesis) of the EBR or GA, seedlings were dark-germinated on different concentrations of each hormone. Figure 6-8 shows that although there was a clear difference in hypocotyl length in *camp1* mutants compared to the wildtype, hypocotyl length was not significantly changed from the wildtype in response to GA and EBR. Interestingly, there appeared to be a decrease in seed germination of *camp1* plants when compared with non-treated mock and treated wild-type (Figure 6-8B). Both gibberellin and brassinosteroid biosynthetic mutants have markedly decreased germination efficiencies that can be alleviated by application of brassinosteroids (Steber and McCourt 2001, Clouse 2011). Because the growth and responsiveness of *camp1* to GA_3 and EBR are not consistent with the typical GA or EBR mutants, some complex interplay between these hormones (or some regulatory component) and *CAMP1* gene might be occurring, although there is no clear evidence for it or a clue regarding the mechanism.

High-throughput sequencing of the F2 population resulting from *camp* and *Ler* narrowed down the potential region of the relevant mutation to a ~2Mkb section on chromosome 2. Among

the potential causative SNPs, the mutation in AT2G07505, encoding a protein of unknown function, causes a premature stop. Whether an additional copy of this gene can rescue the *camp* phenotype will help to determine whether this SNP is the causative mutation for the *camp* phenotype. As a parallel approach, binary BAC clones with known locations in the *Arabidopsis* genome (JAtY library, http://orders2.genome-enterprise.com/libraries/arabidopsis/jaty.html) could be used for phenotype rescue experiments.

METHODS AND MATERIALS

Plasmid Rescue and Tail PCR to Identify Causative Mutation

The T-DNA insertion project that resulted in this mutant line utilized the pDAP101 vector that contains the entire pBluescript vector sequence in the T-DNA insertion cassette, enabling one to perform plasmid rescue as a strategy to identify gene sequences flanking the insertion site(s). Plasmid rescue was performed on a pooled *camp1* genomic DNA. Genomic DNA was isolated, digested with HindIII and the plasmid was re-circularized (Mandal, Lang et al. 1993). Fragments were gel-purified and allowed to self-ligate before transforming into XL-10 Gold ultra-high competency cells (Agilent Technologies). Plasmids were purified, digested to identify unique plasmids, and 3 clones were chosen based on distinct restriction digestion patterns. Sequencing was then initiated first with T-DNA specific sequences and later with nested primers on plasmid DNA to identify plant-derived sequences neighboring the T-DNA insertion(s).

Mapping of Illumina Miseq run

The reads were mapped to TAIR 10 genome using Bowtie2 (Langmead, Trapnell et al. 2009). The resulting SAM file was converted to BAM file using Samtools version 0.1.16, sorted and indexed, and converted into pileup format using respective commands in the Samtools. The pileup file was fed into a custom PEARL script (Austin, Vidaurre et al. 2011). The resulting emap file was used for the analysis.

Generation of Callus Tissue

One issue associated with this project was the difficulty in obtaining enough plant material from *camp1* plants. The *camp1* plants tend to be very small, producing little biomass due to their epinastic leaves and lack of bolting, and isolation of a significant amount of genomic DNA to perform experiments upon which typically requires sacrificing the entire plant. In this case, a tandem approach was taken to generate callus from explants and regenerate plants for genomic DNA isolation and metabolite profiling (Bashandy, Guilleminot et al. 2010).

Characterization of Mutants Potentially Allelic to CAMP1

Single nucleotide polymorphisms (SNPs) and insertions/deletions (indels) which resulted in a stop codon mutation were identified by comparing aligned sequences of *camp1* and TAIR9 or TAIR10 (shown in Table 6-3). Gene candidates with T-DNA mutants available through ABRC stock center were selected (Table 6-2). Homozygous plants were segregated on antibiotic selective media and genotyped using genomic DNA PCR with gene and T-DNA specific primers as described in Chapter 3 (Table 6-2).

Metabolite Profiling using Gas Chromatography-Mass Spectroscopy (GC-MS)

Polar and non-polar metabolites were extracted from four replicates of freeze-dried callus tissue for semiquantitative gas chromatography- mass spectroscopy (GC-MS) analysis (Duran, Yang et al. 2003, Collakova, Goyer et al. 2008). Briefly, 1.00mg ± 0.05mg dry weight of tissue was disrupted with glass beads and extracted with 1:1:1 chloroform/methanol/H_2O. The organic phase containing nonpolar metabolites was dried under a stream of nitrogen, and fatty acid methyl esters were prepared by derivatization in 1 N methanolic HCl at 50°C for 5 h. Samples were dried under a stream of nitrogen gas, and trimethylsilyl derivatives of glycerol and carbohydrates hydrolyzed from triacylglycerols and sugar lipids were prepared. For the analysis of polar metabolites, the aqueous phase was dried and trimethylsilyl or tert-butyldimethylsilyl derivatives were prepared. One microliter of derivatized samples was separated on a gas chromatograph equipped with a flame ionization detector. Heptadecanoic acid (C17:0), norvalin, and ribitol were used as internal standards.

Characterization of Hormone Response

Two replicates of approximately 20 seeds were grown axenically on Murashige and Skoog (MS) basal salt media (Phytotechnology Labs Catalog # M524) supplemented with 10% (w/v) sucrose and 0.8% (w/v) plant agar (Phytotechnology Labs Catalog # A181) adjusted to pH5.7 with no hormone, 1μM gibberellin A_3 (GA3, Phytotechnology Labs Catalog # G500) , 10μM GA3, 0.1μM 24-epibrassinolide (EBR, Phytotechnology Labs Catalog # E244), or 1μM EBR. Seeds were vernalized at 4°C in the dark for 4 days prior to growth under long day conditions (16 hour light/ 8 hour dark) at light intensity between 120-150 μmol/m^2sec or wrapped in aluminum foil at 22°C for 10 days. Light grown seedlings were examined every 2 days while hypocotyls of etiolated seedlings were measured after day 10.

Auxin studies were performed by growing two replicates of approximately 20 seeds each axenically on vertical MS plant agar media for 5 days. The seedlings were then transferred to media supplemented with either 0μM, 0.1μM, 1.0μM, or 10μM L-2,4- Dichlorophenoxyacetic acid (L-2,4-D), a synthetic auxin, and allowed to grow for 3 days under long day conditions (16 hour light/ 8 hour dark) at light intensity between 120-150 μmol/m^2sec. The growth of roots were then measured and used as an indication of hormone sensitivity.

Fixation and Imaging of Plant Tissue

For histological examination, petiole tissue was fixed by vacuum-infiltration at room temperature for 1 hour followed by 1 hour of vacuum infiltration on ice with a 2% paraformaldehyde/0.5% glutaraldehyde in 10 mM sodium phosphate buffer (Thornton and Talbot 2006). Samples were then dehydrated with a phosphate buffer/ethanol series consisting of 10% (v/v) gradients. Each dehydration step was performed twice with the exception of the 100% ethanol, which was repeated three times, on a rotating platform at room temperature for 10 min. Samples were embedded in LR White resin (London Resin Company) and subsequently sectioned on a Sorvall MT2B ultramicrotome, then stained with Toluidine blue/boric acid (0.05% w/v) for 1 min and heat-fixed to slides at 60°C for 1 min. Images were captured under brightfield optics with a Zeiss Axioscope 40 microscope (Carl Zeiss, Inc.).

For scanning electron microscope (SEM) examination, excised leaf tissue was fixed for 16 hours at room temperature using 4% glutaraldehyde in 0.2M sodium cacodylate buffer, pH 7.0, followed by vacuum-infiltration at 4°C for 4 hours. Samples were rinsed with buffer 3 times for 5 minutes each and secondary fixation was performed with 2% OsO_4 in sodium cacodylate buffer overnight. Material was then rinsed in the same buffer 3 times and dehydrated via

ascending ethanol series from 30 to 100% for 15 min intervals. Tissue was then critical-point dried in CO_2, mounted in colloidal silver paste onto aluminum stubs, sputter-coated with gold, and examined using Carl Zeiss EVO40 Scanning Electron Microscope located at Veterinary Medicine, Virginia Tech under guidance of Kathy Lowe.

FIGURES

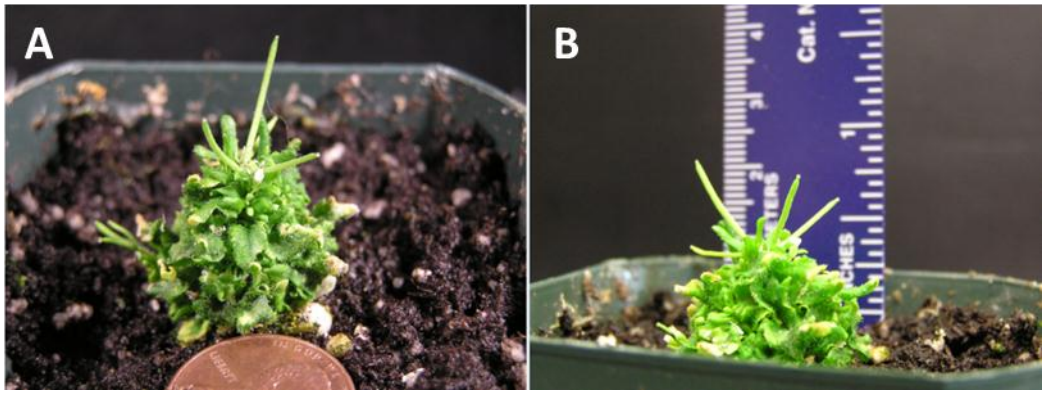

Figure 6-1. *Camp1* mutant plant phenotype.

A) Flowering *camp1* plant next to penny to show small size and B) flowering *camp1* plant next to ruler to show dwarfed height.

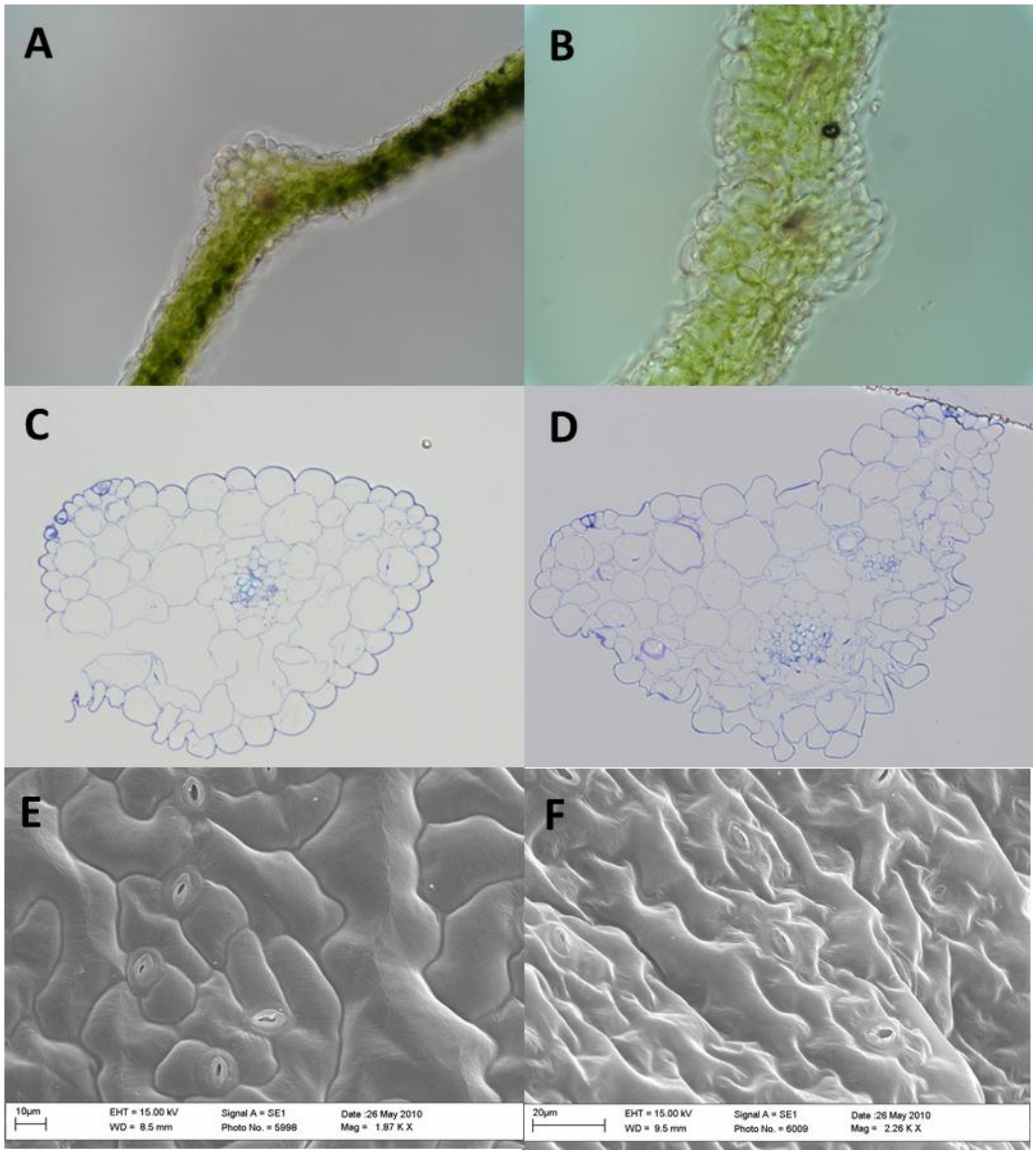

Figure 6-2. Microscopy of camp1 mutant plants to observe cell morphology.

A) cross-section of WT Landsberg erecta leaf and petiole at 20x magnification, B) cross-section of *camp1* mutant leaf and petiole at 20x magnification, C) cross-section of WT Landsberg erecta stem at 40x magnification stained with toluidine blue, D) cross-section of *camp1* mutant stem at 40x magnification stained with toluidine blue, E) scanning electron micrograph of WT Col-0 leaf surface at 1,870x magnification, and F) scanning electron micrograph of *camp1* leaf surface at 2,280x magnification.

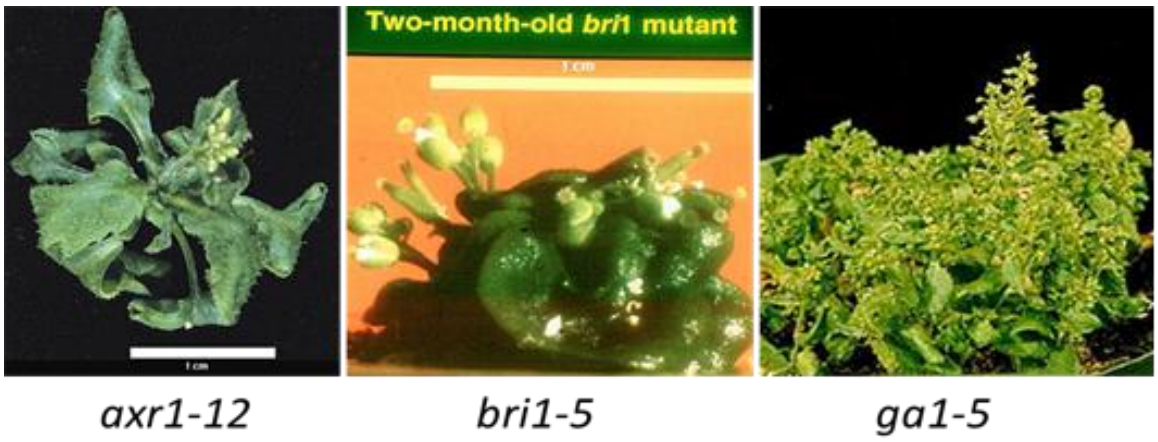

Figure 6-3. Typical phenotype of plant growth hormone mutants.

Axr1-12 (Lincoln, Britton et al. 1990), *bi1-5* (Azpiroz, Wu et al. 1998), *ga1-5* (Cowling 1999) are defective in pathways mediated by auxin, brassinosteroids, and gibberellin, respectively.

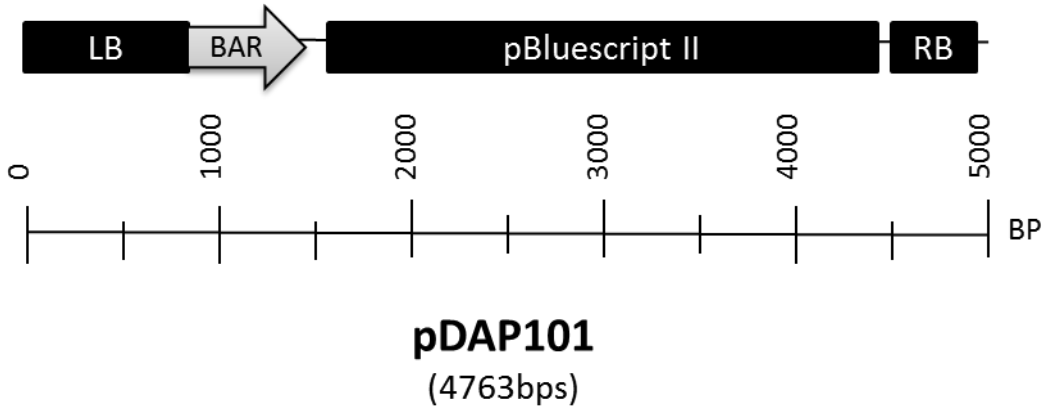

Figure 6-4. pDAP101 cassette used for generating SAIL T-DNA insertion lines.

Left border (LB) and right border (RB) sequences were used to design nested primers to sequence into the flanking genomic DNA (McElver, Tzafrir et al. 2001).

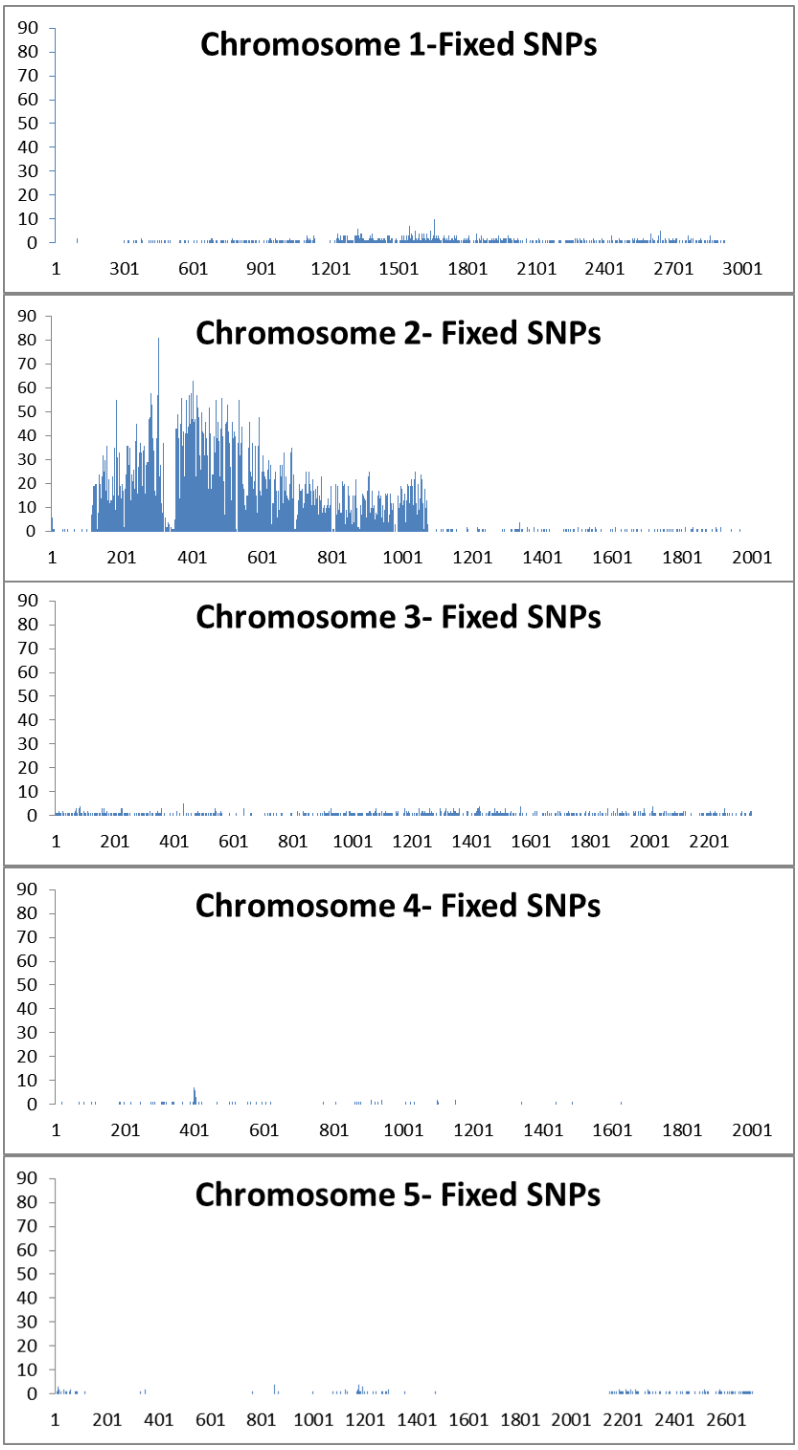

Figure 6-5. Distribution of fixed single nucleotide polymorphisms (SNPs) between camp1 mutant and TAIR10 genomic sequence on all five chromosomes.

The upper arm of chromosome 2 shows much higher representation of fixed SNPs compared to other regions.

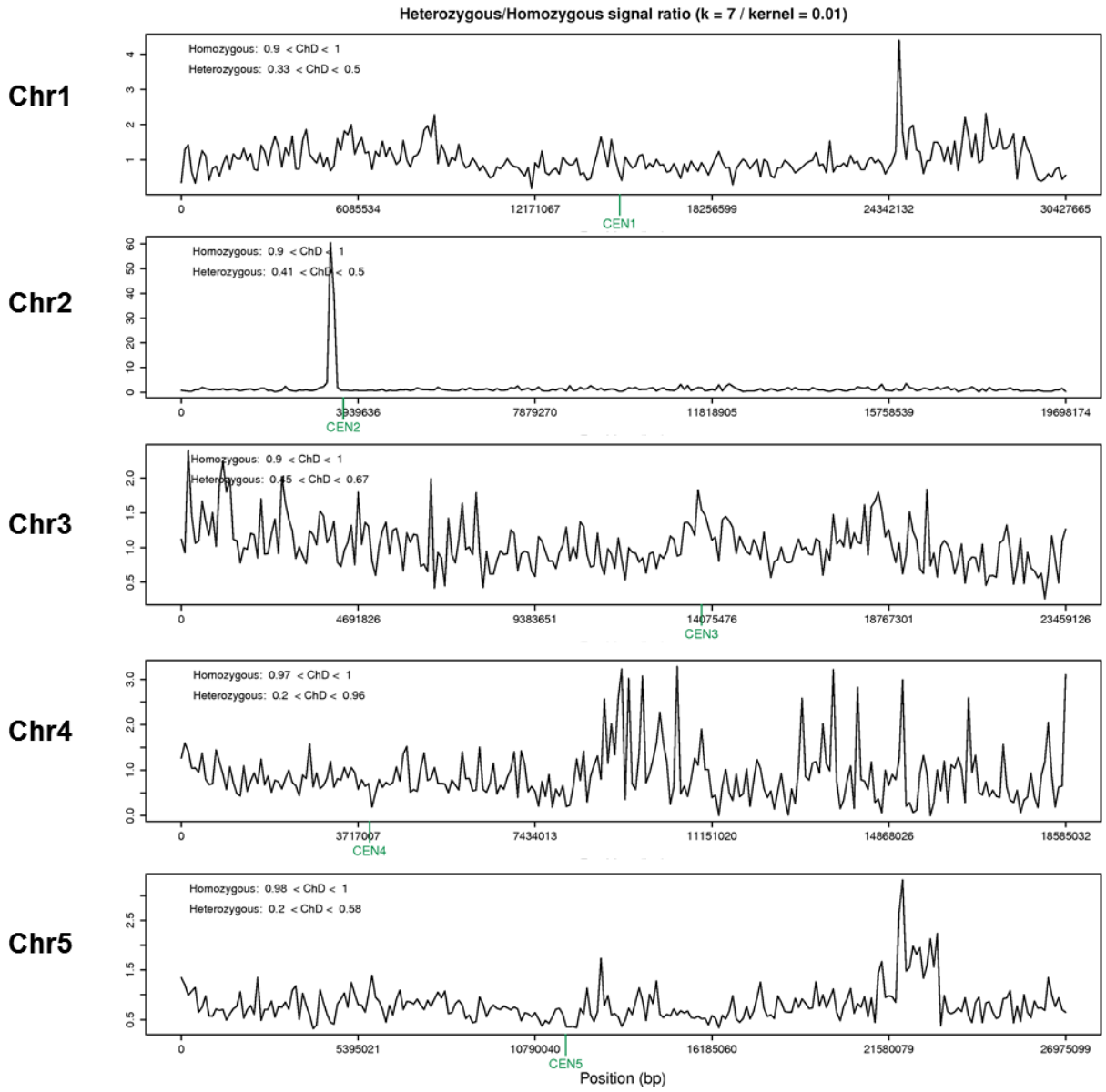

Figure 6-6. The degree of variations within a given single nucleotide polymorphism (SNP) compared to the reference genome, or discordant chastity (ChD) for Chromosomes 1-5 based on mapping of F2 sequences to TAIR10 genome.

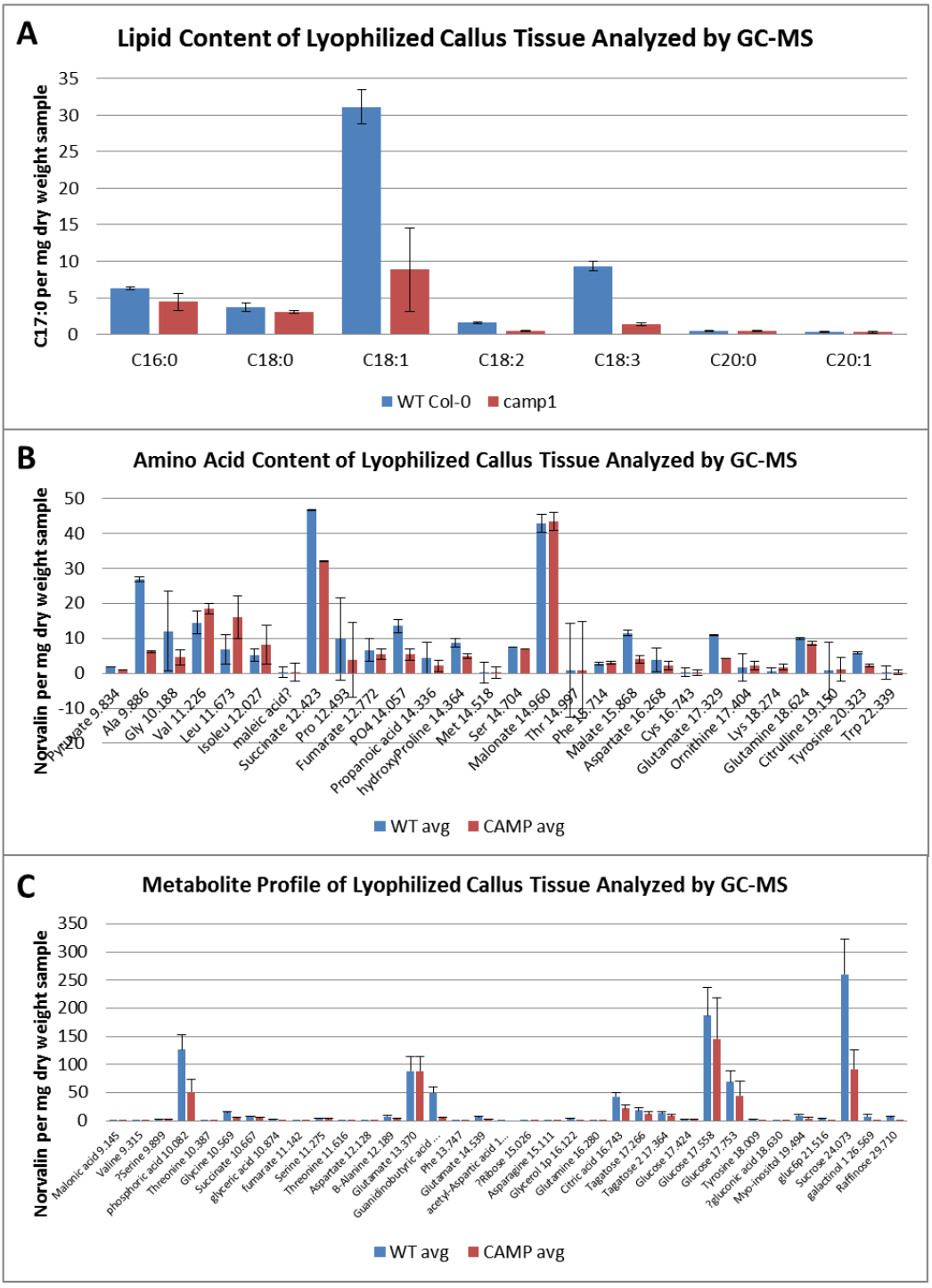

Figure 6-7. Results of metabolite profiling analysis using GC-MS on *camp1* and wild-type Columbia-0 lyophilized callus tissue.

A) lipid profile, B) amino and carboyxlic acid profile, and C) polar metabolite profile.

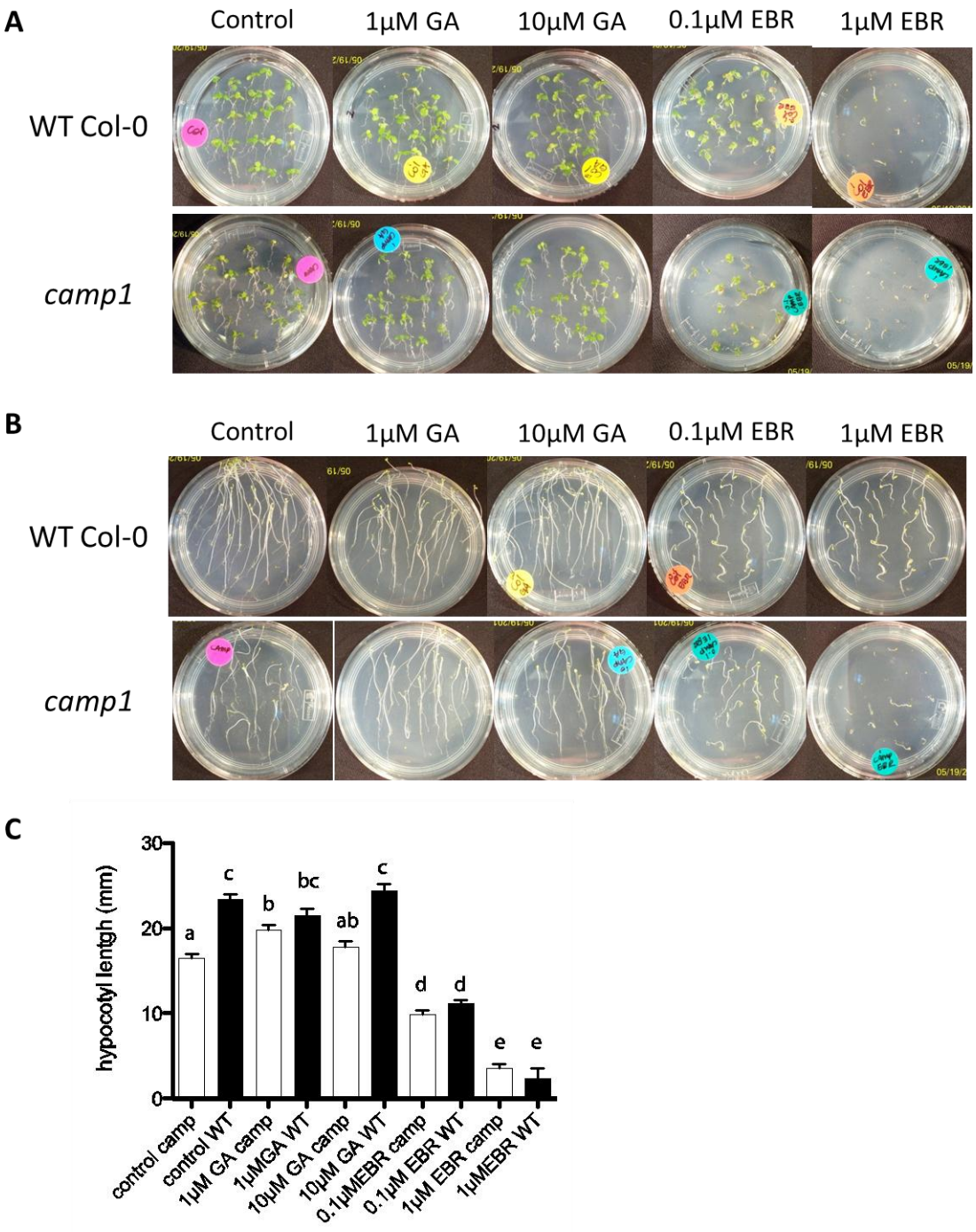

Figure 6-8. Examination of hormone response of 10 day old light- and dark-grown seedlings.

A and B) light-grown and etiolated seedlings, respectively, treated with Gibberellin A_3 (GA) and 24-epibrassinolide (EBR). C) Length of hypocotyls of etiolated plants treated with GA and EBR.

TABLES

Table 6-1. Potential causative single nucleotide polymorphisms (SNPs) of Chromosome 2 identified through mapping of F2 camp1 population to TAIR10 genome.

Chrom.	Position	Ref. base	SNP base	Depth	Discordont chastity	Accession	Tag	Strand	Ref. codon	SNP codon	AA change	BLOSUM 100
2	3125970	C	T	8	1.00	AT2G07505.1	CDS	+	CAA	TAA	Q->*	-10
2	3169984	C	G	8	1.00	AT2G07560.1	3'UTR					
2	3169997	T	C	8	1.00	AT2G07560.1	3'UTR					
2	3170003	T	G	8	1.00	AT2G07560.1	3'UTR					
2	3170015	T	A	8	1.00	AT2G07560.1	3'UTR					
2	3170258	A	R	15	0.87	AT2G07560.1	3'UTR					
2	3170279	C	Y	13	0.85	AT2G07560.1	3'UTR					
2	3171965	C	A	10	1.00	AT2G07560.1	cryptic splice site (4bp)					
2	3172099	A	G	8	1.00	AT2G07560.1	CDS	-	GGT	GGC	G->G	9
2	3241428	T	G	17	1.00	AT2G07773.1	CDS	-	ATT	CTT	I->L	2
2	3241444	C	T	18	1.00	AT2G07773.1	CDS	-	CTG	CTA	L->L	8
2	3241470	T	C	21	1.00	AT2G07773.1	CDS	-	AAC	GAC	N->D	1
2	3257925	A	G	30	0.93	AT2G07672.1	CDS	+	TAT	TGT	Y->C	-8
2	3266717	T	C	42	1.00	AT2G07673.1	CDS	+	ATG	ACG	M->T	-2
2	3269423	A	G	59	1.00	AT2G07674.1	CDS	+	ACA	ACG	T->T	9
2	3272818	A	C	31	1.00	AT2G07676.1	CDS	+	TAT	TCT	Y->S	-2
2	3289461	A	G	22	1.00	AT2G07681.1	CDS	+	AAT	GAT	N->D	1
2	3290780	A	G	18	0.94	AT2G07681.1	CDS	+	AGT	GGT	S->G	-2
2	3347094	T	G	80	0.97	AT2G07695.1	CDS	+	CTT	CTG	L->L	8
2	3347349	T	G	22	1.00	AT2G07695.1	CDS	+	AGT	AGG	S->R	-3
2	3348486	T	C	11	1.00	AT2G07785.1	3'UTR					
2	3350539	T	A	18	1.00	AT2G07599.1	CDS	-	CCA	CCT	P->P	12
2	3350539	T	A	18	1.00	AT2G07599.2	CDS	-	CCA	CCT	P->P	12
2	3359473	T	C	20	1.00	AT2G07798.1	CDS	+	CTC	CCC	L->P	-7
2	3385678	A	C	200	0.95	AT2G07706.1	CDS	-	GTT	GTG	V->V	8
2	3385688	C	T	198	0.94	AT2G07706.1	CDS	-	GGC	GAC	G->D	-4
2	3385694	G	A	236	0.95	AT2G07706.1	CDS	-	CCA	CTA	P->L	-7
2	3386984	T	G	20	1.00	AT2G07708.1	5'UTR					
2	3446641	A	G	11	1.00	AT2G07724.1	CDS	-	ATG	ACG	M->T	-2
2	3468549	G	C	49	0.96	AT2G07732.1	CDS	-	CCG	GCG	P->A	-2
2	3476795	A	G	15	1.00	AT2G07827.1	CDS	+	ATG	GTG	M->V	0
2	3476795	A	G	15	1.00	AT2G07827.2	CDS	+	ATG	GTG	M->V	0
2	3495992	A	G	23	1.00	AT2G07739.1	CDS	-	TTT	TCT	F->S	-5
2	3515513	C	M	8	0.88	AT2G07680.1	CDS	+	GCC	GCM	A->	

Gene candidates identified from mapping of F2 *camp* plants to *Arabidopsis* TAIR10 genome with AGI accession, genome location, and SNP stop codon mutations listed.

Table 6-2. Genes potentially epistatic to camp1 mutant obtained from ABRC for further characterization.

Stop Mutation	AGI #	Description	ABRC Stock
SNP	AT2G14170	ALDEHYDE DEHYDROGENASE 6B2, ALDH6B2	SALK_093983C
indel	AT2G19920	RNA-dependent RNA polymerase family protein	SALK_088175C
indel	AT2G19940	oxidoreductases, acting on the aldehyde or oxo group of donors	SALK_138081C
indel	AT2G23400	Undecaprenyl pyrophosphate synthetase family protein;	SAIL_30_F07
SNP	AT2G24600	Ankyrin repeat family protein	SALK_100250

Arabidopsis biological resource center (ABRC) stock information for *camp* causative mutation gene candidates selected for further investigation.

Table 6-3. Chromosome 2 gene candidates identified from Illumina sequencing of camp1 x WT-Col-0 crosses.

Chromosome location		Stop Mutation	AGI #	Description
1275477	1230506	Indel	AT2G04020	gdsl-like lipase/acylhydrolase superfamily protien, 261aa
1542305	1477533	Indel	AT2G04440	mutation in nudix domain, Nudix hydrolase, 215aa
1938801	1841019	Indel	AT2G05330	unknown, 398 aa
1957144	1858195	Indel	AT2G05360	U-box associated ubiquitination effector family, 358aa
3704925	3486876	Indel	AT2G09840	nucleic acid binding;zinc ion binding , 267
3938577	3712430	Indel	AT2G10260	proteiase family, unk, 547aa
4016966	3788114	Indel	AT2G10440	unk, 935aa
4661846	4393317	Indel	AT2G11626	similar to b-galactosidase protein, 242aa
5630724	5265158	Indel	AT2G13510	unknownm 284aa
5649196	5277579	Indel	AT2G13550	unknown, 181aa
6056533	5648805	Indel	AT2G14288	unk, 246aa
7915150	7347075	Indel	AT2G18190	P-loop containing nucleoside triphosphate hydrolases superfamily protein, 494aa
8603511	8016300	Indel	AT2G19920	RDRP4, 927aa
8613362	8025981	Indel	AT2G19940	oxidoreductases, acting on the aldehyde or oxo group of donors, NAD or NADP as acceptor;copper ion binding, 401aa
9884557	9235562	Indel	AT2G23220	CYP81D6, 515aa
9965194	9309047	Indel	AT2G23400	Undecaprenyl pyrophosphate synthetase family protein; tandem to the next gene (at2g23410), 253aa
3579326	3369804	SNP	AT2G07750	DEA(D/H)-box RNA helicase family protein (minus HelC domain)
3586168	3376649	SNP	AT2G07760	ZF TF
5981716	5576281	SNP	AT2G14170	METHYL-MALONATE SEMI-ALDEHYDE DEHYDROGENASE
6727002	6242342	SNP	AT2G15420	ubiquitin fusion degradation UFD1 family protein, 561aa
7956640	7386210	SNP	AT2G18320	F-box associated ubiquitination effector family protein, 106aa
10453830	9778567	SNP	AT2G24600	Ankyrin repeat family protein, 601aa

LITERATURE CITED

Austin, R. S., D. Vidaurre, G. Stamatiou, R. Breit, N. J. Provart, D. Bonetta, J. Zhang, P. Fung, Y. Gong, P. W. Wang, P. McCourt and D. S. Guttman (2011). "Next-generation mapping of Arabidopsis genes." Plant J **67**(4): 715-725.

Bashandy, T., J. Guilleminot, T. Vernoux, D. Caparros-Ruiz, K. Ljung, Y. Meyer and J. P. Reichheld (2010). "Interplay between the NADP-linked thioredoxin and glutathione systems in Arabidopsis auxin signaling." Plant Cell **22**(2): 376-391.

Clouse, S. D. (2011). "Brassinosteroids." Arabidopsis Book **9**: e0151.

Clouse, S. D., M. Langford and T. C. McMorris (1996). "A brassinosteroid-insensitive mutant in Arabidopsis thaliana exhibits multiple defects in growth and development." Plant Physiol **111**(3): 671-678.

Collakova, E., A. Goyer, V. Naponelli, I. Krassovskaya, J. F. Gregory, 3rd, A. D. Hanson and Y. Shachar-Hill (2008). "Arabidopsis 10-formyl tetrahydrofolate deformylases are essential for photorespiration." Plant Cell **20**(7): 1818-1832.

Cowling, R. J. and N. P. Harberd (1999). "Gibberellins control Arabidopsis hypocotyl growth via regulation of cellular elongation." Journal of Experimental Botany **50**(337): 1351-1357.

Davenport, R. (2002). "Glutamate receptors in plants." Ann Bot **90**(5): 549-557.

Duran, A. L., J. Yang, L. Wang and L. W. Sumner (2003). "Metabolomics spectral formatting, alignment and conversion tools (MSFACTs)." Bioinformatics **19**(17): 2283-2293.

Langmead, B., C. Trapnell, M. Pop and S. L. Salzberg (2009). "Ultrafast and memory-efficient alignment of short DNA sequences to the human genome." Genome Biol **10**(3): R25.

Lincoln, C., J. H. Britton and M. Estelle (1990). "Growth and development of the axr1 mutants of Arabidopsis." Plant Cell **2**(11): 1071-1080.

Mandal, A., V. Lang, W. Orczyk and E. T. Palva (1993). "Improved Efficiency for T-DNA-Mediated Transformation and Plasmid Rescue in Arabidopsis-Thaliana." Theoretical and Applied Genetics **86**(5): 621-628.

McElver, J., I. Tzafrir, G. Aux, R. Rogers, C. Ashby, K. Smith, C. Thomas, A. Schetter, Q. Zhou, M. A. Cushman, J. Tossberg, T. Nickle, J. Z. Levin, M. Law, D. Meinke and D. Patton (2001). "Insertional mutagenesis of genes required for seed development in Arabidopsis thaliana." Genetics **159**(4): 1751-1763.

Raffaele, S., A. Leger and D. Roby (2009). "Very long chain fatty acid and lipid signaling in the response of plants to pathogens." Plant Signal Behav **4**(2): 94-99.

Ross, J. J., I. C. Murfet and J. B. Reid (1997). "Gibberellin mutants." Physiologia Plantarum **100**(3): 550-560.

Steber, C. M. and P. McCourt (2001). "A role for brassinosteroids in germination in Arabidopsis." Plant Physiol **125**(2): 763-769.

Thornton, C. R. and N. J. Talbot (2006). "Immunofluorescence microscopy and immunogold EM for investigating fungal infection of plants." Nat Protoc **1**(5): 2506-2511.